Development of a predictive asset rating tool for decision support in an electrical distribution network

Tuan Nu'man bin, Tuan Ab Rashid
(Numan Rashid)

A thesis presented for the degree of
Doctor of Philosophy
in
Electrical and Computer Engineering
at the
University of Canterbury,
Christchurch, New Zealand.

2019

I dedicate this thesis to my family. Without your patience, understanding, support, and most of all love, the completion of this work would not have been possible.

ABSTRACT

The optimization of network capacity utilization is becoming increasingly important in an electrical distribution network with the variation in load demand due to seasonal changes and uptake of new technologies such as photovoltaics, batteries, electric vehicles and distributed generation. The proliferation in the use of these technologies introduces uncertainties in future load demands and increases the risk of asset stranding. This then represents an opportunity for network planners and operators to re-evaluate their existing infrastructure with the aim to optimize the electrical components operation and return on investment.

This thesis introduces a novel method to evaluate and optimise the network capacity utilization for network planning, operation and management. A predictive asset rating model for 33kV electrical distribution has been developed and implemented in Unison Network Limited as part of this research. The thermal behaviour of the electrical components to its surrounding was studied utilising sensors installed along the circuits and based on historically captured data available from the public and at localised area. The predictive asset rating model performs network evaluation based on probabilistic method to evaluate the dynamic utilisation of the network and reliability in the event of changes to the operating conditions and the network configuration. The model was developed using MATLAB to carry out different simulation scenarios for network planning and operation.

The thesis begins by introducing the current state of electrical distribution networks. The rating and modelling of electrical components is then introduced, covering international standards and similar research in the area of study. The impact of environmental conditions and load demand to the available capacity of the network are then discussed. Results in the area of capacity planning, constraint analysis and network expansion planning is presented, highlighting the model's ability to predict capacity utilisation and constraints on the network.

Deputy Vice-Chancellor's Office

Postgraduate Office

UNIVERSITY OF CANTERBURY
Te Whare Wānanga o Waitaha
CHRISTCHURCH NEW ZEALAND

Co-Authorship Form

This form is to accompany the submission of any thesis that contains research reported in co-authored work that has been published, accepted for publication, or submitted for publication. A copy of this form should be included for each co-authored work that is included in the thesis. Completed forms should be included at the front (after the thesis abstract) of each copy of the thesis submitted for examination and library deposit.

Please indicate the chapter/section/pages of this thesis that are extracted from co-authored work and provide details of the publication or submission from the extract comes:
Section 4.3 contains figures that's co-authored and published across multiple EEA conference
Section 2.5 is adapted from "Global and Local Trends of Grid Intelligence Based on Dynamic Rating Application".

Please detail the nature and extent (%) of contribution by the candidate:
Data gathering, running simulation, researching and the majority of the manuscript 95%. The co-authors offered criticisms which the candidate worked into the manuscript.

Certification by co-authors

If there is more than one co-author then a single co-author can sign on behalf of all. The undersigned certifies that:

- The above statement correctly reflects the nature and extent of the PhD candidate's contribution to this co-authored work

- In cases where the candidate was the lead author of the co-authored work, he or she wrote the text.

Name: *Dr Andrew Lapthorn* Signature:  Date: *9 October 2019*

LIST OF PUBLICATIONS

The following is a list of papers and awards presented that have been accepted during the research presented in this thesis.

CONFERENCE PAPERS

N. Rashid, A. Lapthorn, T. S. Jalal, B. v. Vliet (2017), "What's my Rating? Asset Capacity Utilisation with a Smart Grid", in *Electricity Engineer's Association (EEA) Conference*, Wellington, New Zealand, June 2017, pp.1-9.

N. Rashid, A. Lapthorn (2016), "Evaluation and Optimization of Network Capacity Utilization for Electric Distribution", in *IEEE International Conference on Power System Technology (POWERCON)*, Wollongong, Australia, October 2016.

N. Rashid, A. Lapthorn, T. S. Jalal, B. v. Vliet (2016), "Global and Local Trends of Grid Intelligence Based on Dynamic Rating Application", in *Electricity Engineer's Association (EEA) Conference*, Wellington, New Zealand, June 2016, pp.1-9.

T. S. Jalal, N. Rashid, K. a. Murrani, B. v. Vliet (2015), "Challenges in Implementing Intelligent Computation Algorithms for Smart Distribution Networks", in *Electricity Engineer's Association (EEA) Conference*, Wellington, New Zealand, June 2015, pp.1-9.

N. Rashid, T. S. Jalal, K. a. Murrani, B. v. Vliet (2014), "Practical experience on dynamic rating implementation in distribution networks to improve asset utilisation", in *Electricity Engineer's Association (EEA) Conference*, Auckland, New Zealand, June 2014, pp.1-9.

T. S. Jalal, N. Rashid, B. v. Vliet (2012), "Implementation of Dynamic Transformer Rating in a Distribution Network", in *IEEE International Conference on Power System Technology (POWERCON)*, Auckland, New Zealand, October 2012, pp.1-5.

AWARDS

Unison Networks Limited (2017), "Unison's Predictive Asset Rating," in *Electricity Engineer's Association (EEA) ESI Engineering Excellence Award*, Wellington, New Zealand, Awarded, June 2017.

Unison Networks Limited (2017), "Unison's Predictive Asset Rating," in *Deloitte's Innovation in Energy Award*, Auckland, New Zealand, Finalist, June 2017.

CONTENTS

LIST OF FIGURES

LIST OF TABLES

Chapter 1

INTRODUCTION

1.1 INTRODUCTION

Electrical distribution networks (EDN) are made up of thousands of electrical components that are arranged and interconnected together to form a working power delivery system. The network operators faces a number of challenges in ensuring a reliable power supply from its existing infrastructure to its customers. Some are due to variables such as load growth, ageing infrastructure and abnormal operating events. In New Zealand, the electricity demand had been increasing at an approximately 2.5 percent rate per year since the 1970s and is projected to continue growing at 1.5 percent per year through to 2050 [Electricity Authority of New Zealand 2018]. The projected increase in demand strongly relates to economic growth and increased customer connections. It is however observed that the uptake of new technology such as battery storage and photovoltaic (PV) systems has caused the demand to reduce, as experienced by large EDN in New Zealand [Unison Networks Limited 2015, Vector Limited 2015]. The overall electricity consumption in New Zealand had reduced by 1.2 percent per year from 2010 to 2013 and then again in 2015 to 2018 [Ministry of Business, Innovation & Employment 2018]. Apart from the consumption, the variations of the load usage by the consumers also impose a challenge for network planning. The variation between low and high customer demand can be as high as 31% for different operating and environmental conditions [Electricity Authority of New Zealand 2018]. Network operators face abnormal operating events that can interrupt the electricity supply to its customers due to permanent or transient faults, further requiring the existing infrastructure to handle the increased load to maintain a reliable power supply. These challenges then represents an opportunity for network planners and operators to re-evaluate its existing infrastructure and

optimise the electrical components operation and return of investments.

The utilisation of an individual component in EDN is dependent on its design and ability to handle power, also taking into account additional information such as the operating environment [Willis 2004]. Network planners have historically relied upon static ratings (SR) to define the maximum allowable current (ampacity) passing through electrical components, which are set as the operational limits. Many of the environmental conditions used to calculate these limits (such as ambient temperature, soil temperature, wind speed, solar radiation) are assumptive in nature. To be conservative, planners select values that represent the worst-case scenario based on historically observed conditions in the service area. This leads to a SR that is conservative for most conditions and potentially exceeds the true ampacity for unfavourable conditions. Given the uncertainties in future load demand and possible risk of asset stranding due to consumer technological shifts, network operators are looking at opportunities to operate their assets considerably closer to the practical limits. With the advancement of technology and increased monitoring of assets through smart grid initiatives, operators are able to use additional data metrics and turn them into useful and actionable information. By actively monitoring changing environmental conditions, these data metrics can be used to better understand the network operating conditions to then optimise the network utilisation. One of the methods to address the uncertainties in the true ampacity of an electrical component is by evaluating the real-time thermal rating or dynamic rating (DR).

DR has been studied and applied in the electricity industry since the 1980s, predominantly in electric transmission and overhead line applications [Ausen *et al.* 2006, Raniga and Rayudu 2000, Shun Hsien *et al.* 2006]. The high cost and lengthy time involved to upgrade existing infrastructures sees transmission network applying DR to evaluate the component's rating and identify periods of capacity gains and constraints without the needs to upgrade its existing infrastructure. The approach to apply DR was not relevant in the past for operator of EDN as upgrading the existing network are more straight forward since the network covers a smaller service area compared to the transmission network. However, with the variation of demand and uncertainties in the uptake of new technology, an increased application of DR in the EDN can be seen to ensure the networks are optimised to achieve the most benefit [Michiorri 2010, Yang and Strickland 2014a].

The implementation of DR in EDN varies for different network configuration and system requirements but relies on the availability of data, a system to process the data and an evaluation of the processed data. With increased number of components and environmental conditions being monitored in the field, operators are facing challenges and looking at better ways to convert the increasing amount of field data into information that can be used for decision making. This leads to the concept of "big data", looking at solutions to challenges experienced when capturing, processing, analysing and visualising these data. These have led to different solution of DR implementation to be investigated by different institutions to suit the specific needs of the EDNs which will be highlighted in Chapter 2 of this thesis. It was found that these solution doesn't fully meet the need of future EDN where there exist an uncertainties in demand, varying electrical components installed on the network and ability for the DR implementation to make the decision required in the area of capacity utilisation across network operation, planning and asset management. To meet these shortfall, a solution through the use of the developed predictive asset rating tool has been investigated in this thesis. The model aggregates parameters that impacts the asset capacity utilisation and evaluates the rating of interconnected electrical components to generate additional matrix for decision support in an EDN. The developed solution will be discussed in detail throughout this thesis.

In 2010, Unison Networks Limited (Unison), a network operator based in Hastings, New Zealand, has embarked on a journey towards achieving a smarter grid. The definition of smart grid varies across different application, the following definition of smart grid has been adopted by Unison [Unison Networks Limited 2015]:

"The application of real time data, communications technologies and emerging trends in electricity distribution to improve capacity utilisation, enhance lifecycle asset management and provide additional service on the modern network, thereby optimising network investment to the benefit of all stakeholders."

Increased monitoring of the electrical components and environmental conditions is present in the Unison network to obtain better understanding of the network operating conditions for improved decision making. The capacity utilisation of power transformers (PTX), underground cables (UGC) and overhead lines (OHL) have been studied on Unison's high voltage (33kV) network

for this PhD. This thesis outlines the development and implementation of a novel method to evaluate the network capacity utilisation using a probabilistic model in the event of changes to the operating conditions and the network configuration. The method from here on denoted as predictive asset rating (PAR).

1.2 RESEARCH OBJECTIVES

The primary objective of this research is to develop and implement the PAR tool in an EDN in order to optimise the capacity utilisation of the electrical components in a safe and reliable manner where network uncertainties exist. To be able to achieve the objective, the following work had been carried out:

i. identify the sensitivity of PAR application to environmental data,
ii. identify technological requirement to implement PAR,
iii. develop novel algorithms and software,
iv. evaluate application of PAR for varying network scenarios events,
v. provide recommendations on constraints and benefits for PAR implementation.

The PAR model for Unison had been developed based on the following specifications:

i. allow easy integration with existing software environment,
ii. allow flexibility in modelling and implementation,
iii. includes data processing capabilities,
iv. considers health and safety requirements,
v. considers component life,
vi. provides likelihood of rating utilisation,
vii. provides information that supports business decision making.

1.3 THESIS OUTLINE

Chapter 2 provides an overview of the basic theory of component ratings in an electrical distribution network. These components are power transformers, underground cables and

overhead lines. Literature on modelling and monitoring methodology of the electrical components is presented. The principle of thermal rating is highlighted, outlining the effect of environmental parameters onto electrical components. The chapter finishes with a section on evaluating power system reliability.

Chapter 3 details the modelling used for implementation. The models for each electrical component studied are given based on industrial standards and relevant work on dynamic rating. The second part of the chapter details the modelling of the environmental parameters for sparsely located monitoring sites and provides an overview of the impact to the electrical components. The chapter finishes with a section on modelling the power system reliability based on the Monte Carlo method.

Chapter 4 presents the development work of dynamic rating implementation in an EDN. The datasets and model used for the study are described covering the environmental data and the electrical component studied. The algorithm and its implementation is then described and the validation steps taken are presented.

Chapter 5 discusses the results of predictive asset rating implementation in an electrical distribution networks. The simulation of varying environmental conditions and their impact to different electrical components is presented here. Details of the implementation are given including models used, steps involved in the algorithm and the power system simulation and evaluation.

Chapter 6 presents the future work that can be carried out following this research. Additional simulation and further consideration from the model presented in this thesis are discussed to present possible scope for future research and application areas. The main findings of this thesis are also discussed and concludes the research.

Chapter 2

BACKGROUND

2.1 OVERVIEW

In this chapter the background of this research is first introduced. The electrical distribution network and the connected electrical components are presented. The utilisation of the network is then discussed covering its impact to network operations, planning and asset management. The chapter finishes with a discussion on the challenges faced by electrical distribution in the area of capacity utilisation. A novel tool is proposed which evaluates and provide information required to support management decisions in the area of capacity utilisation for electrical distribution network.

2.2 INTRODUCTION

Electrical distribution networks (EDN) are made up of thousands of electrical components that are arranged and interconnected together to form a working power delivery system. In a distribution network, a distribution substation receives power from a sub-transmission circuit and steps down voltages using power transformers (PTX). These transformers are used to provide electrical supply to many distribution circuits that are interconnected and consist of overhead or underground electrical components. A typical power delivery system in New Zealand is shown in Figure 2.1.

In New Zealand, the electricity demand had been increasing at an average of 2.5 percent rate per year from 1975 to 2010 and decreased by 1.2% from 2010 to 2013. The demand is now back

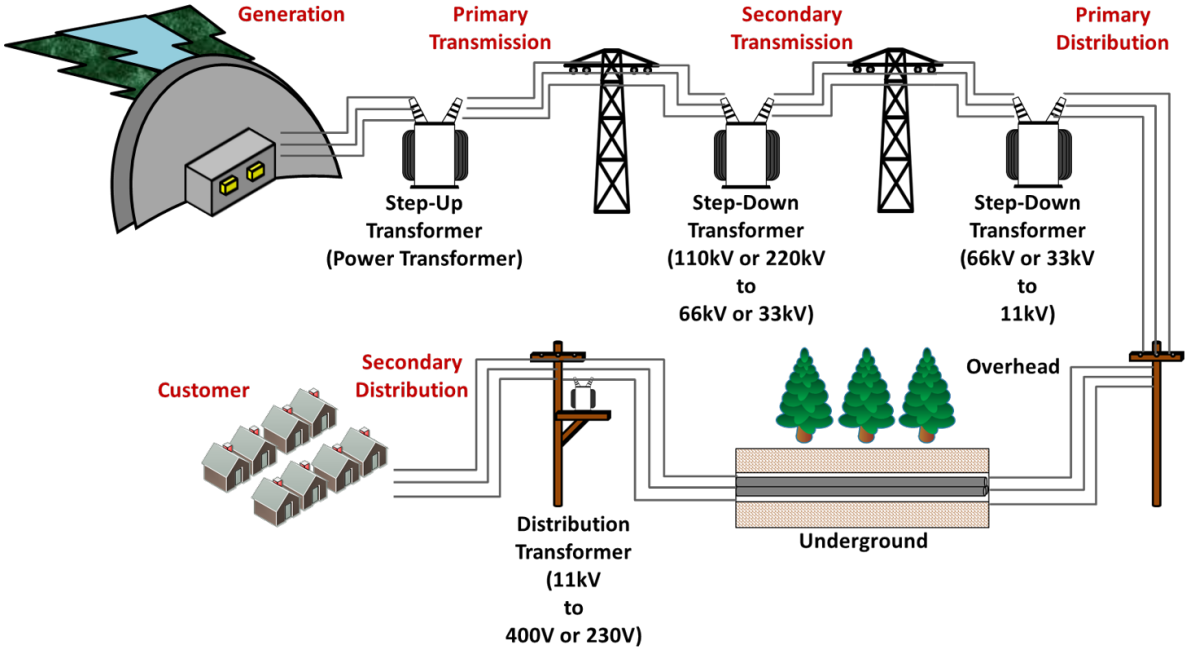

Figure 2.1 Typical power delivery system in New Zealand

on the increasing trend at 1% per year since 2013 [Ministry of Business, Innovation & Employment 2018]. The overall electricity consumption in New Zealand varies by sector with industrial showing the highest consumption, followed by residential, commercial and agriculture covering 37%, 32%, 24% and 7% respectively for the period ending 2015 as illustrated in Figure 2.2.

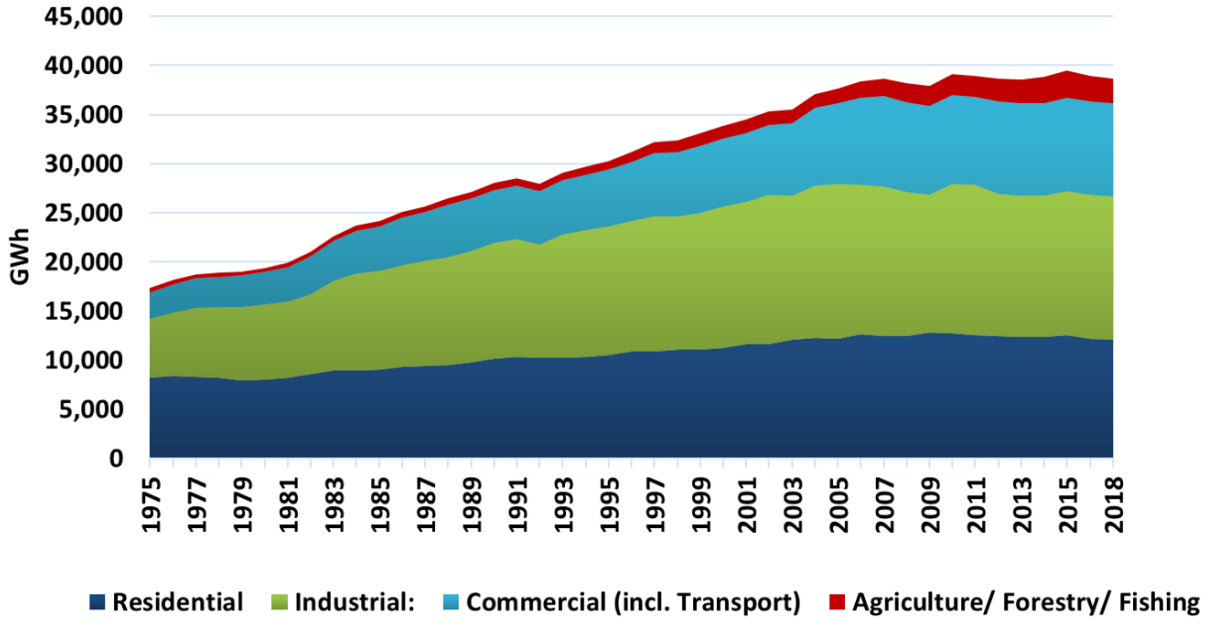

Figure 2.2 Electricity Consumption in New Zealand by Sector (data available from [Ministry of Business, Innovation & Employment 2018])

Transpower New Zealand is the owner of New Zealand's national transmission grid and provides the infrastructure for electric power transmission that allows consumers to have access to generation from a wide range of sources. Network operator then distributes the power to its service area. As demand for electricity varies over time, supply must change almost instantly to support this demand. Electricity consumption has been observed to follow strong daily and seasonal patterns as illustrated in Figure 2.3. The total demand for North Island, New Zealand can be seen fluctuating, increasing during winter in May and drops again during summer period in November. The variation between low and high demand such as between summer night and winter evening can be as high as 35%.

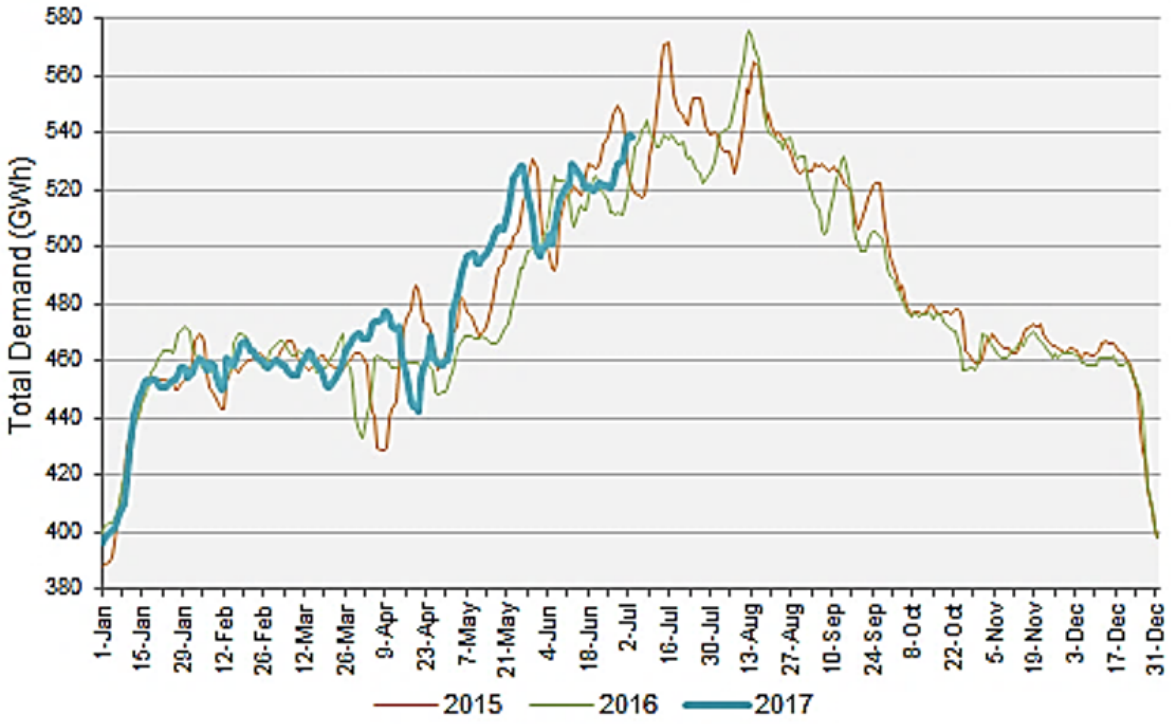

Figure 2.3 North Island, New Zealand Electricity Demand (Rolling 7 days) (reprinted from [Transpower New Zealand 2017])

The fluctuation in demand and consumption imposes a challenge for network operators when planning the capacity and operating the network. An increase in the number of connected installation control points (ICPs) can result in an increase of demand beyond the available installed capacity of the network which would require the network to be upgraded to meet the load demand. As network operators in New Zealand are subject to regulatory provisions under the Commerce Act 1986, their service charges to the consumer are limited [Commerce

Commission 2017]. Conversely, as consumers become more efficient in their use of electricity with the availability of energy-efficient appliances and the uptake of distributed generation, the demand is likely to reduce, again impacting the revenues of network operators. A study, commissioned by the Electricity Commission, on the uptake of energy-efficient appliances and technologies in New Zealand projected that potential reduction of NZ's base energy consumption to be as much as 23% by 2016 [KEMA 2007]. It can be seen from Figure 2.2 that the difference of electricity consumption in 2007 and 2015 is indifferent, with a difference of 33 GWh (the estimated saving for residential was 2,633 GWh by 2016). As the amount saved are not measured in the total NZ energy consumption, the discrepancies in the values are likely due to the savings being hidden from the change of demographic in New Zealand. There has been a growth in the gross domestic product (GDP) since the 2005 statement of opportunity (SOO) used by the study which would consequently lead to an increase in electricity demand [Electricity Authority Commission 2017]. With a better estimate on the likelihood of consumers uptake of technology and a more granular load profile, robust scenario modelling can be established by evaluating the occurrences of events. As the sectors discussed are directly connected to an EDN, a reduction in demand would then require the operation of the existing network infrastructure to also be efficient and optimised to maintain the return on network investment.

Initial use of electricity in New Zealand has been recorded since 1885. The electrical components that have been installed since then would have been retired or replaced with newer components to maintain network reliability and continuity of supply. The design specification of an electrical components and its exposure to thermal stress during operation underpins its rating and useful life. Standards such as "Power transformers, Part 7: Loading guide for oil-immersed power transformers", AS/NZS-60076.7 [AS/NZS TC EL-008 2013b] and "Electric cables - Calculation of the current rating", IEC 60287 [IEC TC 20 2006] have been developed to provide network operators guidelines to safely operate the components on their network without overheating or excessively degrading its useful life. Traditionally the rating and the capacity utilisation of these components are determined based on conservative and static values due to limited knowledge and technology available to monitor operational conditions. Considerable interests by different institutions have been seen to monitor the environmental and thermal state of the components to optimise the utilisation of the EDN [Yang and Strickland 2014b, Degefa *et al.* 2014]. In

the literature, the study is better known as real time thermal rating or dynamic rating (DR). Electrical component operating conditions such as the environmental conditions, circuit loading and temperature are seen utilised to provide additional insight into decision making in an EDN [Douglass and Edris 1999]. The next section provides a background on approach taken by different EDN to evaluate the rating and make decision based on the capacity utilisation of their network.

2.3 FUNDAMENTAL COMPONENTS OF A DISTRIBUTION NETWORK

To evaluate the current state of a distribution network in the area of capacity utilisation, the fundamental components required for power delivery have been studied. This involved the study of PTX and the circuits used to deliver the power from the source to the load centres. As circuits consist of section with overhead lines (OHL), undeground cables (UGC) or combination of the two (hybrid circuit), each of these will be evaluated separately and later evaluated collectively to achieve the rating of the network. The presence of DR evaluation on electrical components and its potential to network operators are highlighted focusing on the following criteria:

(a) **Real time system viewing**: Ability to actively evaluate the available capacity and operational event.

(b) **Fault and constraints determination**: Ability to prompt potential thermal limits on the network.

(c) **Network optimisation and expansion planning**: Ability to provide predictive evaluation and optimise electrical components.

2.3.1 Power Transformers

Transformers are designed to transform voltage from one voltage level to another. At the distribution level, the voltage is stepped down from a higher voltage to a lower voltage level at the consumer end. The transformer loading range varies from kilo Volt-Ampere (kVA) to mega Volt-Ampere (MVA). The standard term used for power transformers are based on power transformers having the loading capability of 2.5 MVA to 100 MVA whilst distribution transformers

are for transformers with maximum rating of up to 2.5 MVA [IEC TC 14 2005]. This research focuses on power transformers with loading capability between 2.5 MVA to 100 MVA and from here on are referred to as just transformers.

A transformer's loading capability is determined by evaluating the operating condition with respect to the thermal limits of its parts during operation. This is to ensure the condition of its materials are not excessively deteriorating due to thermal stress. Excessive heating causes the material within a PTX to operate abnormally and can lead to a fire or a premature failure. The international standards prepared by Institute of Electrical and Electronics Engineers (IEEE) in IEEE C57.91 [IEEE C57.91 2012] and by International Electrotechnical Commission (IEC) in IEC 60076.7 [IEC TC 14 2005] provide guidelines on the loading capability of transformers. The latter standard is also adapted by Standards Australia and New Zealand (AS/NZS) in AS/NZS 60076.7 [AS/NZS TC EL-008 2013b] to provide guidelines for New Zealand operating conditions. These guidelines provide calculations and practical considerations to ensure the transformers are operated safely.

Transformers experience heating and cooling during their operation, which can be used to evaluate its operating temperature. The illustration shown in Figure 2.4 shows a typical heat transfer experienced by a transformer with oil natural and air forced (ONAF) cooling. Based on the heat transfer experienced, thermal models have been developed and used widely by network operators to evaluate the hottest temperature within a PTX. For an ONAF PTX, its hot-spot temperature can be modelled looking at the ambient temperature, top oil temperature and winding temperature, given as [IEEE C57.91 2012],

$$\theta_{h(n)} = \theta_a + \Delta\theta_{oil(n)} + \Delta\theta_h \tag{2.1}$$

where $(\theta_{h(n)})$ is the hot-spot temperature, (θ_a) is the ambient air temperature, $(\Delta\theta_{oil(n)})$ is the top oil temperature rise over ambient temperature, and $(\Delta\theta_h)$ is the hot-spot temperature rise over oil temperature rise. The subscript n denotes the evaluation at each time step of the transformers operation.

Using the thermal model, the hot-spot temperature of a transformer is evaluated to ensure it

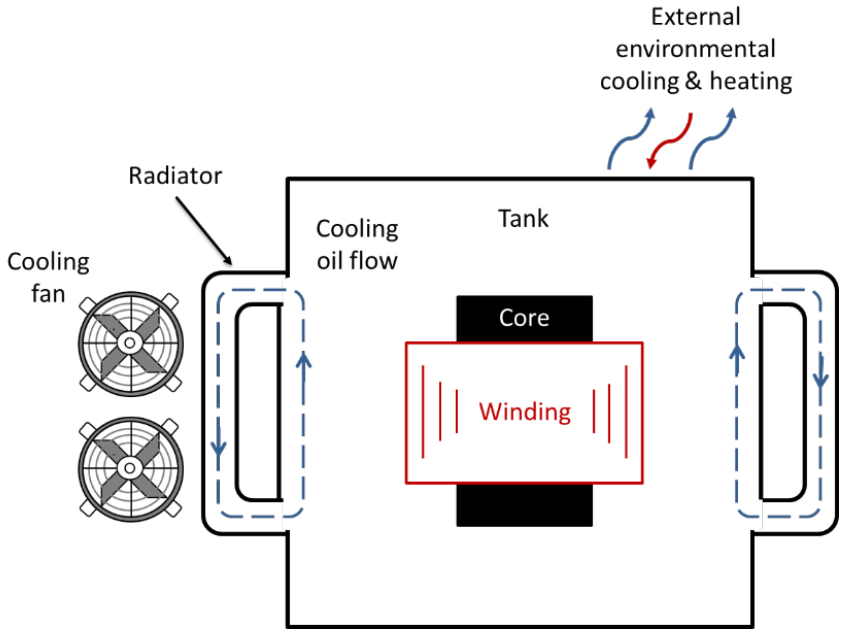

Figure 2.4 Heat transfer of an ONAF transformer

is operating within the thermal limit. With exposure to a higher operating temperature, when operating the transformer closer to its thermal limit, the work by [AS/NZS TC EL-008 2013b] suggests the evaluation of the transformer's loss of life, L, based on the relative ageing rate of the paper material used at the windings, V_n, to represent the deterioration rate caused by the exposure to the hot-spot temperature at each calculation time step, t_n, given as,

$$L = \sum_{n=1}^{N} V_n \times t_n \tag{2.2}$$

Interest in the area of optimising the capacity utilisation of a transformer and evaluating its condition sees institutions and utilities applying and validating the standard method. This research includes work that advances the exponential model of power transformer heating to allow consideration for non-linear cooling of transformers [Swift *et al.* 2001]. The equivalent circuit derived by the work is re-illustrated in Figure 2.5 which represents the heat transfer from winding-to-oil-to-air.

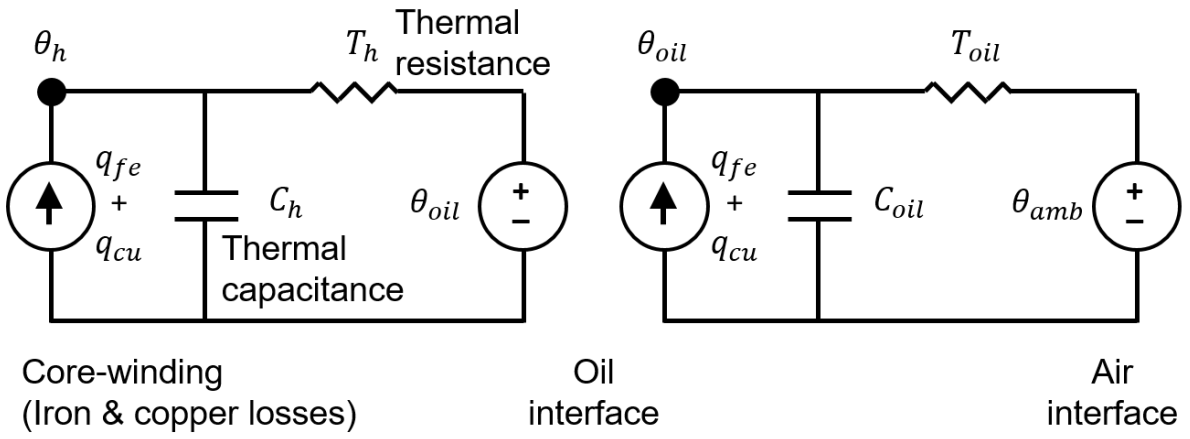

Figure 2.5 Circuit representation of transformers heat transfer, re-illustrated based on [Swift *et al.* 2001]

The thermal model considers the oil, winding and external environment interface allowing a more granular calculation and monitoring of the transformer loading capability. For a DR application, a continuous stream of data are important to ensure the calculation are updated in a timely manner. The work by [Nuijten *et al.* 2005] discusses the implementation of the model on 27 of their transformers ranging from 18 MVA to 100 MVA equipped with top-oil and environmental temperature sensors. The study found that the DR implementation on their network provides their network operator a quick-scan of present and future loadings. The new information provides their operators greater confidence in the headroom available during emergency situations. A detailed analysis of different models for PTX is discussed further in Chapter 3.

2.3.2 Underground Power Cables

Underground power cables are used to distribute electric power from the source to the consumer. Underground cables are insulated and their physical construction determines their ability to carry current. For an electrical distribution network, the sizing of underground cables varies between, but not limited to, a conductor with a cross sectional area of 16 mm^2 to 800 mm^2. A conductor with bigger cross sectional area has a higher current carrying capacity. The use of better conductive materials also further improves the carrying capacity of the cable. To study the loading capabilities of an underground cable, the thermal resistance of the cable construction is calculated to evaluate the ability for the heat generated by the current in the conductor to be dissipated to the environment. This concept was first introduced in *"The calculation of the*

temperature rise and load capability of cable systems" by [Neher and McGrath 1957] and later adapted and improved in *"Electric cables - Calculation of the current rating"*, IEC 60287 [IEC TC 20 2006] to incorporate additional findings. Since then, a series of improvements to the rating evaluation of underground cables have been introduced to the electrical industry. A notable work is in the area of solving the heat transfer equation for underground cables numerically to provide an improved approximation of the temperature distribution in the soil surrounding the cables as covered in IEC TR 62095 [IEC TC 20 2003]. The work in IEC 60287 provides a guideline on the calculation of the current rating for various cable configurations such as in duct, direct buried, grouped and combinations of these. The inaccuracy of the model lies in its approximation of the cable as a line source placed in an infinite homogeneous surrounding medium. This limits its application for cable configuration with multiple heat sources, which has been improved through the approach taken by IEC TR 62095 [IEC TC 20 2003].

An underground cable experiences heating and cooling during its operation. The illustration shown in Figure 2.6 shows the typical heat transfer experienced by an UGC. The heat transfer across the UGC can be represented as an equivalent circuit to evaluate the thermal losses at each of the cable layers where the losses, W are presented as a source and thermal resistance, T_n as an impedance as shown in Figure 2.7. T_3 is the thermal resistivity at the most outer layer of the cables just before the external environment, T_4 [IEC TC 20 2006].

The work presented in IEC 60287 suggests different thermal resistances, T_1 to T_4 to be considered for different cable constructions. This is valid as different cable configurations have varying ability to dissipate heat. Most DR applications for UGC are seen taking this approach which covers common cable configuration such as adjacent circuit in parallel to one another and cables that has been backfilled with a common soil type [Chand and Brown 2017, Shun Hsien *et al.* 2006].

As the configuration varies with application and can be more complex than those covered by the standard, the work in IEC TR 62095 proposes heat transfer across the cable to be broken down into smaller regions to provide a finer temperature distribution. The finite element method (FEM) is one of the numerical methods suggested to solve the thermal model when a mixed cable configuration exists [IEC TC 20 2003].

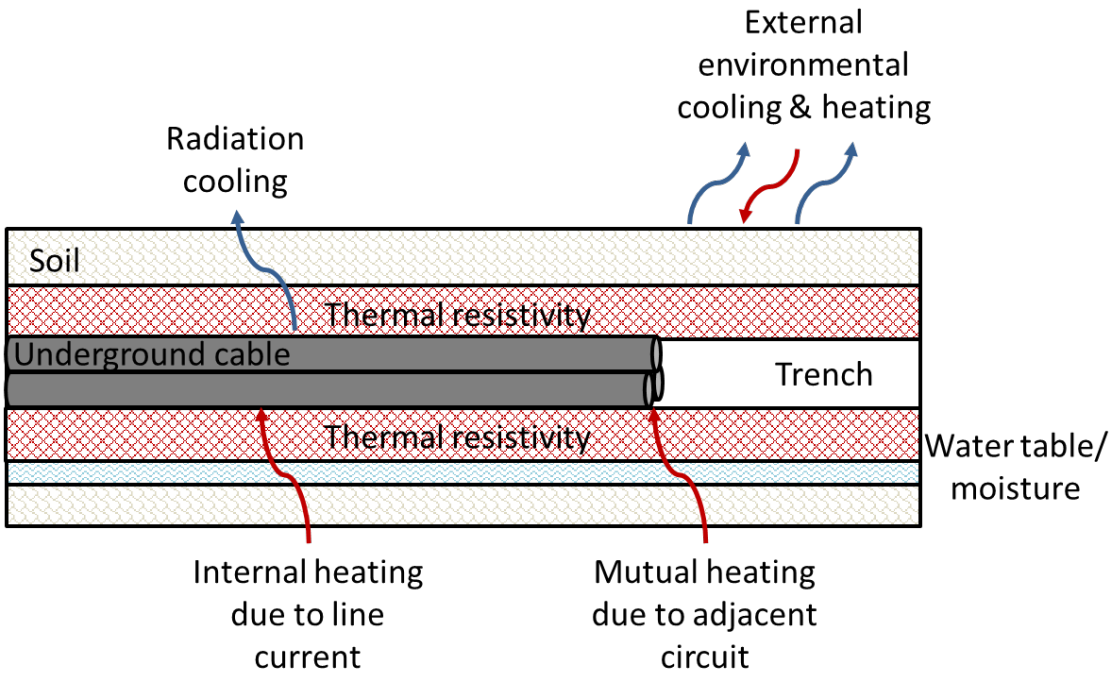

Figure 2.6 Heat transfer of cables in group

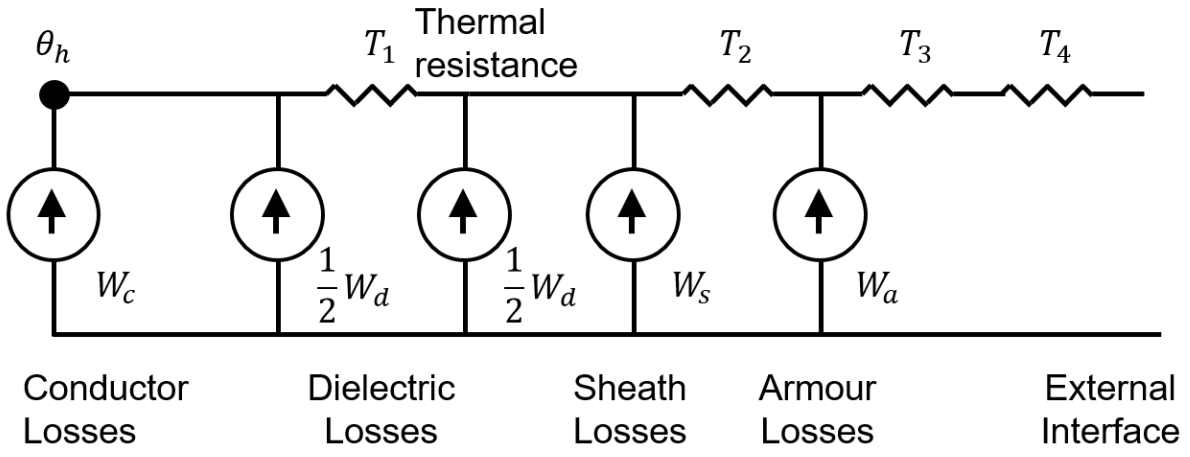

Figure 2.7 Circuit representation of cables heat transfer

Based on the heat transfer principle of a solid with an internal heat generation, the temperature distribution of a cable configuration can be evaluated as,

$$\frac{1}{\alpha} \cdot \frac{\partial \theta}{\partial t} = \frac{\partial^2 \theta}{\partial x^2} + \frac{\partial^2 \theta}{\partial y^2} + W_{gen} \cdot T \tag{2.3}$$

where, θ is the unknown temperature inside a trench of a cable configuration that has internal

heat generation W_{gen} from the conductive materials at the cable conductor and screen wires. Solving (2.3) for θ allows the temperature inside the trench to be calculated and the location of the hot-spot temperature to be identified. The temperature solution from (2.3) via FEM has been compared against the analytical method in IEC 60287. [Baazzim *et al.* 2014] found that the use of FEM provides a more accurate and reliable computations of underground cable loading capability compared to IEC 60287 as it provides flexibility and control of the cable construction and is well suited when additional heating or cooling is present. The work by [Mushamalirwa *et al.* 1988] highlighted that computation time requirement to solve the finite-element model was of concern in the past, this is now less relevant with the advancement in technology and improved methodology. This aspect is important as FEM computation used to take days, then hours and with improved modelling this limitation can be further improved. The ability to accurately model temperature distribution through DR evaluation allows operators to have a better understanding of cable's operation and its impact to the overall network. This then allows optimisation on the selection of cable to be used for different environmental conditions.

2.3.3 Overhead Power Lines

Overhead power lines (OHL) are designed to carry electric current and are usually used in tandem with underground cables to distribute electric power from the power source to the consumer. Long strings or spans of overhead power lines are attached to poles and are used to distribute electric power over a longer stretch of the network. Being out in the open, an overhead line is more accessible to evaluate its operating conditions. This also means lines are more susceptible to environmental variations compared to the other asset classes. The illustration shown in Figure 2.8 shows a typical heat transfer experienced by an overhead line.

Environmental variations are beneficial to the line rating when a cooling effect is applied to the asset such as during high wind speed. A heating effect such as the conductor exposure to high solar radiation limits the utilisation of the overhead lines as it increases the net heat of the conductor. Research by the International Council on Large Electric Systems (CIGRE) evaluates the operational capability of an OHL based on the heat it generates and its exposure to external heating and cooling, given as [CIGRE WG B2.12 2002],

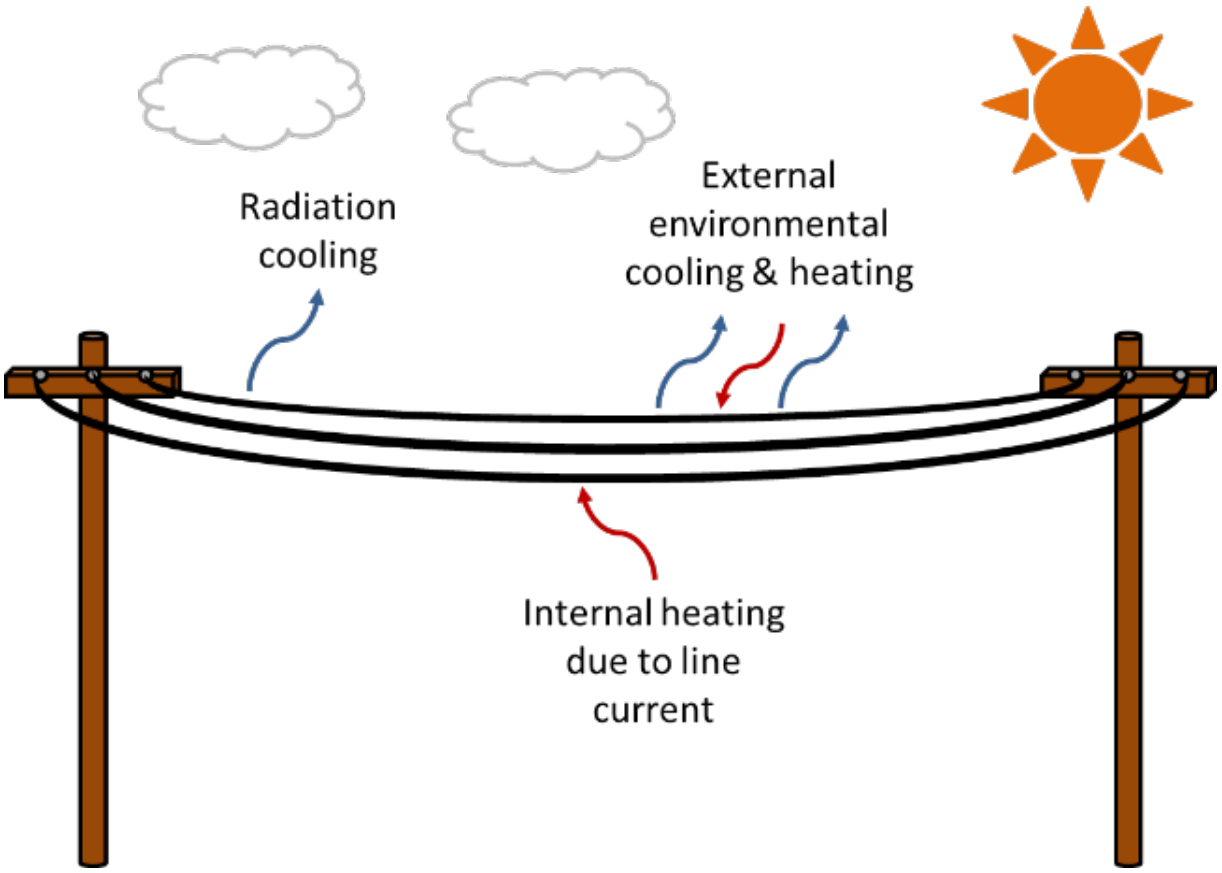

Figure 2.8 Heat transfer of bare overhead lines

$$m \cdot c_p \cdot \frac{d\theta}{dt} = W_{gen} + Q_{sun} - Q_{rad} - Q_{conv} \tag{2.4}$$

where, θ is the unknown temperature of the conductor. A factor is applied for different conductor types represented by m, the conductor's mass and c_p, the specific heat capacity. The OHL heat transfer involves heating and cooling across the conductor evaluated per unit length. The heating is due to the active power losses W_{gen} and absorbed solar energy, Q_{sun}. Cooling is experienced through radiation, Q_{rad} to the environment and convection Q_{conv} due to the heat removed from the surface of the conductor being exposed to air.

The thermal model allows industry guidelines such as *"IEEE Standard for Calculating the Current-Temperature Relationship of Bare Overhead Conductors"*, [IEEE 738 2013] to be prepared to provide utilities the practical requirements for safe installation and utilisation of overhead lines. Operating the overhead lines above its rating introduces risk to the public as the

high temperature causes the overhead lines to sag and reduces the overhead line safety clearance to ground. Research by [Rahim *et al.* 2010] demonstrates the use of the measured sag of the conductor to validate the thermal model used for their DR application and shows that the thermal and mechanical model can both be used in tandem to ensure both the safety and operational benefits are achieved. The sag measurement technique mainly focuses on a certain span and can only be applied to OHL. Additional interfaces will be required to consider other components on the network. Operationally without a DR evaluation, the line clearances are assumed to be within the regulatory limit as long as the lines are not operated above the stated manufacturer's rating and the design specification. With monitoring in place and calculation performed in a continuous manner, the line clearances can be modelled and operators can be notified after a certain threshold thus enabling real time system viewing and constraint determination.

2.3.4 Circuit Breaker

A circuit breaker is used to control, protect and isolate electrical components. It operates as a switch which allows currents to flow through between two adjoining electrical components when closed and break the connection when opened. Circuit breakers can be designed to either use oil, air, gas, vacuum or a hybrid which encompass of air and gas technologies. The level of currents that it can break depends on its current rating which varies for different arc-suppressing material. The characteristics of breakers are given by international standards such as *"High-voltage switchgear and controlgear - common specifications"*, IEC 62271 or AS 62271. The temperature limit of the material that makes-up a circuit breaker varies from 75 degrees celsius (°C) to 180°C [AS TC EL-007 2012]. The most limiting material of a circuit breaker (if used) is the bare-copper contact of an air type circuit breaker which has a maximum operating temperature of 75°C. The temperature limit of other contacts are shown in Table 2.1

The circuit breakers selected for a circuit are normally rated higher than the current carrying capacity of the circuit. The reason for this is to ensure in the event of a fault, the circuit remains isolated and restricts damage caused to the rest of electrical components. A circuit breaker mainly acts as a control point and has less pre-eminence in thermal rating applications compared to the other electrical components discussed. The configuration of the electrical components and

Table 2.1 Temperature limit of circuit breaker materials, reprinted from [AS TC EL-007 2012]

Contacts material and the type of dielectric	Maximum Temperature (°C)	Maximum Temperature Rise (°C) at Ambient Air Temperature < 40°C
Bare-copper or bare-copper alloy		
- in air	75	35
- in SF_6	105	65
- in oil	80	40
Silver-coated or nickel-coated		
- in air	105	65
- in SF_6	105	65
- in oil	90	50
Tin-coated		
- in air	90	50
- in SF_6	90	50
- in oil	90	50

positioning of circuit breakers is however important as it directly links to the reliability of the electricity supply. In delivering a reliable power supply, there are different ways the network can be configured as shown in Figure 2.9. The solid square represents a circuit breaker whilst the line represents the electrical network.

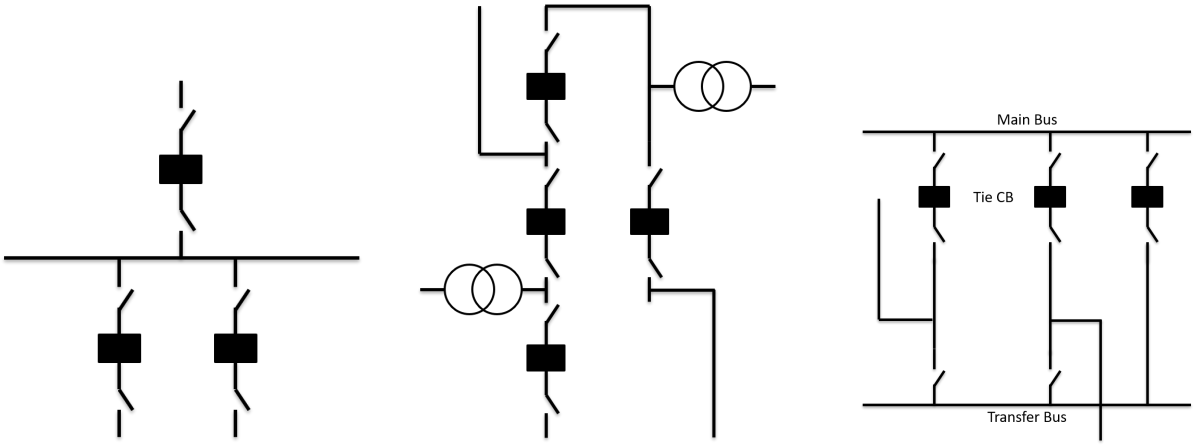

(a) Single bus (b) Ring bus (c) Main and transfer bus

Figure 2.9 Circuit breaker positioning for different network configuration, re-illustrated based on [Brown 2009]

A common substation configuration such as the ring bus allows for an alternative circuit to be utilised during network contingency in the event of a failure [Brown 2009]. A series of circuit breakers will operate to isolate the faulty circuit and redirect the electricity from an adjacent circuit to maintain the network reliability. During a contingency event, the adjacent circuit is

back-feeding the load from the faulty circuit on top of its base load. Therefore, prior to operating the circuit breaker, network operators are required to have awareness on the available capacity of the adjacent circuit. This criteria is identified as important for network operators to support their decision making process to achieve real time system viewing and identify constraints. With increased data matrices from DR evaluation, relevant information can be tailored to the requirement of network operators and support their decision making process.

2.3.5 Attached Components

Apart from the electrical components already discussed, there are also smaller accessories that make up an electrical distribution network. This includes cable termination, cable joints, cable bushing and other contact materials. As discussed in Section 2.3.4, different contact materials will have varying maximum temperature and maximum temperature rise depending on the material and the type of dielectric used. The selection of components lies in engineering knowledge to ensure accessories with the correct current rating are installed such that it allows safe operation of the circuit involved under stress and normal operating conditions. For DR applications, the attached components are treated as a vessel and have no control on the circuits attached. Research by network operators in Great Britain represents the number of attached components with varying condition factors for its consideration in their network risk evaluation [WG DNO UK 2017]. A DR application that's employed with a risk evaluation provides an increased assurance that the network is operated safely.

2.4 ENVIRONMENTAL PARAMETERS MODELLING

The electrical components exposure to the external environmental parameters can vary due to seasonal variations, terrain and coverage. Studying the behaviour of these variations is fundamental to the application of DR to evaluate the components temperature based on the surrounding environmental conditions.

The environmental temperature fluctuates annually and daily, affected by variations in solar radiation, atmospheric conditions and wind speed, each of which can be measured using sensors

available within a weather station. Based on the heat transfer presented earlier for the different electrical components in Section 2.3, changes to the surface environmental conditions are of importance for PTX and OHL as it affects the components operating temperature. The environmental temperature has been argued to be cyclic in nature and more prominent in countries with seasonal temperature. This has led to the traditional practice of operating the electrical component at seasonal maximum continuous ratings. In an ideal scenario, near worst-case scenarios for each season are used to evaluate the component rating. Departing from the ideal, the environmental conditions per site will change over-time and the component's rating should be re-evaluated. An important aspect to highlight is that, although departing from the ideal, the likelihood of an environmental condition to occur can still be measured based on the observed occurrences to evaluate its impact to the electrical distribution network [Anders 1990, Billinton and Li 1994].

For UGC, soil thermal properties are more important as it determines the ability for the heat generated by the conductor to dissipate to the external environment. The soil's ability to draw the heat out varies for different soil types and moisture content. The interest on performing soil measurement began since mid-1940 and measurement techniques such as the thermal needle approach, have been evaluated and introduced by the Electric Power Research Institute (EPRI) in *"Soil Thermal Resistivity and Thermal Stability Measuring Equipment"* [EPRI EL-2128 1981]. The technique was recognised and adopted as a standard for soil temperature and thermal resistivity measurements in [IEEE 442 1996, ASTM D5334-14 2014]. The soil temperature measurement at the cable depth using the thermal needle approach only allows for measurement at a fixed location. The model used for soil mapping by [Mitas and Mitasova 2005] provides a technique to approximate unmonitored sites based on known environmental conditions. Detailed comparison of different interpolation techniques for spatial set of data such as Kriging and inverse distance weighted (IDW) were discussed, with the later providing better control when working with limited measurement points. Both techniques have been used for interpolating scattered data points of climatic phenomena, soil properties, ground elevations and population densities and well known in Geographic Information System (GIS) application [Mitas and Mitasova 2005]. The ability to incorporate the interpolation technique for DR application will provide network operators information on the environmental conditions at unmonitored site to

identify the optimal electrical components required to meet the demand. Most DR applications have been found lacking this ability as the emphasis has been on installing monitoring equipment [Adapa and Douglass 2005].

2.5 DYNAMIC RATING APPLICATION GLOBALLY

As network operators move towards a smarter grid with improved monitoring and awareness of network operating conditions, the amount of additional technology required to implement DR is reduced. Depending on the environmental and component conditions, DR applications vary and may not apply to all the components available on the network. The next subsections provide examples of projects carried out in different parts of the world relating to DR applications for varying environmental and operational conditions. The list of projects does not cover all the DR applications globally but is provided to highlight the requirement of DR in a globally challenging era where disruptive innovation exist and optimisation is the key to yield benefits from existing investment.

(a) **United Kingdom (U.K.)**

In the U.K., £500 million was made available by Office of Gas and Electricity Markets (OFGEM) through the Low Carbon Networks (LCN) fund from 2010 to 2014 to support utilities in the testing and trialling of smart grid technologies and solutions. The funds are applied towards projects that assist network operators in understanding the provision of security of supply subject to value for money as the UK moves towards a low carbon economy. Examples of applications relating to DR in the U.K. are found in the work undertaken by UK Power Networks and Scottish Hydro Electric Power Distribution (SHEPD)[Michiorri *et al.* 2011].

UK Power Networks, London, maintain electricity cables and lines across the South East and East of England ensuring continuity of supply. They are one of the recipients of the LCN fund with £28 million allocated towards research in the area of demand side response, distributed generation, impact of electrical heating and transport load and the use of technology and tools towards improving network planning and operation. As part of the research they investigated the use of an Active Network Management (ANM) platform that

monitors critical grid locations, performs a specified action based on monitored conditions and controls electricity flow to maximise the use of the grid for demand response. SHEPD, Scotland, investigates the ANM deployment with a DR system to achieve real time rating of their overhead line circuits located at a constraint location on its network. Based on the studies carried out by SHEPD, with DR systems their average circuit curtailment was estimated to reduce by 48% which allows a connection of an additional 4 megawatts of additional generation units onto their existing infrastructure without having major network reinforcement.

(b) **United States of America (U.S.)**

In the U.S., under the Smart Grid investment Grant (SGIG) program, over $500 million of grants in government-sponsored projects have been applied towards electric distribution smart grid investment, covering 13% of the total SGIG projects. The project includes investment in devices, equipment and software to enable smart grid functions for various electrical components. An example of a DR application in the U.S. is the work undertaken by CenterPoint Energy [Castillo *et al.* 2012].

CenterPoint Energy, Texas has distribution substations that deliver power to about 5 million customers. The steady load growth and load demand experienced at each distribution transformer have lead them to introducing a transformer monitoring system using an automation controller in 2012. The solution implemented is based on the thermal model presented in "IEEE Guide for Loading Minirel-Oil-Immersed Transformers and Step-Voltage Regulators", [IEEE C57.91 2012] to monitor critical substation transformers assets. The solution allows CenterPoint Energy to detect abnormalities in the transformer loading capability and to then selectively schedule maintenance as required. The application is expected to enable condition based maintenance and avoid unexpected outages due to abnormal operating conditions.

(c) **Asia**

In Asia, there have been several advances in DR applications to improve monitoring of underground cables' temperature and circuit loading. The increased number of high rise structures and increasing load demand in large cities are likely to define research requirements for underground cables, as utilities work towards optimising the use of their existing infrastructure. An example of a DR application in Asia is the work undertaken by SP

PowerGrid Ltd. (SP PowerGrid) [Li 2005].

SP PowerGrid in Singapore make use of distributed temperature sensing (DTS) equipment to monitor the surrounding temperature of the underground cable to then predict the cable rating. The DTS equipment uses fibre optic cables that are laid along the length of the underground cables to determine the surrounding temperature. An advanced thermal model was developed based on the cable standard, *"Electric cables - Calculation of the current rating"*, IEC 60287 [IEC TC 20 2006] to estimate the cable surrounding soil thermal parameters. The application allows SP PowerGrid to improve their rating selection under normal loading and emergency loading conditions.

(d) **Europe**

Under the work carried out by the European Commission Joint Research Centre (JRC), over €3 billion of investments have been made from 2002 to 2014 towards smart grid projects, with a significant increase in investment by EDBs during the 2011 to 2013 period. Smart grid applications are categorised into seven different categories with smart network management covering €850 million (26%) of the total budget as shown in Figure 2.10. The smart network management category considers implementations focusing on increasing the operational flexibility of the electricity grid with a goal to improve the observability and controllability of the networks. These include dynamic rating, real-time asset monitoring, grid monitoring and other tools that observe and control the behaviour of the network. An example of a DR application in Europe is the work undertaken by N.V Nuon Energy (Nuon) [Nuijten *et al.* 2005].

Nuon, Netherlands implemented a pilot DR system on their existing 150kV overhead lines and underground cables in 2005. In identifying the thermal limit along underground circuit, an extensive soil survey was carried out to identify and rank the bottlenecks. The most limiting section on the cable's capacity is then used as the main DR indicator for the underground section. The limiting section for overhead lines is determined by identifying line clearances that restrict the line loading. Based on Nuon's experiences their DR system provides grid controllers with a quick-scan of present and possible future loadings. Under emergency situation, the network operators are also able to identify possible outage and failure scenarios.

(e) **New Zealand**

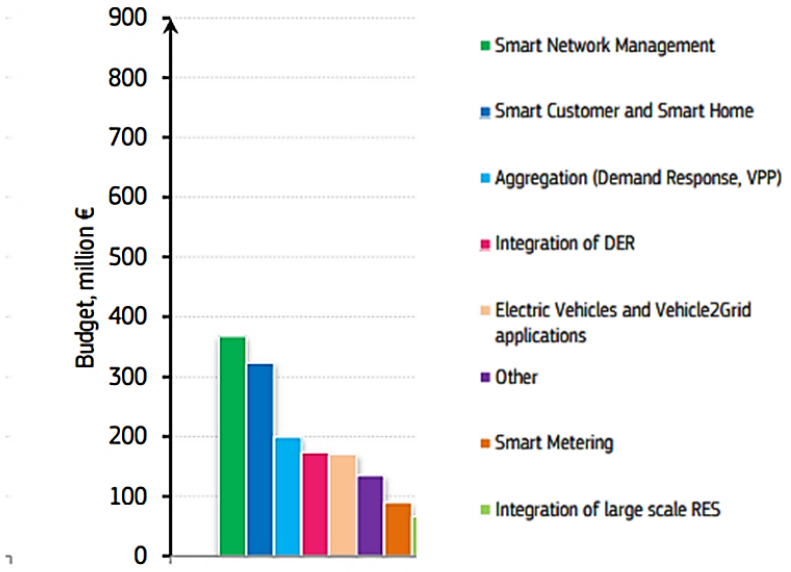

Figure 2.10 Investment per smart grid application category in Europe (reprinted from [European Commission JRC 2014])

Some of the work on DR in New Zealand has been carried out before smart grid was coined. Early adoption of DR has been found on the transmission network and used to distribute long stretch of OHL from generation sites located in rural region to a more populated area. Maximising the capacity utilisation of existing network is favourable to justify the initial investment. Uncertainty in demand and cost-benefit of an investment however increases the challenges of making a justified investment. DR has been used to provide improved awareness of the network capacity utilisation and greater control of asset capability. Increased applications of DR can be seen and are not limited to OHL. An example of such advancement in New Zealand is the different work undertaken by Transpower New Zealand on their OHL and UGC. [Raniga and Rayudu 2000, Chand and Brown 2017]

In 1996, Transpower New Zealand trialled the implementation of DR on two of their 220kV OHL. Several tension monitoring devices were used to evaluate the line clearance and the OHL rating. Each device was able to measure the conductor tension up to 50 towers away which provides a good justification for application on a transmission network. Based on the implementation, it was found the capacity gain on their OHL can be up to 2 times more than the static rating for 20% of the time. The work has enabled them to have

real time system viewing and identifying constraint determination when operating the DR on-demand [Raniga and Rayudu 2000].

For practicality reasons, such as urban areas where line clearance issues exist and areas where vehicle access is limited, the use of OHL is less favourable, and the use of UGC can be justified. Since the cost of an UGC installation is normally higher than that of an OHL, it is important for network operators to understand the condition, performance and utilisation of the installed UGC to maximise its useful life. Detailed modelling of the cable construction, temperature measurement and graphical user interface are some of the aspects that ensure DR end-user have confidence and visibility of the UGC performance [Chand and Brown 2017].

2.6 DISCUSSION

In a regulated electricity market such as New Zealand where revenue is capped, each capital investment on the network has to be justified and prioritised to ensure a reliable supply of electricity whilst keeping the cost down for the consumers. Network operators face a number of challenges in ensuring a reliable power supply to its customers. As presented in Section 2.2, this includes challenges such as planning a network with varying load demand. Over-investment can results in stranded or under utilised assets and under-investment can result in a capacity shortage during high demand. To maintain a reliable supply of electricity, capacity shortage on a circuit would require network operators to investigate and provide a solid justification on network reinforcement, due to limited funds available. Infrastructure that has deteriorated and showing poor reliability would also need to be managed and plans set-up to distribute the cost of maintenance and replacement to maintain a healthy operational cost.

The planning of an EDN focuses on designing a network that allows each of the electrical components to be utilised in synergy to meet the load demand. The configuration and utilisation of the circuit on a distribution network determines its reliability. One of the keys to maintaining network reliability is to obtain as much information on the system as fast as possible, to quickly relieve the network constraint. Through DR's ability to provide real time system viewing, the potential to back-feed a circuit is readily known from increased knowledge of the network's

operating conditions [Adapa and Douglass 2005]. The work by [Schell *et al.* 2012] initially identified a capacity constraints when integrating two distributed generation system onto their existing infrastructure. However, with the visibility of their DR implementation, an improved knowledge of the circuit capacity was available, with an increase of potential capacity of up to 50%, thus delaying the investment needed to increase the circuit capacity. Most utilities have the ability to determine alternative circuits during network contingency through load flow analysis based on static rating (SR) values. These rating however may not represent the true available capacity at the time of operation which limits the selection of alternative circuits. Through DR the load flow analysis is able to account for the actual available capacity on the circuit when restoring the network.

EDN are exposed to varying environmental and operational events that influence the electrical component's operating temperature. Under extreme weather conditions the possibility of the components to be thermally overloaded are likely, leading to outages due to thermal stresses. The time it takes for electrical components to reach its maximum operating temperature varies with the load applied. A higher temperature limit for a fixed time frame was found possible to a lightly loaded components without excessively reducing the useful life of the components [AS/NZS TC EL-008 2013b]. Through DR, the component operating temperatures are calculated over time to provide insight into fault and constraints determination. The improved knowledge of the asset utilisation allows load transfer to be performed more effectively as discovered by [Adapa and Douglass 2005] thus improving their power system reliability.

The implementation of DR to optimise the network utilisation in EDN varies for different network configuration and system requirements but relies on the availability of data such as the circuit loading and environmental conditions to evaluate the electrical components operating conditions due to heating and cooling. An interface would also be required to send, capture and process the data to perform evaluation and gain insight [Raniga and Rayudu 2000]. With increased number of components and environmental conditions being monitored in the field, network operators are facing challenges and looking at better ways to convert the increasing amount of field data into information that can be used for decision making. These have led to different approaches of DR implementation to be investigated to suit the needs of different EDNs. An embedded hardware implementation for DR has been seen to provide an active control system at the substation relay

which processes the operational and environmental data on-site to evaluate the optimisation opportunities of the network [Michiorri 2010]. The research uses a combination of international standard and factors from its national standard in United Kingdom to calculate the component's rating. As installation configurations vary and not all are presented in the standard, there is room for improvement to easily up-scale a DR application. The components available on a network dictate the effort required for a DR application to a wider network. Depending on the majority of the components available on the network, the selected DR application can be focussed on a single component type, such as the DR development work carried out for just OHL [Ausen *et al.* 2006]. The approach involves a replica of the overhead conductor installed in parallel to the actual conductor. A controller that is attached to the replica conductor is used to evaluate the rating of the actual conductor without having a direct attachment to it. The approach allows modelling of the actual component without having an outage to install the required hardware. The approach however will not justify the required cost to install the replica to monitor multiple span, a tension monitoring equipment would be better justified [Raniga and Rayudu 2000]. As the hardware only models OHL, the DR development work does not apply for PTX and UGC.

The research on DR focuses on the evaluation of electrical components actual rating capability for varying operating conditions. Research on OHL is the most studied due to its exposure to varying operating conditions and seen as having the most variable potential capacity [Raniga and Rayudu 2000]. The work on UGC also sees a lot of interest and models developed to simulate its surrounding thermal parameters during operation due to limited direct access to perform thermal measurements along the UGC. A distributed temperature sensing (DTS) monitoring system has been used to measure the temperature along the UGC using fibre optic cables. The thermal parameters of the soil along the UGC can then be estimated using the measured temperature values [Li 2005]. The study on PTX focuses on not only its loading capability but also its condition assessment due to the high cost of the component. Through DR, an abnormality during operation found on the transformer thermal loading and condition assessment allows selective scheduled maintenance to avoid prolonged exposure to abnormal operating conditions [Nuijten *et al.* 2005].

Increased monitoring of component operating and environmental conditions has allowed network

operators to make use of the available data to support decision making. The application of DR enables grid intelligence on an EDN and provides information for decision making. DR has been presented to allow operational rules to be established from real time system viewing, identifying fault and constraints and allows selective network reinforcement. Initial DR applications only sees researchers focusing on one part of the problem at a time. This leads to a lack of holistic view on the integration with other parts of the network involved and was highlighted as an issue for DR implementation [Castillo *et al.* 2012]. Over time, more components are being considered for DR application which provides improved control of the network, utilising different part of the network to improve system reliability [Nuijten *et al.* 2005, Michiorri *et al.* 2011]. Different models are seen applied to evaluate the thermal rating of various components and can vary either through a simplified approach based on empirical tables to present the de-rating and up-rating factor, or detailed modelling based on heat transfer, solving it analytically or a finer approximation using numerical analysis such as the finite-element method.

Existing DR applications available in literature are seen to focus mainly on pre-existing installed components and also lacks an evaluation of the DR application impact across different part of the business, either network planning, operation or asset management where decisions are required. The identified gap is a comprehensive decision support tool that allows network operators to evaluates the capacity utilisation across the installed and planned electrical components depending on varying operational scenarios and provides a measurable criteria. This research investigates different ways the developed tool are used in decision making process for EDN. This research proposes to introduce a tool to score and evaluate different electrical components based on its rating, constraints and loss-of-life during operation to benefit network operation, planning and asset management.

2.7 SUMMARY AND CONCLUSIONS

This chapter has introduced the basic concepts, data structure and asset parameters that are relevant to determine the assets' capacity utilisation. Research on evaluation of capacity utilisation based on thermal ratings for different asset classes has shown capacity gain and improved reliability management on electrical distribution networks. Thermal rating evaluation based on

hardware installations provides confidence in the thermal rating calculations. The approaches however were described as more costly and only caters for specific network configurations which limits a wider network application. The use of computational tools and interpolation of known data points were discussed and found to provide a better alternative for a wider network implementation. A novel solution has been proposed to quantify the asset capacity utilisation and provides criteria for network operators, planning and asset management to perform management decisions. The detailed modelling and implementation of the tool on a distribution network is further discussed in Chapter 3 and Chapter 4 of this thesis.

Chapter 3

SYSTEM DEVELOPMENT: MODELLING

3.1 OVERVIEW

In this chapter, the development of the predictive asset rating (PAR) system model is presented. The model has been developed at Unison Networks Limited (UNL), New Zealand, as part of this research. This chapter introduces the modelling techniques considered for inclusion into the PAR system, covering the modelling of electrical components, environmental conditions, and evaluation criteria. The chapter finishes with a discussion on the comparison of the different rating evaluation models and criteria used for management decision.

3.2 MODELLING OF ELECTRICAL COMPONENTS

Distribution networks consist of components that are connected together to make up a power delivery system. These components are exposed to varying environmental conditions during operation. Based upon standard practice, the component utilisation is determined by its ability to remain operational without excessively degrading its condition. During operation, the heat generated by the flow of current through the component's body, increases its temperature and the surrounding environment. Because environmental conditions vary, the components are exposed to effects of cooling and heating from parameters such as high wind speed for cooling and high solar radiation for heating. The overall temperature of these components can be approximated by modelling the heat transfer that occurs between the components and the surrounding environment. The following section discusses the underlying model to determine the rating of power transformers, underground cables and overhead lines based on a heat transfer model. Relevant

standards and literature are first highlighted, followed by suggested improvement which has been developed and implemented to allow the following:

(a) *Ease of implementation*: the model are able to easily integrate with common data that network operators have.
(b) *Flexible*: the model are able to consider different operating scenario and environmental conditions.
(c) *Modular*: the model is developed as a building block which can be simulated on its own or combined.

3.2.1 Power transformers

At the distribution level, there are two main categories of transformers, liquid filled and dry type. The dry type transformers are generally used in areas with high health and safety restrictions in cases of fire risk such as mining sites and underground sub-stations. This study focuses on EDB that mainly uses liquid filled transformers from here on referred to as just a power transformers (PTX).

A PTX consists of core and windings that is immersed in a tank of mineral oil as illustrated in Figure 3.1a. The oil provides an insulation layer and keeps the heat producing elements within the transformers tank cool during operation through natural or forced convection. When the transformer operates, the temperature of the oil increases, reducing its density and specific gravity, thus rising up and circulates upwards through the inlet of the cooler and later flows through the radiator as the fluid starts to cool down and back to cooling the winding. The cooling of the oil can also be accelerated through forced cooling via the use of fans and pumps to allow improved heat transfer rate [Kulkarni and A. 2004]. The oil flow in different type of transformers is illustrated in Figure 3.1.

The different designation of cooling refers to the method used for dissipation of heat from the oil to the atmosphere. Whether the oil circulates in the tank naturally through natural process, or accelerated by force using pump or directed if the cooling oil has been directed to flow through the windings. Due to the flow of the oil the transformers will have varying temperature across its

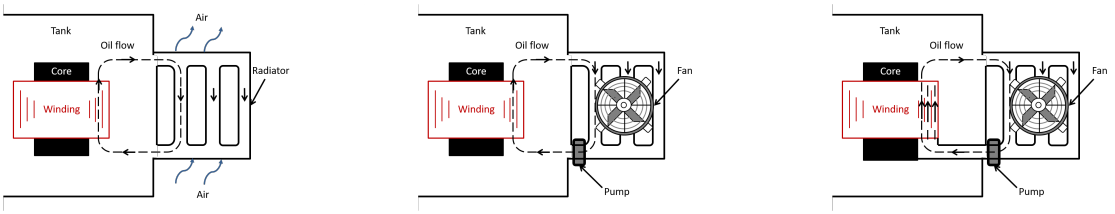

(a) Oil Natural-Air Natural (ONAN) (b) Oil Forced-Air Forced (OFAF) (c) Oil Directed-Air Forced (ODAF)

Figure 3.1 Transformer cooling types, re-illustrated based on ([Kulkarni and A. 2004])

tank. This process can be illustrated as a simplified thermal model shown in Figure 3.2b. If we assume that the transformer windings are heating the oil at a constant rate, the oil temperature will have a linear increase from the bottom of the winding to the top. When considering the hottest spot within a transformer body, θ_h, this thermal model would then approximate the spot to be at the top of the winding where the oil is at its hottest temperature. Additionally, the winding would also be experiencing heating from the stray losses leading to temperature rise across the winding.

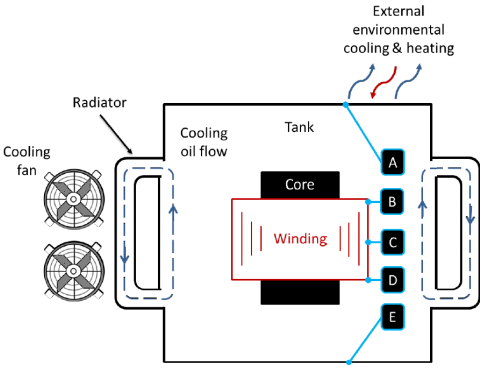

(a) Heat transfer of power transformer

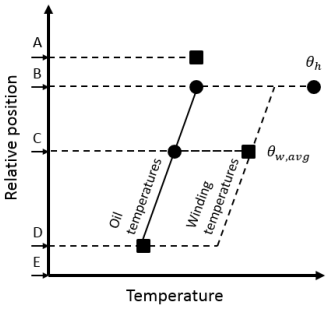

(b) Thermal model representation of power transformers, re-illustrated based on [AS/NZS TC EL-008 2013b]

Legend:	**A**	: Top-oil temperature	$\boldsymbol{\theta_h}$	: Hot-spot temperature
	B	: Oil temperature at top of winding	$\boldsymbol{\theta_{w,avg}}$	: Average winding temperature
	C	: Average oil temperature	●	: Calculated point
	D	: Oil temperature at bottom of winding	■	: Measureable point
	E	: Bottom of the tank		

Figure 3.2 Simplified relative positions and temperature gradient within transformer's tank

Depending on the type of cooling, either forced or natural, the transformers will have varying temperature rise within its tank. The thermal characteristics of different type of transformers

is determined by performing a heat-run test for a set duration and monitor the relative increase of the different parts of the transformers relative to steady-state value. An illustration for the hot-spot-to-top-oil is shown in Figure 3.3 [AS/NZS TC EL-008 2013a].

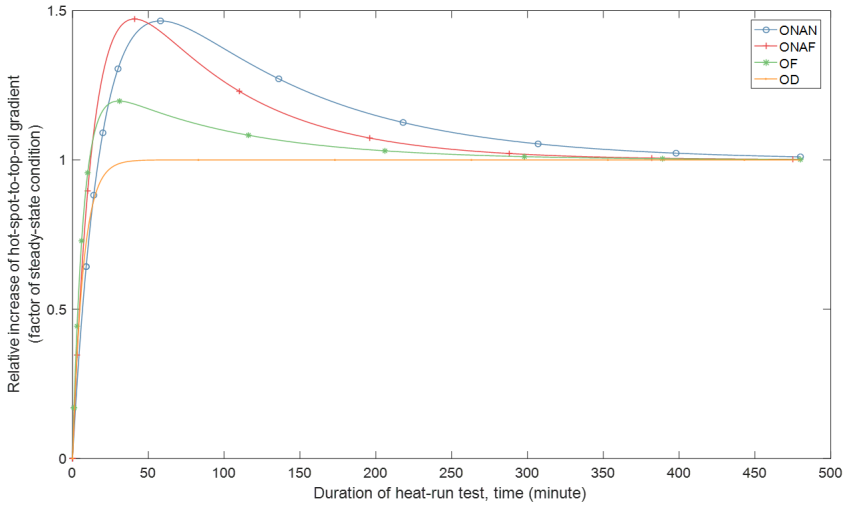

Figure 3.3 Relative increase of a temperature gradient[AS/NZS TC EL-008 2013a]

The transformer's thermal characteristics provides a measure of the transformers operating condition against different cooling and heating that it experiences. To evaluate the potential capacity utilisation of a transformer, different transformer models are explored, highlighting important findings and then providing suggested modifications and applications to allow for evaluation by an EDN.

3.2.1.1 Analysis of models for rating of power transformers

The aim in evaluating the transformer rating is to determine the hottest temperature within a transformer's tank for a given loading and cooling type such that the temperature does not lead to accelerated ageing of the transformers. This rule has been well embraced in the power transformers loading guide since 1945 by American Institute of Electrical Engineers transformer subcommittee [AIEE 1945]. The advancement in temperature monitoring technology through fibre optic sensors allows for temperature measurements within the transformer tank to be performed and has led to better understanding of power transformer thermal characteristics and advancing its thermal model. This has been well captured by the international standard *"IEEE Guide for Loading Mineral-Oil-Immersed Transformers and Step-Voltage Regulators"*,

IEEE C57.91 [IEEE C57.91 2012] and similar adaptation in IEC 60076.7 [IEC TC 14 2005] and AS/NZS 60076.7 [AS/NZS TC EL-008 2013b] to incorporate the findings to its national operating conditions. The evaluation of the thermal model in AS/NZS 60076.7 are similar in parts to [IEC TC 14 2005], referencing to its work. The two are mentioned interchangeably in this report when analysing the power transformers model.

The evaluation of temperature in °C for transformer rating calculations looks at the heat transfer experienced by a transformer and is modelled by evaluating three major thermal components given as [IEEE C57.91 2012]

$$\theta_h = \theta_a + \Delta\theta_{oil} + \Delta\theta_h \tag{3.1}$$

where, θ_a is the ambient temperature, $\Delta\theta_{oil}$ is the top oil temperature rise over ambient temperature rise and $\Delta\theta_h$ is the hot spot temperature rise over oil temperature rise. The thermal components looks at the dependencies on each part of the transformers body, from the heating of the winding, to the heating of the oil and to the cooling of the oil by air. The heat transfer process can be represented as an equivalent circuit as shown in Figure 3.4, showing source as heating, resistor as thermal resistance and capacitor as thermal capacitance. Monitoring the changes of these thermal variables over time is the key to thermal rating application. The thermal variables are dependent on the transformer cooling type as discussed later in (3.6) and (3.7).

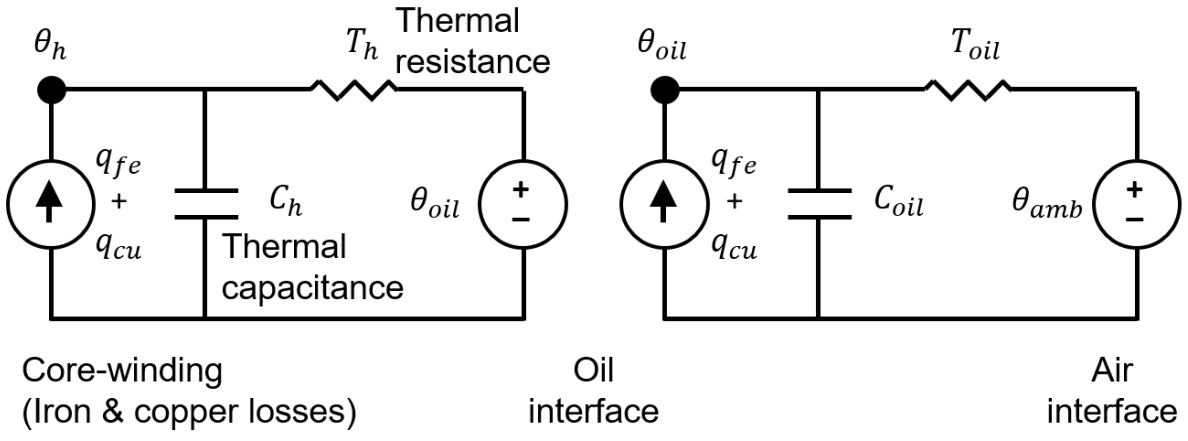

Figure 3.4 Circuit representation of transformers heat transfer, re-illustrated based on [Swift *et al.* 2001]

In exploring the time response (in minutes) of the top oil and hot spot temperature rise during transient conditions, [IEEE C57.91 2012] presented an exponential equation of the temperature rises driven by the time constant of the oil, τ_{oil} and time constant of the winding, τ_w. The temperature rise at different time step relates to the thermal constant by

$$\Delta\theta_{oil} = (\Delta\theta_{oil,r} - \Delta\theta_{oil,i}) \cdot (1 - e^{-\frac{t}{\tau_{oil}}}) + \Delta\theta_{oil,i} \tag{3.2}$$

for temperature rise of the oil, $\Delta\theta_{oil}$, and

$$\Delta\theta_h = (\Delta\theta_{h,r} - \Delta\theta_{h,i}) \cdot (1 - e^{-\frac{t}{\tau_w}}) + \Delta\theta_{h,i} \tag{3.3}$$

for temperature rise of the winding, $\Delta\theta_h$.

The temperature rise of the oil and winding relates to the ratio of the loading from initial (subscript i) to the rated load (subscript r). The relationship varies for different PTX depending on its cooling mode. The PTX thermal characteristics is obtained by performing a heat-run test as illustrated earlier in Figure 3.3. The relationship between the top-oil to a change in load is [IEEE C57.91 2012],

$$\Delta\theta_{oil,n} = \Delta\theta_{oil,r} \cdot \left[\frac{K_n^2 \cdot R + 1}{R + 1}\right]^x \tag{3.4}$$

and the relationship for the winding temperature to a change in load is

$$\Delta\theta_{h,n} = \Delta\theta_{h,r} \cdot K_n^{2y} \tag{3.5}$$

where, $\Delta\theta_{oil,n}$ and $\Delta\theta_{h,n}$ is the top-oil rise over ambient temperature and hot spot rise over top-oil temperature respectively at the time considered and the terms $\Delta\theta_{oil,r}$ and $\Delta\theta_{h,r}$ is the parameters at rated load. The term R is the rated load and K_n is the ratio of load considered to the rated load. The effect of change in resistance due to the changes in load is accounted by the transformers oil exponent, x, whilst the winding exponent, y account for the effect of change in

resistance and oil viscosity [IEEE C57.91 2012]. The exponent values for various cooling mode are shown in Table 3.1.

The oil in a transformer acts as a coolant to remove the heat from the windings. The oil temperature rises as it comes into contact with the transformer's winding and becomes cooler at the bottom of the winding as the oil circulates in the tank and radiator. Depending on the transformers cooling mode (either natural or forced oil flow), the thermal capacity of the oil varies. For natural cooling of the oil, the empirical formula of its thermal capacity, C (Ws/K) is [AS/NZS TC EL-008 2013b]

$$\begin{aligned} C = {} & 0.132 \cdot (\text{mass of core and coil assembly in kilograms}) \\ & + 0.0882 \cdot (\text{mass of the tank and fittings in kilograms}) \\ & + 0.4 \cdot (\text{mass of the oil in kilograms}) \end{aligned} \tag{3.6}$$

whereas forced cooling of the oil would allow a higher thermal capacity of the oil given as

$$\begin{aligned} C = {} & 0.132 \cdot (\text{mass of core and coil assembly in kilograms}) \\ & + 0.132 \cdot (\text{mass of the tank and fittings in kilograms}) \\ & + 0.58 \cdot (\text{mass of the oil in kilograms}) \end{aligned} \tag{3.7}$$

This leads to a varying oil time constant, τ_{oil} in minutes at the rated load, which is a function of thermal capacity, C, average oil temperature rise above ambient at rated load, $\Delta\theta_{oil,r}$ and losses at rated load, P_r evaluated as [AS/NZS TC EL-008 2013b]

$$\tau_{oil} = \frac{C \cdot \Delta\theta_{oil,r} \cdot 60}{P_r}. \tag{3.8}$$

The hot spot temperature rise is associated with the heating from the transformer's winding. The winding time constant depends on the mass and thermal capacity of the winding evaluated as [AS/NZS TC EL-008 2013b]

$$\tau_w = \frac{m_w \cdot C \cdot g}{60 \cdot P_w} \tag{3.9}$$

where, τ_w is the winding time constant in minutes at rated load, m_w is the mass of the winding in kg, C is the specific heat capacity of the conductor material, g is the difference between the winding and oil temperature at rated load and P_w is the winding loss in Watts. As illustrated in Figure 3.4, the thermal resistance and capacitance both affects the hot-spot temperature in a transformer.

The heat-run test carried out by transformer's manufacturers allows EDN to make use of the thermal characteristic obtained for steady state condition. As the core size and fittings varies for different transformer manufacturer, the best accuracy is achieved by obtaining test results. This is of course not always practical as some transformers have been installed prior to the availability of fibre optic sensors installation within the transformers windings. Based on standard design specification and conservative heat-run test results, the use of transformer thermal characteristics listed in Table 3.1 [IEC TC 14 2005] has been adopted.

Table 3.1 Recommended thermal characteristics for exponential equations [AS/NZS TC EL-008 2013b]

Constant parameters	Transformer cooling mode			
	ONAN[1]	ONAF[1]	OF[1]	OD[1]
Oil exponent, x	0.8	0.8	1.0	1.0
Winding exponent, y	1.3	1.3	1.3	2.0
Constant, k_{11}	0.5	0.5	1.0	1.0
Constant, k_{21}	3.0	2.0	1.3	1.0
Constant, k_{22}	2.0	2.0	1.0	1.0
Time constant, τ_{oil}	150	150	90	90
Time constant, τ_{wl}	7	7	7	7

[1]**Note:**
ONAN - Oil Natural Air Natural
ONAF - Oil Natural Air Forced
OF - Oil Forced
OD - Oil Directed

For dynamic rating applications, changes of loading and environmental conditions are monitored over time. Evaluating the hot-spot temperature based on the heat transfer equation in (3.1) for a changing input by solving the exponential equation in (3.2) and (3.3) for each time step allows the evaluation of the transformer rating. The exponential equation however, does not allow

flexibility in considering additional heating and cooling finding its implementation to be limited for a step-change in load. To allow better approximation of the temperature with respect to the load changes and external environmental conditions, the evaluation of (3.1) based on the difference equation is considered [AS/NZS TC EL-008 2013b]. The algorithm involves evaluating the output sample, θ, at time, n based on the past input samples, $(n-1)^{th}$, the present input samples, n^{th} and the past output samples $\theta(n-1)^{th}$ for each of the evaluation in the time domain, t. The evaluation of an output based on the difference equation from here on are denoted with a letter D. Based on difference equation, the hot-spot temperature from (3.1) is then given by [AS/NZS TC EL-008 2013b]

$$\Delta\theta_{h(n)} = [\theta_{o(n-1)} + D\theta_{o(n)}] + [\Delta\theta_{h1(n)} - \Delta\theta_{h2(n)}] \tag{3.10}$$

where,

$$D\theta_o = \frac{Dt}{k_{11} \cdot \tau_o} \cdot \left[\left(\frac{1 + K^2 \cdot R}{1 + R} \right)^x \cdot (\Delta\theta_{or}) - (\theta_o - \theta_a) \right]. \tag{3.11}$$

The term $\Delta\theta_{h1(n)}$ and $\Delta\theta_{h2(n)}$ in (3.10) relates to the hot-spot temperature rise before and after the effect of changing oil flow as it passes the hot-spot. Based on [AS/NZS TC EL-008 2013b] this effect can be modeled as

$$D\Delta\theta_{h1(n)} = \frac{Dt}{k_{22} \cdot \tau_w} \cdot \left[k_{21} \cdot \Delta\theta_{hr} K^y - \Delta\theta_{h1(n)} \right] \tag{3.12}$$

and

$$D\Delta\theta_{h2(n)} = \frac{Dt}{\left(\frac{1}{k_{22}} \right) \cdot \tau_o} \cdot \left[(k_{21} - 1) \cdot \Delta\theta_{hr} K^y - \Delta\theta_{h2(n)} \right] \tag{3.13}$$

The terms were defined in previous equations. The two hot-spots are considered separately when evaluating the rating of transformers to take into account of the fact that the oil flow moves at a slower rate as it moves away from the winding and starts cooling down. Different approach to

rating evaluation of transformers has been presented in Chapter 2. The difference equation from (3.10) has been adopted in the PAR system. To allow flexibility in evaluating different type of transformers, equations (3.11), (3.12) and (3.13) have been integrated with the transformer's thermal characteristic presented in Table 3.1. The transformer's operation state, such as fan information and tap location, has also been incorporated to switch between the different thermal constants.

3.2.2 Underground power cables

An underground power cable consist of a metallic conductor at its core and constructed together with additional protective layers to maintain continuous operation whilst buried underground. Some typical cable configurations are shown in Figure 3.5.

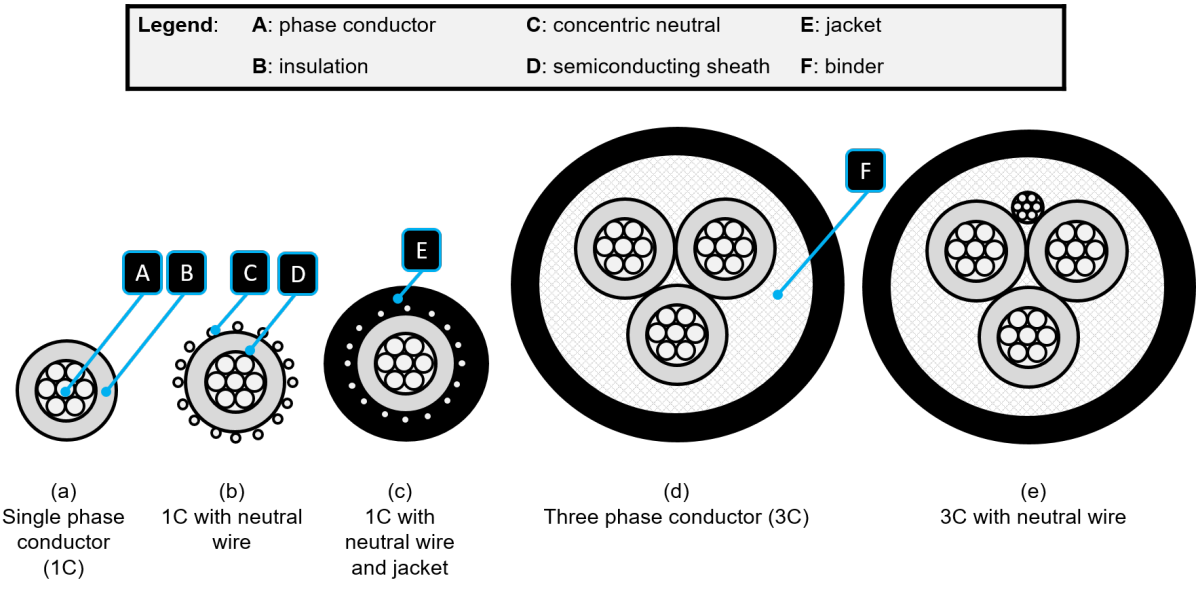

Figure 3.5 Typical cable cross sections (re-illustrated based on [Willis 2004])

The simplest cable configuration consists of a one phase conductor with an insulation material as illustrated in Figure 3.5(a). To provide a return path for fault current, a neutral wire is used which can be embedded onto the cable configuration as illustrated in Figure 3.5(b) instead of using a separate neutral wire. Newer cables are often configured with an outer jacket to provide additional protective layer to minimise water ingress and corrosion of the neutral wire as illustrated in Figure 3.5(c). Using three single-phase cables, a three-phase circuit can be

achieved. Alternatively, a single cable with three fully-insulated phase conductors can be used as illustrated in Figure 3.5(d) and Figure 3.5(e). The later consist of a neutral wire to avoid the need of having a separate neutral wire.

3.2.2.1 Analysis of models for rating of underground cables

In 1932, an article entitled *"Calculation of the Electrical Problems of Underground Cables"* by [Simmons 1932] was recognised by the industry as a guideline on the subject of underground cable rating at the time. In an effort to further improve the calculations and to accurately model cables that are laid in ducts, Neher and McGrath published a paper, *"Temperature and Load Capability of Cable Systems"* extending the work of Simmons to evaluate for varying cable construction [Neher and McGrath 1957]. Their paper highlights the rating procedures and presents a study on the effects of the loading cycle and the temperature rise of the conductor for different cable construction. Since then, the work has been internationally accepted by EDBs leading to the standardisation of rating procedures in the 1980s by the IEC electric cable technical committee, TC 20, in IEC 60287 for maximum continuous rating [IEC TC 20 2006] and in IEC 60853 for transient and cyclic studies [IEC TC 20 1985].

The aim in evaluating the cable current rating is to determine the conductor temperature for a given current loading or, conversely, to determine the tolerable load current for a given conductor temperature. The procedure involves evaluating current-dependent heat producing elements and voltage-dependent heat losses from insulation. The rating for an underground cables is calculated by modelling the rate at which the heat is transferred through each layer of the cable's cross section, from the conductor to its external environment. Based on Joules first law, as an electric current flows through a conductor, the amount of heat being generated is proportional to the square of the current multiplied by the electrical resistance of the conductor such that,

$$W_c \propto I^2 \cdot R \cdot t \tag{3.14}$$

where, W_c is the amount of heat (W/m) generated by the conductor, I is the electric current (amps) flowing through the conductor, R is the electrical resistance (Ω/m) of the conductor and

t is the duration of the load. Cables are also composed of an insulation made of a dielectric material which behaves as a capacitor to reduce the effect of electromagnetic interference. As the field dissipates through the insulation, the electric charges that flows through the insulation at a lower voltage level are negligible. However at a higher voltage level and as the cable ages or becomes damaged, the charges are able to flow through more freely causing additional heating. The heating associated with the dielectric loss, W_d (W/m), can be evaluated as [IEC TC 20 2006],

$$W_d = \omega \cdot C \cdot U_0^2 \cdot \tan \delta \tag{3.15}$$

where, ω is the system frequency in radians per second, C is the capacitance (F/m) of the insulating material, U_0 is the system voltage to earth and $\tan \delta$ is the loss factor of the insulation at system frequency. The conductor temperature (θ_c) rise above ambient temperature (θ_a), $\Delta\theta_{UGC}$ can then be considered to be composed of two components. The temperature rise due to the thermal losses in the cable, $\Delta\theta_c$ and the temperature rise due to dielectric loss, $\Delta\theta_d$, given by the following relationship [Neher and McGrath 1957],

$$\Delta\theta_{UGC} = \theta_c - \theta_a = \Delta\theta_c + \Delta\theta_d \tag{3.16}$$

The heat generated by a single conductor is distributed radially to the external environment. The rate of heat dissipation (W/m) through each layer is dependent on the thermal resistance (°.C.m/W) of the layers. The temperature rise in the cable can then be expressed as the combination of all the heat transfer at each layer as a factor of the heat generated giving

$$\Delta\theta_c = W_c \cdot \sum_{n=1}^{N} \lambda_{cn} \cdot T_n \tag{3.17}$$

and

$$\Delta\theta_d = W_d \cdot \sum_{n=1}^{N} \lambda_{dn} \cdot T_n \tag{3.18}$$

where, W_c and W_d are the heat losses in one conductor, N is the number of layers from the conductor to the external environment, λ_{cn} is the ratio of the losses at successive layer to the total losses of the conductor in the cable, λ_{dn} is the ratio of the losses at successive layer to the total losses of the insulation in the cable. An illustration of the layers as an equivalent circuit where the heat losses are presented as a source and thermal resistance, T_n, as an impedance is shown in Figure 3.6

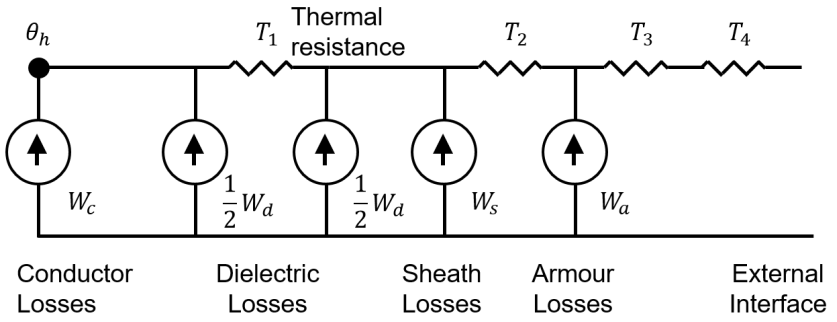

Figure 3.6 Thermal model circuit representation for an underground cable

Through the equivalent circuit, it can be seen that each layer within an underground cables will have a direct influence onto the final hot-spot temperature, θ_h. Evaluating these losses over time would allow a thermal rating application to be achieved at varying time-steps. Rearranging equation (3.14), (3.15), (3.16) and (3.17) to evaluate the current, I leads to

$$I = \left[\frac{\Delta\theta_{UGC} - \Delta\theta_d}{R_{ac} \cdot \sum_{n=1}^{N} \lambda_{cn} \cdot T_n} \right]^{0.5} \tag{3.19}$$

where, R_{ac} is the alternating current resistance per unit length (Ω/m) of the conductor at the maximum operating temperature. Solving (3.16) analytically allows the evaluation of temperature for a given loading whilst (3.19) leads to the evaluation of current for a given conductor temperature. The equation is evaluated to determine the temperature, $\Delta\theta_{UGC}$ that allows the hottest spot across the cables to remain below the operating temperature limit as to not accelerate the degradation of the insulation material.

Cables are surrounded by external environmental conditions which affect their operating condition, denoted by T_4. Monitoring and accurately evaluating the impact of external environmental conditions onto the cables allows a study of its rating utilisation looking at the cable's heat trans-

fer to the external environment, Q (W/m). For the heat transfer problem shown in Figure 3.7, the Kennelly formula has been used by [Neher and McGrath 1957] to evaluate the temperature distribution to a point, $P(x, y)$ by assuming the temperature rise across the Earth's surface being zero and is uniform. This was proven true by [Bauer and Nease 1957] by taking multiple measurements along a cylindrical heating elements buried at varying depth. Doing so then leads to the assumption that a heat source, $+Q$, will have an image of it with a heat sink, $-Q$, giving the temperature rise at point, ΔT_p as,

$$\Delta\theta_p = \frac{Q \cdot T_{earth}}{2\pi} \ln\left(\frac{d'_{earth}}{d_{earth}}\right) \tag{3.20}$$

where, Q is the heat source, T_{earth} is the thermal resistivity of the earth, L is the depth to the centre of the heat source and d_{earth} is the distance to the heat source which is in contact with the earth.

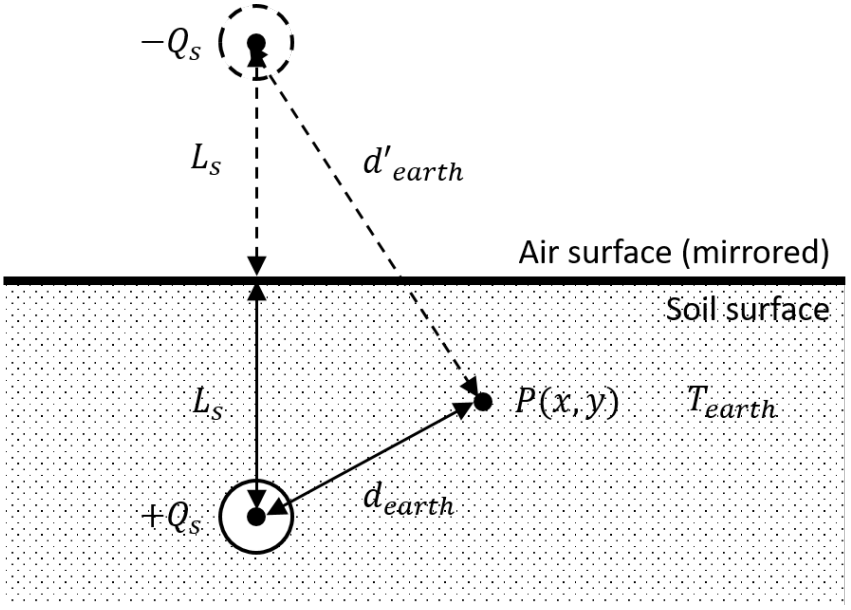

Figure 3.7 Heat distribution based on solution of image

This procedure, however, leads to reduced accuracy due to the approximation of T_{earth} in a complex construction that has multiple circuits and changing thermal resistivity layers of the earth. It also considers the heat transfer from the centre of the cable to its external layer to be uniform. An alternative model to improve the approximation has been suggested by using a finite element method (FEM) in *"Electric cables -– Calculation of the current rating — Finite*

element method", IEC TR 62095, [IEC TC 20 2003]. For an underground construction with a surface temperature $\theta(x, y, t)$ changing over time, t that has underground cables buried in a spatial location at depth, y (meter) and positioned horizontally at x (m), the temperature distribution within the cable laying can be evaluated as a solid with a heat conduction equation, given as [IEC TC 20 2003]

$$\frac{1}{\alpha}\frac{\delta\theta}{\delta t} = \frac{\delta^2\theta}{\delta x^2} + \frac{\delta^2\theta}{\delta y^2} + W_{gen,n} \cdot T_n \tag{3.21}$$

where, $W_{gen,n}$ is the heat generation from the cable n, T_n is the effective thermal resistivity of the immediate material and α is the thermal diffusivity of the medium. The solution of the partial differential equation (PDE) (3.21) evaluating for temperature, θ represents the temperature distribution within a cable laying. Numerical approximation techniques such as the finite difference method (FDM) and FEM can be used to solve the PDE. However, due to the limitation of FDM in approximating a curved surface [IEC TC 20 2003], the method is not considered for modelling the underground cables. The FEM approach involves transforming the heat equation into a system of equations containing a set of carefully chosen elements to solve the PDE by assigning a selection of points called nodes onto the surface with an assumed temperature values, $\theta_{1\rightarrow n}$. Then, refining the nodes into smaller domains known as elements will lead to several element that covers the surface. The illustration in Figure 3.4 shows an example of approximating a two-dimensional surface (x, y) as a triangular plane with temperature, θ in the z-axis.

This leads to the approximation of the curved surface as a linear combination of the element function to evaluate the approximation of the temperature distribution, $\theta(x, y)$. A comparison between the analytical method presented in equation (3.16) [IEC TC 20 2003] and FEM by [Baazzim *et al.* 2014] found that the analytical method by IEC over-estimates the ampacity of the cables when comparing for different ambient temperature, cable depth and thermal resistivity. The comparison for varying depth is shown in Figure 3.9 which shows over-estimates in the IEC method at shallower depth. The author invites the reader to view the reference for the remaining comparison.

The rating evaluation based on (3.19) are found to be narrowly confined to calculation of a rating

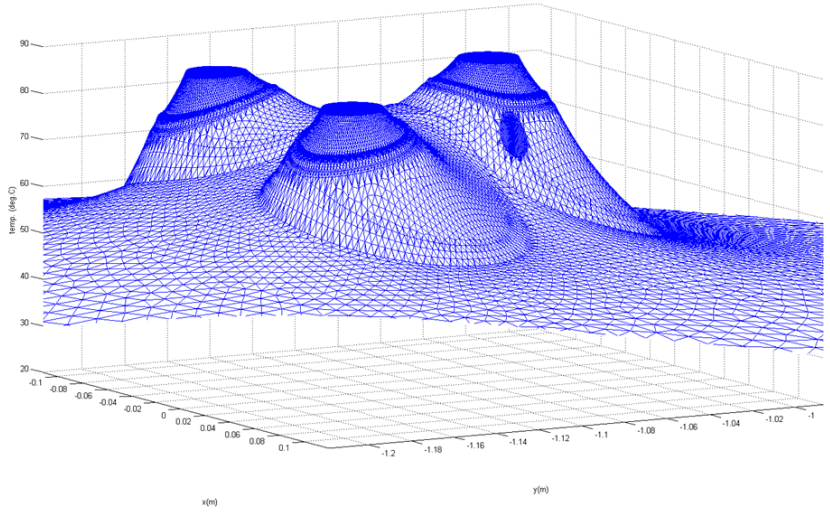

Figure 3.8 Modelling of a two-dimensional scalar function using triangular elements

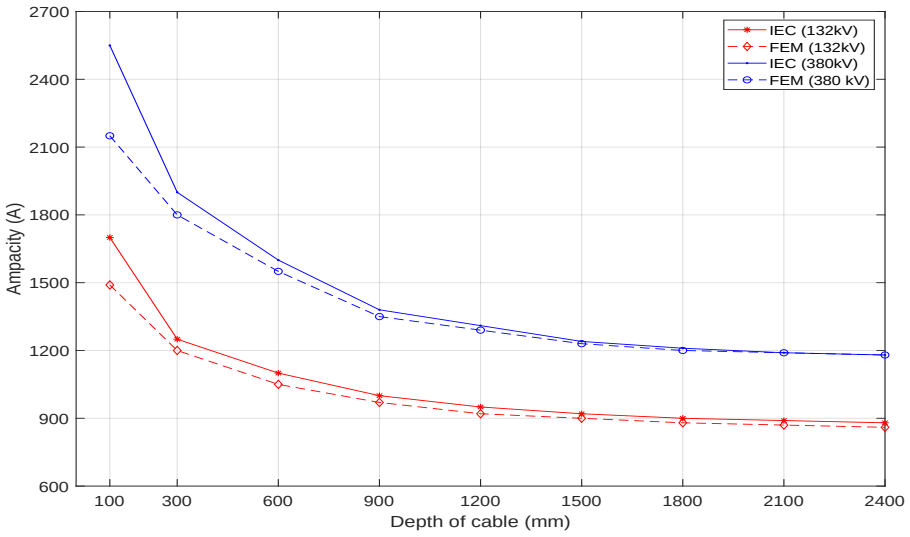

Figure 3.9 Comparison of IEC and FEM ampacity calculation at varying depth, re-illustrated based on [Baazzim *et al.* 2014]

given a temperature constraint. They are less useful when installations deviate significantly from those covered (such as the presence of heterogeneous soil layers or when one wishes to calculate a temperature other than that of the conductor) making the model based on FEM more favourable for rating and temperature evaluation across the cable layers.

For a cable construction with a temperature distribution defined as (3.21) having a cross sectional region, Ω, with boundary, $\delta\Omega$, the solution condition based on Dirichtlet boundary value problem

(BVP) can be defined as

$$\begin{cases} \frac{\delta^2\theta}{\delta x^2} + \frac{\delta^2\theta}{\delta y^2} = \frac{1}{\alpha}\frac{\delta\theta}{\delta t} + W_{gen} \cdot T, & \text{in } \Omega \\ \theta = \theta_B, & \text{on } \delta\Omega \end{cases} \tag{3.22}$$

The boundary relates to the fact that an arbitrary cross section will be considered (eg. a 5m x 10m region), the temperature outside the region is considered as having the same temperature as the boundary. The temperature $\theta = \theta(x, y, t)$ at each point x, y and time, t can be obtained by solving (3.21) based on the BVP, such as the work presented in IEC TR 62095 [IEC TC 20 2003] using FEM to evaluate the region, given as,

$$\frac{\delta\chi}{\delta\Theta} = \sum_{e=1}^{E} \frac{\delta\chi_e}{\delta\Theta_n} = H\Theta + Q_c\frac{\delta\Theta}{\delta t} - K = 0 \tag{3.23}$$

where, χ_e is the function that describes the temperature distribution within an area of interest, Θ_n is the FEM nodal values and E is the number of elements. The third equality represent the temperature distribution as matrix where, H is the heat conductivity matrix, Q_c the heat capacity matrix and K is a vector which expresses the distribution of heat sources and heat sinks over the region of interest. To evaluate the temperature distribution based on FEM on a continuous basis, the matrices, the nodal values and its derivatives have to be re-evaluated based on the change of heating and environmental conditions as presented in equation (3.21). As the number of elements can be significantly large (eg. a 200,000 x 200,000 matrix used to discretise a 5m x 10m region as shown in Figure 3.8), the evaluation for each element is very time consuming. To improve this step for thermal rating application, the following factorisation of equation (3.23) is proposed:

Substituting H with L, where,

$$\begin{aligned} L = (&A \cdot ConductivityIdentity \cdot A' + \\ &B \cdot ConductivityIdentity \cdot B'). \end{aligned} \tag{3.24}$$

Substituting Q with M, where,

$$M = (C \cdot DensitySpecHeatIdentity \cdot C' + \\ diag(C \cdot DensitySpecHeatIdentity \cdot C')). \tag{3.25}$$

and, substituting K with Q, where,

$$Q_j = \sum_{i=1}^{n} \frac{q_i Area_i}{3} \tag{3.26}$$

and

$$ConductivityIdentity_{ij} = \begin{cases} \frac{1}{T_i}, i = j \\ 0, i \neq j \end{cases} \tag{3.27}$$

$$DensitySpecHeatIdentity_{ij} = \begin{cases} \rho_i \cdot c_i, i = j \\ 0, i \neq j \end{cases} \tag{3.28}$$

The factorisation in (3.24) and (3.25) represent the matrices in (3.23) as products of matrices that themselves relate to the mesh structure and thermal properties within the cross section. Where, matrix A, B and C is the partial derivative of the triangulation in x, y and unit height respectively. This way, when an environmental condition value changes, a new mesh does not have to be generated to consider the new environmental conditions.

3.2.3 Overhead power lines

Overhead lines can be categorised into two-types, bare conductors and insulated conductors. The lines are made up of several strands of conductors. A higher tensile strength conductor can be used as reinforcement as illustrated in Figure 3.10 to reduce the amount of the line sag during operation. For an insulated overhead line, the insulation layer will be visible at the outmost layer.

An insulated overhead line is modelled as a cable in air taking into account the solar radiation

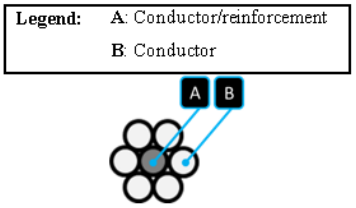

Figure 3.10 Cross-section of bare overhead line conductor

and wind speed to evaluate its rating. The model of an insulated cable has been described earlier in section 3.2.2 and described as having thermal resistive layers that slows down the heat transfer rate. Bare conductors on the other hand have an improved heat transfer capability as the generated heat from the conductor is able to easily escape to the external environment. These conductors are strung from one pole to the next whilst transmitting electrical energy. Being out in the open, overhead equipment is more exposed to weather and requires additional consideration to public safety during its operation. Common types of distribution pole configuration are shown in Figure 3.11.

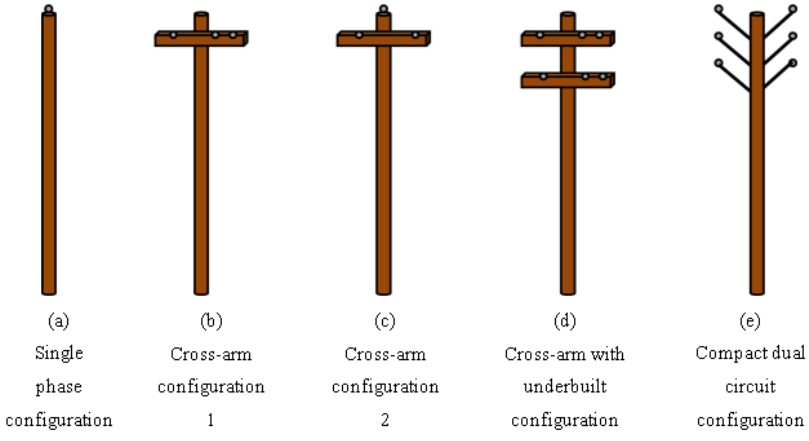

Figure 3.11 Common types of distribution pole configuration (re-illustrated based on [Brown 2009])

Due to additional concerns to public safety, the rating of overhead is evaluated not only based on a thermal model, but also looking at the mechanical model for different conductor type and pole configurations.

3.2.3.1 Analysis of models for rating of overhead lines

The rating of overhead power lines has been well studied. Its application for dynamic line rating (DLR) has also been well utilised in primary transmission and more recently for secondary transmission and distribution. The model used in the design and rating of an overhead line are categorised based on its, structure: studying the mass of the pole and conductor; electrical design: modelling of the conductor temperature and the available clearance of a live line to an underlying object; and based on its mechanical design: modelling of the stress applied to the conductor to ensure it is able to remain in operation. An illustration of the overhead line measurement is shown in Figure 3.12.

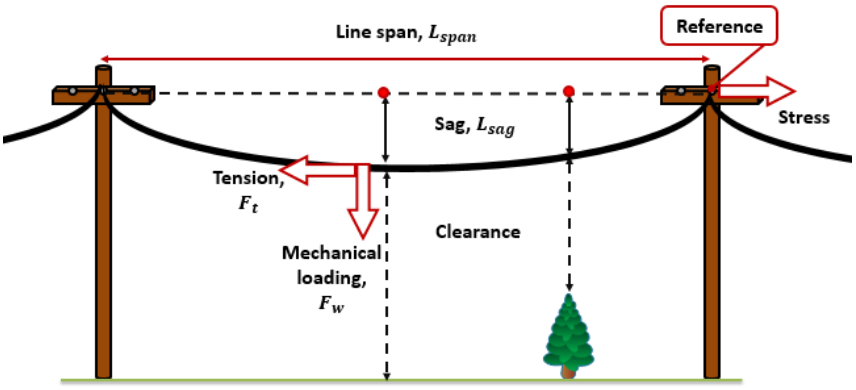

Figure 3.12 Illustration of overhead line measurement

To ensure public safety, the sag of an overhead line should be minimised and must meet regulatory requirements. The mechanical loading and tension of the line are analysed to evaluate the line sag. Based on the catenary shape of the sag, the work by [Wadhwa 2012] modelled the sag as a hyperbolic cosine function and looking at the normalised force (kN), $F_{t,h}/F_w$ acting on a point along the span that contributes to the sag elevation, given as

$$L_{sag} = \frac{F_{t,h}}{F_w} \cdot \left(\cosh \left(\frac{L_{span}}{F_{t,h}/F_w} \right) - 1 \right) \tag{3.29}$$

where, L_{sag} (m) is the elevation from a reference point, L_{span} is the distance along the line from reference point, $F_{t,h}$ (kN) is the horizontal tension component of the conductor and F_w is the total mechanical loading of the line. (3.29) is further approximated by [CIGRE WG

B2.12 2002] based on the Maclaurin series expansion of $\cosh(x)$ reducing the sag model to a parabolic function given as

$$L_{sag} \cong \frac{L_{span}^2}{2 \cdot F_{t,h}/F_w} \tag{3.30}$$

The approximation is valid for general span length such that the inequalities of $(L_{span}^2 \cdot F_w^2)/(12 \cdot F_{t,h}^2) \ll 1$ satisfies [CIGRE WG B2.12 2002].

The mechanical loading, F_w of an overhead line is distributed along the span. The total mechanical loading is determined by evaluating the vector sum of the load along the horizontal and vertical direction, given as

$$F_w = \sqrt{F_{w,h}^2 + F_{w,v}^2} \tag{3.31}$$

The vertical loading, $F_{w,v}$ consists of the conductor weight per unit length and in some cases the weight of snow and ice are also considered [AS/NZS 7000 2016] and is evaluated as,

$$F_{w,v} = g \cdot (m + \rho_{ice} \cdot \pi \cdot r \cdot (d + r)) \tag{3.32}$$

where, g is the gravitational acceleration (m/s^2), m is the conductor mass (kg/m), ρ_{ice} is the density (kg/m^3) of the snow/ice, r is radial snow/ice thickness (m) and d is the overall conductor diameter (m) that is exposed to wind. The horizontal loading, $F_{w,h}$ are modelled based on the wind pressure (Pa,) P acting on the line, given as [AS/NZS 7000 2016]

$$F_{w,h} = P\,(d + 2 \cdot r) \tag{3.33}$$

The tension of a line, F_t is influenced by the temperature of the conductor, θ, vertical and horizontal loading of the line and the age of the conductor. The relationship between the tension and stress of an overhead is modelled by looking at the stress at a known reference condition and the desired condition. A method to model the relationship is by having a controlling tension

that produces the longest unstressed conductor, such that [AS/NZS 7000 2016],

$$S_0 = \frac{S}{1 + \frac{F_{t,h}}{E \cdot A} + x_{lexp} \cdot \theta + \varepsilon} \tag{3.34}$$

where, S_0 is the unstressed conductor length (m) at 0 $^\circ C$, ε is the creep strain (mm/km), a measure of permanent elongation of the cable as it experiences everyday tension whilst strung, E is the elasticity (MPa) of the conductor and x_{lexp} is the coefficient for linear expansion of the conductor. The stressed conductor length, S, of a span length, L_r, based on the parabolic function given in (3.30) is [AS/NZS 7000 2016]

$$S = L_r + \frac{L_r^3}{24 \cdot C^2} \tag{3.35}$$

For changing loading conditions the unstressed conductor length is evaluated by looking at the initial (subscript i) and desired (subscript f) condition and given as [AS/NZS 7000 2016]

$$1 + \frac{F_{t,hi}}{E \cdot A} + x_{lexp} \cdot \theta_i + \varepsilon_i = S_0 = \frac{S_f}{1 + \frac{F_{t,hf}}{E \cdot A} + x_{lexp} \cdot \theta_f + \varepsilon_f} \tag{3.36}$$

The terms are as defined in (3.33). For a homogeneous conductor, the horizontal tension, $F_{t,h}$ is simply $F_{t,h} = \sigma \cdot A$. By introducing additional reinforcement material with improved tensile strength, the horizontal tension are increased. A higher tension constraints leads to a reduced sag elevation during operation which ultimately allows higher circuit loading for the same weight. The conductivity, tensile strength and loading weight of common types of overhead line are shown in Table 3.2.

For an overhead line conductor that has electric current flowing through it, the amount of heat loss it generates is modelled as Joule's first law, the square of the current multiplied by the electrical resistance of the conductor as given in (3.14). Being out in the open, the conductor also experiences additional heating and cooling, to and from the environment through convection and radiation. The phenomena is modelled as a heat transfer across the overhead line given as

Table 3.2 Mechanical and electrical properties of common types of overhead line (reprinted from [Brown 2009]

Type	Conductor description	Conductivity (%)	Strength (%)	Weight (%)
CU	Stranded copper	100	100	100
AAC	All aluminium conductor	64	39	30
AAAC	All aluminium alloy conductor	55	75	30
ACSR	Aluminium conductor steel reinforced	64-65	55-111	31-35
ACAR	Aluminium conductor alloy reinforced	71-73	55-63	36-37
ACSS	Aluminium conductor steel supported	66-67	50-98	39-51

[CIGRE WG B2.12 2002]

$$m \cdot c_p \cdot \frac{d\theta}{dt} = W_{generation} + Q_{sun} - Q_{radiation} - Q_{convection} \tag{3.37}$$

where, θ is the conductor temperature, m is the mass of the conductor and c_p is the specific heat capacity of the conductor. The term on the right hand side represents at the heat transfer experienced by the conductor, evaluating: the heat generation per unit length due to active power losses (W/m), W_{gen}; the solar energy heat absorbed per unit length (W/m), Q_{sun}; the emitted radiative heat per unit length (W/m), Q_{rad}; and the heat removed from the surface by convection per unit length (W/m), Q_{conv}. Several approach have been suggested in literature to evaluate the heat gain and losses across the overhead lines [IEEE 738 2013, CIGRE WG B2.12 2002]. For this study, the heat gain and losses based on [CIGRE WG B2.12 2002] were found to be sufficient and the parameters required to evaluate the heat transfer equation are readily available. Substituting the heat gain and losses model from [CIGRE WG B2.12 2002] into (3.37) gives

$$\begin{aligned} m \cdot c_p \cdot \frac{d\theta}{dt} =& k_j \cdot I^2 \cdot R_{dc} \left[1 + \alpha \left(\theta - 20\right)\right] + \\ & \alpha_s \cdot S \cdot D - \\ & \pi \cdot D \cdot \varepsilon \cdot \sigma_B \left[(\theta_s + 273)^4 - (\theta_a + 273)^4\right] - \\ & \pi \cdot \lambda_f \left(\theta_s + \theta_a\right) \cdot Nu \end{aligned} \tag{3.38}$$

where, Q_{sun} is evaluated from the absorptivity of conductor surface, α_s, solar radiation, S

(W/m^2) and outer conductor diameter, D (m). In Q_{rad} and Q_{conv}, θ_s is the conductor surface temperature (°C) and θ_a is the ambient air temperature. ε is the emissivity and varies from 0.23 for new conductors to 0.95 for weathered conductors. Nu is the Nusselt number given by $Nu = B_1(Re)^n$ for forced convective cooling and $Nu = A_2(Gr.Pr)^{m_2}$ for natural convective cooling. σ_B is the Stefen-Boltzmann constant. The constants are listed in Table 3.3. R_f is the conductor surface roughness given by $R_f = d/[2.(D-d)]$ The equation involves constants and thermal properties of material at known temperature as listed in Table 3.3

Table 3.3 Constants for overhead line model

Constants	Description and values
Re	Stranded (all surfaces): 10^2 to $2.65{\cdot}10^3$ Stranded ($R_f <= 0.05$): $> 2.65{\cdot}10^3$ to $5{\cdot}10^4$ Stranded ($R_f > 0.05$): $> 2.65{\cdot}10^3$ to $5{\cdot}10^4$
$\mathbf{B_1}$	Stranded (all surfaces): 0.641 Stranded ($R_f <= 0.05$): 0.178 Stranded ($R_f > 0.05$): 0.048
n	Stranded (all surfaces): 0.471 Stranded ($R_f <= 0.05$): 0.633 Stranded ($R_f > 0.05$): 0.8
$\mathbf{A_2}$	Gr.Pr (10^2 to 10^4): 0.85 Gr.Pr (10^4 to 10^6): 0.48
$\mathbf{m_2}$	Gr.Pr (10^2 to 10^4): 0.188 Gr.Pr (10^4 to 10^6): 0.25

As bare conductor introduces the risk of electrocution to the public, the statutory clearances between the conductor and underlying object also need to be maintained to ensure its continuous operation. In most cases the statutory clearances limits the operation of the overhead rather than high temperature. Evaluating the conductor temperature, θ using (3.38) and calculating the amount of sag using (3.30) on a span-by-span basis allows the rating of the overhead circuits to be determined.

3.3 MODELLING OF ENVIRONMENTAL CONDITIONS

The dynamic rating calculation of network components relies on the evaluation of actual environmental parameters as opposed to critical values used for static rating. Different sets of inputs are required for different components to evaluate its rating under varying operating conditions. Favourable environmental conditions allows the components to cool faster thus allowing it to operate at an optimal condition, vice versa for unfavourable conditions.

3.3.1 Measuring environmental conditions

Ambient air temperature: Ambient air temperature is measured through the use of a thermometer. To obtain an accurate temperature reading, platinum resistance thermometers, PT100, are used in this study to monitor the ambient air temperature. A resistance thermometer measures the temperature based on the temperature-to-resistance relationship [IEC TC 65 2008].

Soil thermal properties: The soil thermal resistivity (R_{soil}) has been measured based on the thermal needle method presented in IEEE 442 [IEEE 442 1996]. The thermal needle is connected to a power and temperature logger in a pedestal at a field measurement site. A power level (q) has been set to give at least 4 °C temperature rise over one logarithmic cycle of time. Assuming the line heat source having an infinite length that dissipates heat in an infinite medium, the model used to evaluate the soil thermal resistivity is [IEEE 442 1996]

$$R_{soil} = 4\pi \frac{T_2 - T_1}{2.303 \cdot q \cdot \log\left(\frac{t_2}{t_1}\right)} \tag{3.39}$$

Where, R_{soil} is the soil thermal resistivity in °C.m/W, q is the heat dissipation per unit length in W/cm. T_1 and T_2 are the temperature in °C measured at two arbitrary times, t_1 and t_2 in minutes.

It was found that the two main soil parameters relevant to heat transfer are the soil moisture (η) and thermal diffusivity (α). The study of different soil types to the heat transfer carried out in IEC 60853 *"Calculation of the cyclic and emergency current rating of cables"* [IEC TC

20 1985] leads to the relationship of η and α given as,

$$\alpha = \frac{10^{-3}}{R_{soil} \cdot d \cdot (0.82 + 0.042 \cdot \eta)} \tag{3.40}$$

Depending on the soil monitoring application, for a measured soil moisture (η), the soil thermal resistivity (R_{soil}) can be approximated based on (3.40) and vice versa for a measured soil thermal resistivity.

3.3.2 Probability distribution model

A probability distribution represents the probability of a measureable set of data. A higher number of occurrences of a value during an experiment leads to higher probability of achieving those values. For each of the measured values, a probability distribution is determined to estimate the environmental conditions. In selecting a distribution model, the following criteria were specified:

(a) *Flexible*: selected distribution model is able to be fitted to different set data.
(b) *Accurate*: selected distribution model is able to be fitted with confidence.
(c) *Fast and simple*: selected distribution model must not involve complex integration such that it reduces the speed of calculation.

The distribution model is required to be flexible as the environmental conditions have varying probability of occurrences. A clear example is a comparison between wind speed and solar radiation, where the solar radiation is always zero when the Sun is not visible. This then filters out distribution model that have a fixed shaped such as the Gaussian and exponential distribution. These leads to three distributions, Weibull, Kumaraswamy and beta distribution which have been used in similar research to study the probability distribution in an electrical distribution network. As the speed of calculation also needs to be minimal to prevent excessive wait time for the network operator during decision making and environmental data that have values between $-\infty < x < +\infty$, the generalised beta distribution (GBD) was selected as the distribution model. A beta function $B(a, b)$ is a mathematical function defined by [Johnson *et al.* 1995]

$$B(a,b) = \int_0^1 x^{a-1}\,(1-x)^{b-1}\,dx \tag{3.41}$$

where, a and b are the shape parameters for the beta distribution. The probability density function (PDF) of a beta distribution is defined as

$$f(x|a,b), PDF = \frac{1}{B(a,b)} x^{a-1}\,(1-x)^{b-1} \tag{3.42}$$

and the cumulative distribution function (CDF) of a beta distribution is defined as

$$F(x|a,b), CDF = \frac{1}{B(a,b)} \int_0^x x^{a-1}\,(1-x)^{b-1}\,dx \tag{3.43}$$

However, as the environmental condition varies and does not always falls in the range of, $0 \leqslant x \leqslant 1$, the generalised form of the beta distribution are introduced. Through linear transformation, scaling the range, $0 \leqslant x \leqslant 1$ to a new variable, y with range $c \leqslant y \leqslant d$, where $x = (y-c)/(d-c)$, allows the generic form of the beta distribution. This transforms the PDF presented in (3.42) to [Johnson *et al.* 1995],

$$f(y|a,b,c,d), PDF = \frac{F(x|a,b)}{d-c} = \frac{1}{B(a,b)} \cdot \frac{(y-c)^{a-1} \cdot (d-y)^{b-1}}{(d-c)^{a+b-1}} \tag{3.44}$$

and the CDF is the area under the curve of a generalised beta PDF with range $c \leqslant y \leqslant d$,

$$F(y|a,b,c,d), CDF = \frac{1}{B(a,b)} \int_c^d \frac{(y-c)^{a-1} \cdot (d-y)^{b-1}}{(d-c)^{a+b-1}} dy \tag{3.45}$$

When substituting $c = 0$, and $d = 1$, the generalised beta function in (3.45) reduces to the CDF of beta distribution in (3.43). The PDF of a GBD for different shape parameters is shown in Figure 3.13.

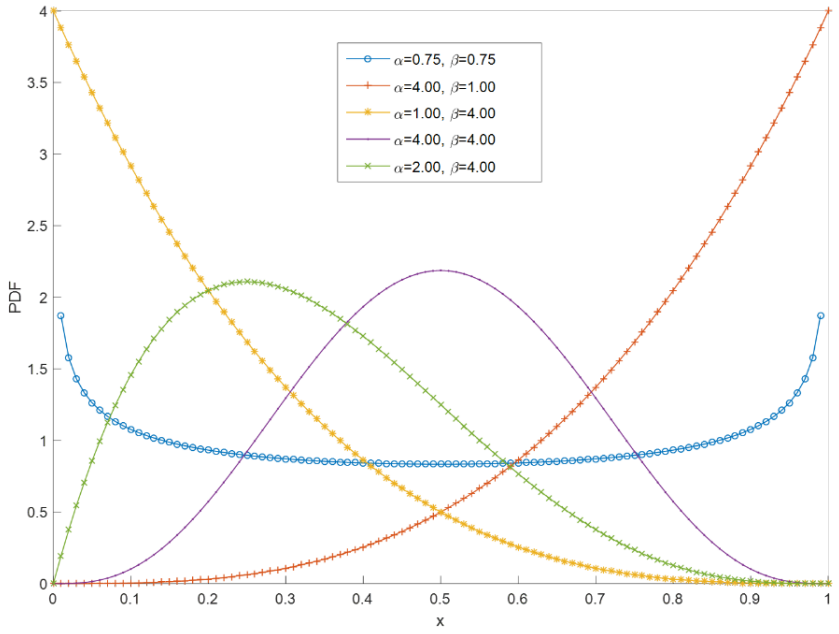

Figure 3.13 PDF of GBD with varying shape parameters

3.3.3 Approximating spatial measurements

The availability of environmental conditions data varies for different parts of the network depending on available monitoring devices. Through historical observation or approximation, the probability of achieving certain environmental conditions can be derived to cover for applications where environmental data are not available. The work on spatial interpolation has been studied extensively in geographical information systems (GIS) to capture geographical information into a database with limited amount of data points. The concept is used in this study to interpolate the environmental data at unmonitored sites. The following criteria were specified in the selection of spatial interpolation techniques:

(a) *Accurate*: selected technique is able to interpolate the environmental data with confidence despite having limited data.

(b) *Fast and simple*: selected distribution model must not involve complex calculation such that it reduces the speed of calculation.

Spatial interpolation methods can be grouped into local neighbourhood, variational and geostatistical approach [Mitas and Mitasova 2005]. As there are several methods available, only the selected method is described in detail. The local neighbourhood interpolation methods are

based on the assumption that a point in space is influenced by nearby points to a set of finite distance. Methods in this group include inverse distance weighting (IDW), natural neighbour, triangulated (TIN) and rectangle-based irregular network. The variational approach on the other hand are based on the assumption that the interpolation function should be smooth and passes through (or close to) the data points normally performed through the spline mathematical function. The geostatistical approach relates to interpolation method based on statistical analysis of the geospatial data, such as Kriging. The comparisons of the different spatial interpolation technique are shown in Figure 3.14.

Spline provides a very smooth interpolation seen in Figure 3.14(e, f) compared to local neighbourhood method seen in Figure 3.14(b, c). The spline method however, requires a large number of recorded points to be able to interpolate accurately. The interpolation based on Kriging method seen in Figure 3.14(d) also provides a very smooth slope compared to the IDW method seen in Figure 3.14(c). The Kriging method however, requires additional processing time to evaluate the spatial correlation of the measured location to the unknown points. Based on the criteria specified, the improved inverse-distance weighting method is selected to be modelled for the interpolation of environmental parameters. The technique was found to provide the best speed with an acceptable accuracy even with the lack of measurement points.

3.3.3.1 Inverse-distance weighting for interpolation of environmental parameters

The inverse distance interpolation technique allows data from irregularly-spaced monitoring station to be interpolated to a wider geographical area. The value of the environmental parameter, Z at any point in a geographical area can be estimated based on the weighted average D for known data points i and collection of data points C near Z. This is presented as [Shepard 1968]

$$Z_k = \begin{cases} \dfrac{\sum\limits_{D_i \in C} (s_i)^2 \cdot z_i}{\sum\limits_{D_i \in C} (s_i)^2} \text{ , if } d_i \neq 0 \text{ for all } D_i \\ \\ z_i \text{ , if } d_i = 0 \text{ for some } D_i \end{cases} \tag{3.46}$$

where, the weighting factor s_i is defined based on the distance of the points, d_i from Z.

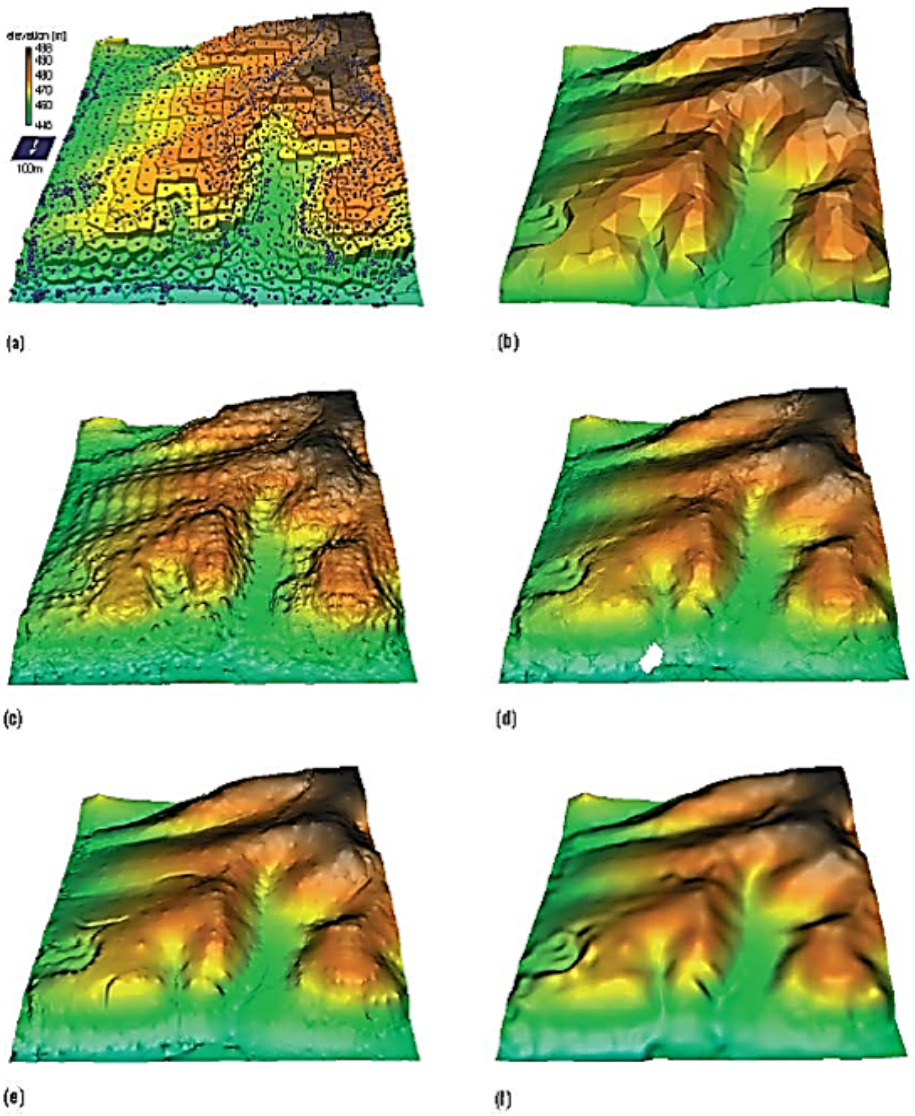

(a) given data and Voronoi polygons	(b) TIN-based linear interpolation
(c) inverse distance weighting	(d) Kriging
(e) spline with tension and stream enforcement	(f) regularised spline with tension and smoothing

Figure 3.14 Comparison of different interpolation methods (reprinted from [Mitas and Mitasova 2005])]

3.4 EVALUATION OF POWER SYSTEM RELIABILITY

An EDN, is exposed to random events that will have varying consequences to the network design, planning and operation. Outages caused by transient faults due to surroundings, third party, planned maintenance and repair work places constraints in network operation and planning. With improved grid monitoring, the goals towards a smarter load transfer to improve power system reliability can be achieved. With the optimisation of component rating through dynamic

rating, adjacent circuits with identified available capacity can be utilised to relieve the constraints on the network.

In the past, the techniques used in determining the reliability criteria of EDBs in the area of design, planning and operation are generally based on deterministic evaluation. Typical deterministic criteria are:

(a) *Design specification*: networks are operated at unity loss of life with the operating condition defined during design.
(b) *Planning network capacity*: networks are planned to have a minimum number of circuits supplying to a load group such that the group maximum demand can be covered by the circuits during outage.
(c) *Operating capacity*: networks are operated to meet the expected load demand with a reserve equal to one or more of the largest units.

The later section discusses techniques considered to evaluate the power system reliability using the developed DRS implemented on an EDN.

3.4.1 Analysis of reliability evaluation methods

EDN consist of interconnected components to provide continuous supply of electricity to its consumer. Each of the components have a reliability criteria which can be used to determine the overall reliability of the system. Several computational techniques have been developed to derive the system reliability. The selection of a reliability evaluation method for this study is decided based upon the following criteria:

(a) Ability to evaluate the impact of environmental conditions onto the system reliability.
(b) Ability to provide a range of probabilistic measure for the system capacity.
(c) Ability to aggregate the reliability of individual network components to represents the overall system reliability.

A review of different approaches to evaluate the system reliability in power system analysis are carried out involving the state-space models, logic diagram and Monte Carlo simulation. For

each method, a brief discussion are presented followed by its relevance in meeting the prescribed criteria. A more detailed discussion of each method are described by [Anders 1990].

3.4.1.1 Markov chains

In the Markov chains method, a system is described by its states and possible transitions between them. A state-space diagram can be constructed to clearly illustrate the number of transitions for each state in the system. The probabilities and frequencies of each state are evaluated to determine the system reliability indices. Consider a state-space model presented in Figure 3.15 to represent two independent electrical component in series to evaluate the capacity constraints of the system.

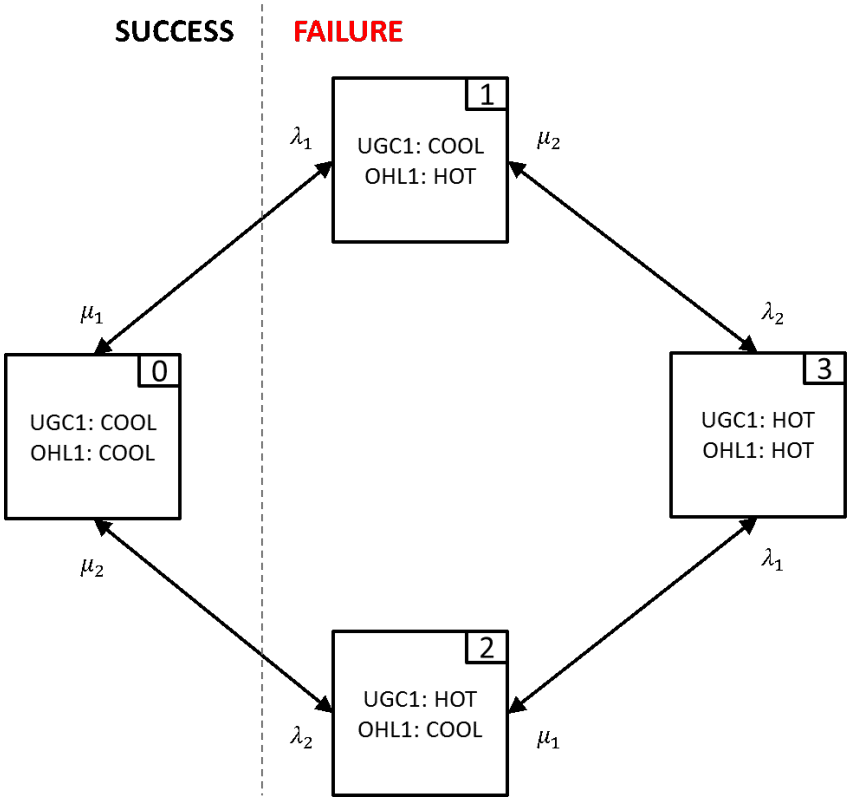

Figure 3.15 State-space diagram representing two independent electrical component in series

The transition rate from success to failure, λ_{SF} and transition from failure to success, λ_{FS} consist of several states with no overlap and can be generally written as [Anders 1990]

$$\lambda_{SF} = \frac{\sum_{i \in S} p_i \sum_{j \in F} \lambda_{ij}}{\sum_{i \in S} p_i} \quad \text{and} \quad \lambda_{FS} = \frac{\sum_{j \in F} p_j \sum_{i \in S} \lambda_{ji}}{\sum_{j \in F} p_j} \tag{3.47}$$

where, p is the probability of each state in the system, i is the combination of state transition from each state to the success state and j is the combination of state transition from each state to the failure state. For a time dependent case, in evaluating the availability of the system, a conditional probability density such that the system will fail at time X given that it has survived through time, t are evaluated as [Anders 1990]

$$\lambda_{SF}(t) = \frac{f_X(t)}{\int_t^\infty f_X(x)dx} \quad \text{and} \quad \lambda_{FS}(t) = \frac{f_Y(t)}{\int_t^\infty f_Y(x)dy} \tag{3.48}$$

where, $f_X(t)$ and $f_Y(t)$ is the probability density function (PDF) of the time the system is in operational and failure state respectively. The availability, A for the system is simply given by the probability the system being in the operating state, $p_S(t)$ where

$$A(t) = p_S(t) = 1 - p_F(t) \tag{3.49}$$

For the state-space model presented in Figure 3.15, the system is only available at state 0, thus

$$A = p_S = p_0 \tag{3.50}$$

In power system analysis, the state-space method has been used to evaluate a system where a transition can be clearly defined. The method would fit well to criteria (b) and (c) however would lead to a complex multistate system representation when evaluating the impact of environmental conditions and multiple components to the system reliability.

3.4.1.2 Enumeration

Enumeration is a logic block representation of the system describing the combinations of component failures that will results in the failure of the entire system. The combination is not necessarily the physical connections but rather the bottleneck of the system. Consider a logic diagram in Figure 3.16 arranged in series and parallel combination to illustrate a circuit with connected electrical components from a single circuit going to a double circuit configuration.

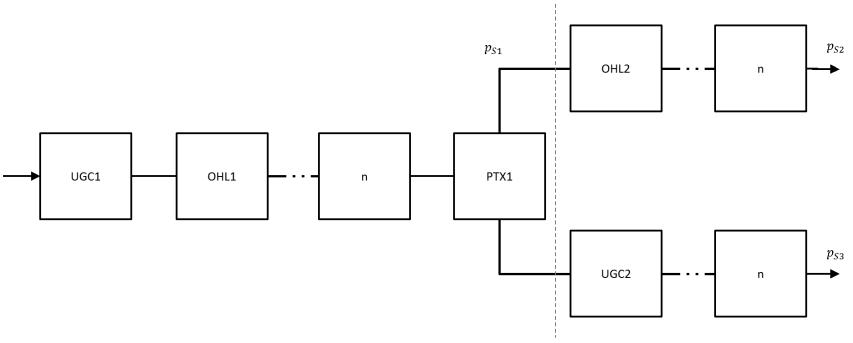

Figure 3.16 Logic diagram representation of series-parallel system

Complex systems are often simplified by evaluating the probability of sub-systems and reducing it to either a series or parallel system. The method would fit well to criteria (a) and (c) to capture impact of environmental conditions at each bottleneck and to then finally aggregate it to represents to overall system reliability.

3.4.1.3 Monte Carlo simulation

Monte Carlo simulation is a numerical simulation procedure involving substituting a set of random variables from a known (or assumed) input probability distribution to evaluate the expected result. The simulation process is repeated until an acceptable approximation of the expected result is obtained. A Monte Carlo algorithm can be represented as a for-loop as shown in Figure 3.17.

In estimating the rating, several iterations of the rating calculations are carried out to identify the probability of achieving an estimated rating value, $E[y(X)]$. Where, $X = X_1, \ldots, X_n$ is a random vector in real coordinate space, $\mathbf{R}^n$ and $y(X)$ is a function of the output model. Based

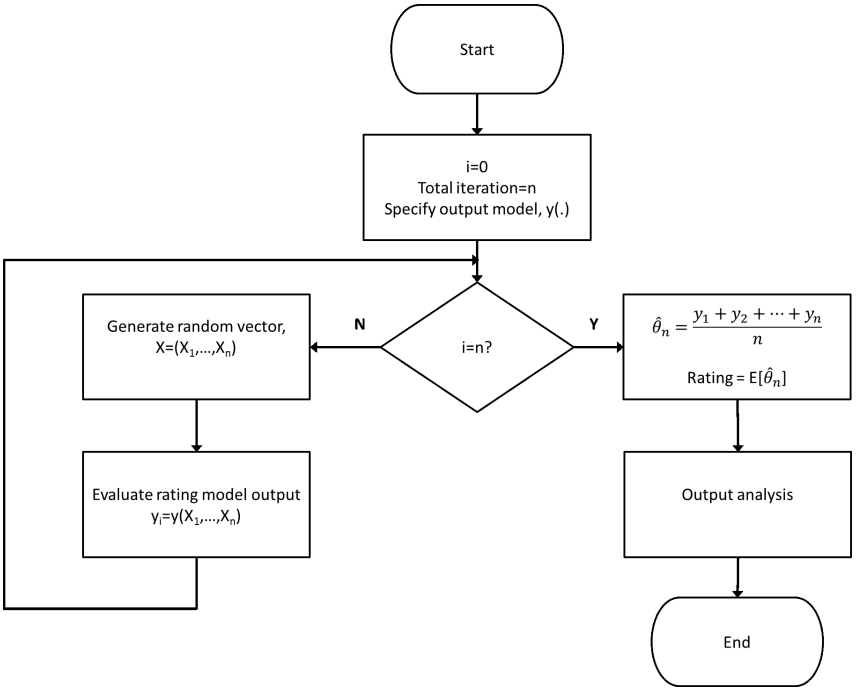

Figure 3.17 An example of Monte Carlo algorithm to estimate rating

on the Strong Law of Large Numbers, the average of the results obtained from a large number of trials converges almost surely to the expected value, θ, that is, $\hat{\theta}_n \xrightarrow{\text{a.s.}} \theta$ when $n \to \infty$.

In power system analysis, Monte Carlo simulation has been used extensively when there are uncertainties in the expected value of the input variables [Billinton and Li 1994]. The Monte Carlo simulation fits the criteria required to evaluate the reliability and security of EDN. The following section presents the model developed to provide network operators, planners and management a probabilistic evaluation of the network reliability and security.

3.5 PREDICTIVE ASSET RATING SYSTEM

The rating of a distribution circuit relies on the minimum component rating along the circuit to ensure none of the component's thermal limits are breached. Dynamic ratings based on a deterministic model have been well implemented by monitoring the environmental conditions and using the data gathered to provide a dynamic rating of the network. Due to problems such as the unavailability of data due to communication errors, uncertainties in environmental conditions and fluctuating load demand leads to challenges when planning and operating an

EDN based on dynamic rating.

Based on the rating model and reliability evaluation presented in previous sections, a new methodology presented in Figure 3.18 has been developed to provide a probabilistic measure of EDN reliability and security for distribution companies moving towards grid modernisation through dynamic rating application. The development covers dynamic rating applications for power transformers, underground cables and overhead lines.

The following explanations are based on the flow diagram seen in Figure 3.18. In step 1 to step 2, the models are initialised with the input data from monitored environmental stations and circuits from an operational historical database, if available. For unmonitored sites, the environmental parameters are approximated based on the IDW model presented in Section 3.3.3.1. In steps 3 to 8, the rating for each electrical components in the circuit is evaluated for possible events in the network based on a Monte Carlo simulation. The expected rating of the electrical components are estimated based on the thermal models and parameters presented in Section 3.2.1 for PTX, Section 3.2.2 for UGC and Section 3.2.3 for OHL. For thermal parameters that are unknown, the model adopts the manufacturer's and international standards recommendation. For each rating evaluation the circuit's capacity utilisation and its thermal values are compared to the components thermal limits and operational constraints. In steps 8 and 9, the circuit's capacity utilisation and operating limits are evaluated to provide a measure of the reliability and security of the circuit in an EDN. The measures are several set of probability criteria calculated from the simulation to cover the DR application for network operation, planning and management.

3.6 SUMMARY AND CONCLUSIONS

This chapter has presented the model development of a novel system for electrical distribution networks known as predictive asset rating. The thermal rating models for different electrical components were discussed referencing industry standards and development in literature. Further refinement has been suggested and made to those models to allow a seamless network wide application. The concept of predictive asset rating to optimise capacity utilisation were introduced and will be discussed further in Chapter 4.

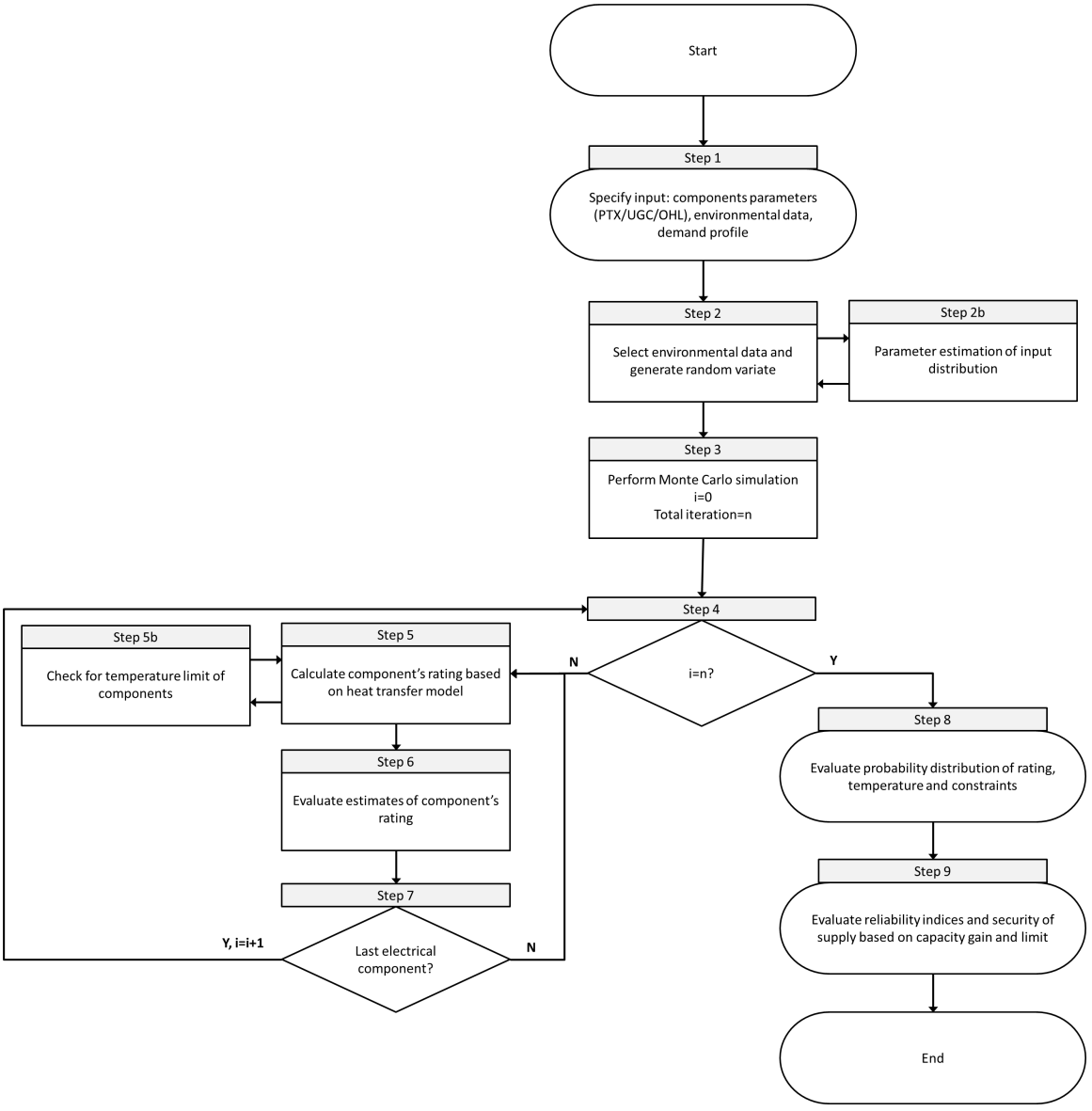

Figure 3.18 Dynamic rating application and evaluation based on probabilistic model

Chapter 4

SYSTEM DEVELOPMENT: IMPLEMENTATION AND VALIDATION

4.1 OVERVIEW

In this chapter, the implementation of the predictive asset rating (PAR) system is presented. The implementation section covers the electrical network under study, the components considered and the datasets used. This chapter provides suggestions on different ways PAR tool is used to provide an alternative methodology for decision support within electrical distribution network. The chapter then covers the validation steps taken to review and proof the model presented in Chapter 3. The validation steps include the electrical component rating model, environmental condition model and the network evaluation model. The comparison of the developed models compared to manufacturer values are then presented, covering power transformers, overhead lines and underground cables. The chapter finishes with a discussion on the application of PAR, covering its benefits for providing decision support for management decisions and challenges faced. The discussion provides information for other electrical distribution networks which are looking at implementing a similar system for their network.

4.2 IMPLEMENTATION OF PREDICTIVE ASSET RATING MODEL

The implementation of the predictive asset rating (PAR) system involves working with different work groups at Unison Networks Limited (Unison). Working with contractors for hardware installation, performing surveys and asset recording. The implementation was also made possible with the help of control room operators, the network & operations group and information

management group at Unison to utilise the different group's areas of expertise and ensure the developed solution is integrated seamlessly with existing infrastructure available at Unison. As discussed in Chapter 2, the implementation of the PAR tool has been developed to improve and provide decision support in the following areas:

(a) **Real time system viewing**: Predictive ability to evaluate the available capacity and operational event.
(b) **Fault and constraints determination**: Predictive ability to prompt potential thermal limits on the network.
(c) **Network optimisation and expansion planning**: Predictive ability to optimise the utilisation of electrical components.

4.2.1 Network model

A subset of Unison's 33kV distribution network covering power transformers (PTX), underground cables (UGC) and overhead lines (OHL) were selected to study the implementation of the developed PAR. The source of electricity from the transmission network is available from two grid exit points (GXP), labelled GXP1 and GXP2 as shown in Figure 4.1. This research focuses on the transformers which step down the voltage from the 33kV circuit to 11kV labelled as T1 and T2 (indicating transformer number 1 and 2) for each zone substation (ZS) of interest. The load flow across the circuits are controlled using circuit breakers (CB) labelled as CB1 to CB12. Based on the sectionalisation of the circuits, they are assigned a unique circuit identification (circuitID) which will be used throughout the discussion when evaluating the rating for varying network configurations using PAR.

To provide a detailed study on the application, a subset of Unison's network is studied, focusing on one region, covering 30,450 out of a possible 110,000 installation control points (ICPs) that could be used in other parts of the region. Under normal operating conditions, GXP1 provides supply to ZS1, ZS2, ZS4, ZS5 and ZS6 whilst GXP2 provides supply to ZS3. Five circuits are connected to GXP1 and seven circuits connected to GXP2 that cover other load areas which are not included in the study.

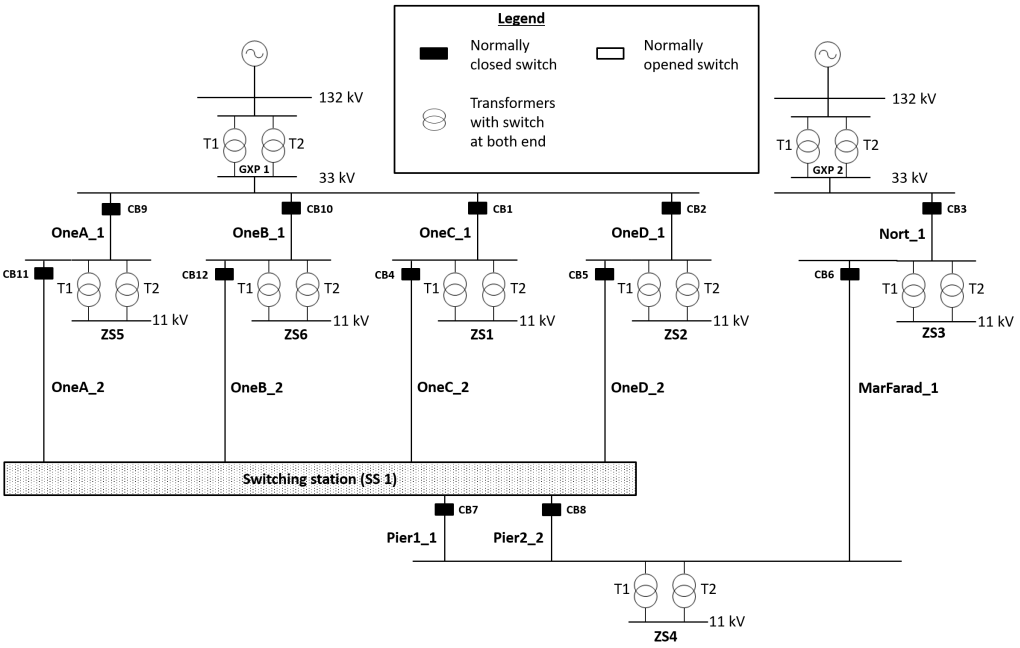

Figure 4.1 Network schematic and circuit naming

The network is configured in a loop system where two sources are available to distribute an alternative supply of electricity in the event of a failure supplying from one source. A geographical representation of the network is illustrated in Figure 4.2. The ONEs circuit is configured as a double circuit, to equally share the load for distribution. Part of the NORT circuit has been clipped-off for geographical representation, it has an overall length of 15km. The different types of PTX, UGC and OHL that have been used for this research are listed in Table 4.1. Each of the components listed will be studied to evaluate different designs and their ability to handle varying operating and network scenarios. The UGC considered are with cross-linked polyethylene (XLPE) insulation, whilst the OHL are the aluminium conductor steel reinforce (ACSR) conductor. Apart from the physical design of the asset which will affect its rating capability, the electrical components were also installed in varying environmental conditions. As part of Unison's Smart Grid initiatives, several types of environmental and asset monitoring equipment have also been installed consisting of weather stations, line tension monitors, soil thermal sensors, distributed temperature sensing equipment and on-site temperature sensors. This research will evaluate the capacity utilisation of the electrical components using PAR under varying conditions and evaluate its impact to network operations, planning and asset management.

Table 4.1 Summary of electrical component

Circuit	Component type description	Percentage of component in the circuit (%)
ONEA	Mixture of UGC and OHL: 8.8 (km)	
	Power cable (AL XLPE 630mm^2)	29
	Overhead line (ACSR Double Dingo 2C 122)	40
	Overhead line (ACSR Jaguar 222)	25
	Overhead line (ACSR Dingo 168)	6
ONEB	Mixture of UGC and OHL: 8.9 (km)	
	Power cable (AL XLPE 630mm^2)	29
	Overhead line (ACSR Double Dingo 2C 122)	40
	Overhead line (ACSR Jaguar 222)	25
	Overhead line (ACSR Dingo 168)	6
ONEC	Mixture of UGC and OHL: 13.3 (km)	
	Power cable (AL XLPE 500mm^2)	7
	Power cable (AL XLPE 630mm^2)	3
	Power cable (CU XLPE 630mm^2)	6
	Power cable (AL XLPE 800mm^2)	9
	Overhead line (ACSR Jaguar 222)	66
	Overhead line (ACSR Panther 262)	9
ONED	Mixture of UGC and OHL: 11.2 (km)	
	Power cable (AL XLPE 630mm^2)	4
	Power cable (CU XLPE 630mm^2)	7
	Power cable (AL XLPE 800mm^2)	11
	Overhead line (ACSR Jaguar 222)	67
	Overhead line (ACSR Panther 262)	11
PIER1	Fully UGC: 1.8 (km)	
	Power cable (AL XLPE 400mm^2)	100
PIER2	Fully UGC: 1.8 (km)	
	Power cable (AL XLPE 400mm^2)	100
NORT	Mixture of UGC and OHL: 9.3 (km)	
	Power cable (AL XLPE 500mm^2)	<1
	Power cable (CU XLPE 500mm^2)	13
	Power cable (AL XLPE 800mm^2)	<1
	Power cable (ACSR Jaguar 222)	7
	Overhead line (ACSR Double Dingo 2C 167)	80
MARFARAD	Fully UGC: 1.8 (km)	
	Power cable (AL XLPE 300mm^2)	100
SUBSTATIONS		
ZS1	2 x Power transformer (ONAN 7.5/ONAF 10)	-
ZS2	2 x Power transformer (ONAN 7.5/ONAF 9)	-
ZS3	2 x Power transformer (ONAN 10/ONAF 20)	-
ZS4	2 x Power transformer (ONAN 10/ONAF 20)	-
ZS5	2 x Power transformer (ONAN 10/ONAF 20)	-
ZS6	2 x Power transformer (ONAN 7.5/ONAF 12)	-

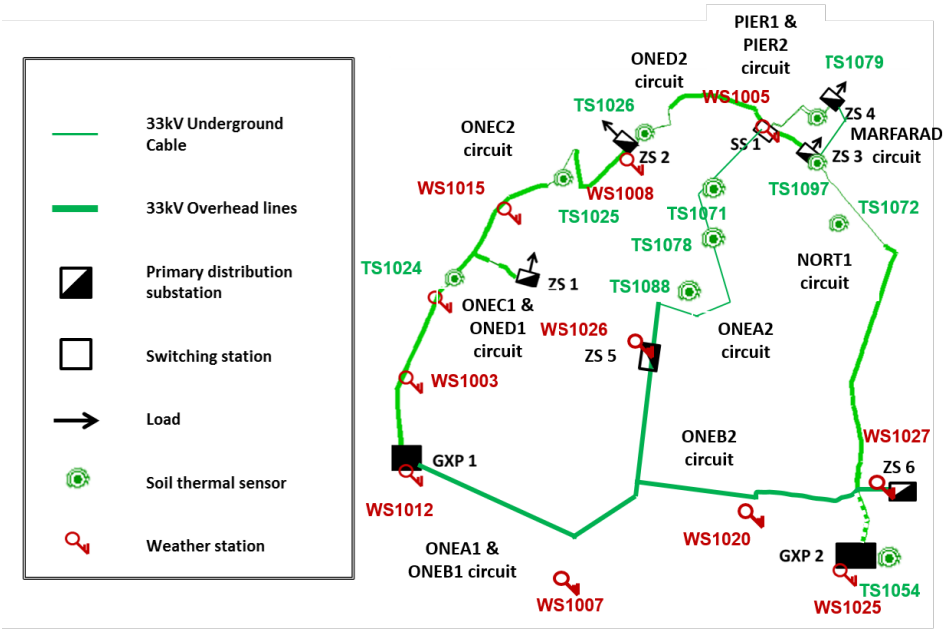

Figure 4.2 Geographical location of distribution network circuit under study

4.2.2 Datasets

The evaluation of the network using PAR is undertaken utilising a data set gathered between 2012 and 2017. The network model, illustrated in Figure 4.1, is based on the configuration in 2015 which will be the main reference for discussion. The network model configuration has been extracted from the common information model (CIM) of Unison's monthly GIS extracts. Any changes to the network can be synchronised to update the network model used for PAR evaluation. The time-series datasets are obtained from the OSIsoft PI historian system available on the Unison premise [OSIsoft 2017]. The historian system interfaces with the supervisory control and data acquisition (SCADA) system and stores time-series data retrieved from field monitoring devices to record trends and historical operational information [Schneider Electric 2017]. To discuss the datasets used by PAR, the data is categorised as follows:

(a) **Static data**: static data such as component make, type, configuration and installation.

(b) **Time-series data**: operational data such as circuit loading and environmental condition.

(c) **Financial data**: data related to cost of an equipment, network upgrade and consequences.

4.2.2.1 Static data

The static data used for this research is sourced from the manufacturer's design and technical specification available on record at Unison. The manufacturer's name plate ratings are used as the baseline for evaluation purposes. This allows a relative comparison and potential improvement or reduction in rating when evaluating the component's rating using PAR. The materials used and its thermal parameters are also captured closely to model the heat transfer across the electrical components. For components that are missing manufacturer's data, a general and calculated value based on international standards discussed in Chapter 3 and the manufacturer's website has been used. Random site audits have also been carried out to ensure the records available are true such as the name plate rating, pole structure configuration and cable cross section depth. The weather station and monitoring station location global positioning system (GPS) coordinates have also been captured. This is especially useful in the approach taken by the PAR model to perform spatial interpolation of environmental parameters at un-monitored sites.

As part of Unison's Smart Grid initiatives project they have installed several field monitoring devices to monitor the operating conditions of their electrical components. The installation of these monitoring devices was made possible by the New Technology team and Unison Contracting. This research makes use of the monitoring devices to study the effect of environmental conditions to network capacity utilisation and risk. The operational data considered includes data that are internal and external to the electrical network. Internal data here is defined as data relating to the day-to-day operation of an electrical component on the network such as the circuit loading, switch operation and network utilisation. External data, on the other hand, are defined as data that's not directly part of the electrical network but has an impact to the operation of an electrical component such as changing environmental conditions and geographical location of the network which has an impact to the overall risk in the operations of electrical components.

The internal data is obtained from the supervisory control and data acquisition (SCADA) system which continuously retrieves network loading data from the field via the communication network. The circuit loading considered for this study is illustrated in Figure 4.3 for the distribution circuit

and Figure 4.4 for the substation loading.

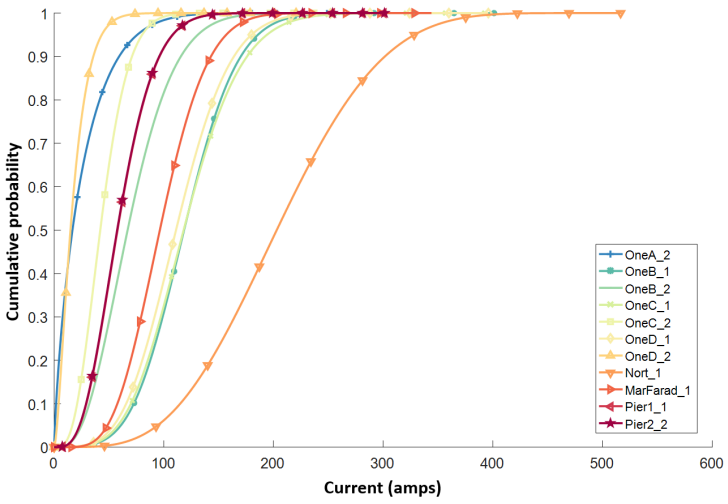

Figure 4.3 Distribution of circuit loading data

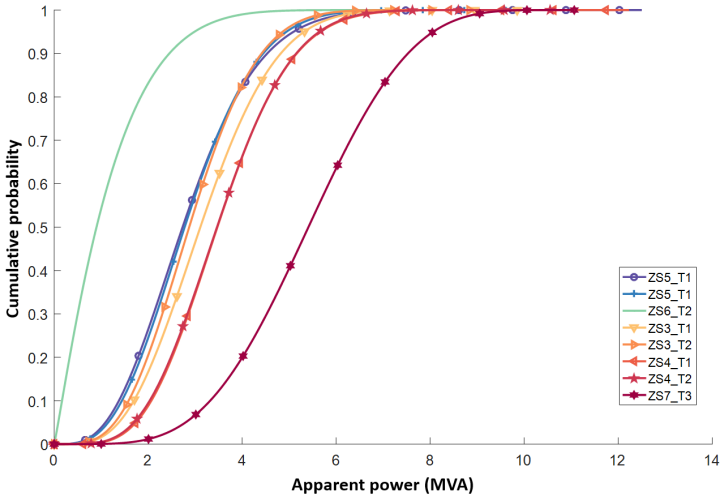

Figure 4.4 Distribution of zone substation loading data

The network loading presented consists of half-hourly data over the 5 year period from 2012 to 2017. The data used for the study is not limited to half-hourly data but shown here to provide a general comparison of the dataset over the same time interval, every 30 minutes. The different time interval of data used by PAR will be discussed further in Section 4.4 of this thesis. It can be seen from Figure 4.3 that the Nort_1 circuit is the highest loaded circuit as it is the only circuit used to distribute the supply from GXP2. For the other side of the network, exiting from GXP1,

the circuit loading is relatively similar due to the double circuit configuration which is true for OneA_1, OneB_1, OneC_1 and OneD_1 averaging at 100 amps. From this part of the network onwards the network splits to different service areas at the zone substation with varying loading as seen in Figure 4.4. The loading of the transformers on the network are generally shared 50-50 between T1 and T2 which leads to similar distribution between the two transformers at the same ZS, which can be seen clearly at ZS4. This is of course not always the case, such as ZS3, where T1 is utilised more, most of the time. Where, distribution loading on the circuit are shared 50-50, the distribution will also match, such as the distribution seen for Pier1_1 and Pier2_2 circuit. The use of PAR for network evaluation takes into account the number of circuits that are adjacent to one another to simulate likely operational scenarios. The consideration of different network loading is achieved through the loadParam data structure which captures, combines and suggests different load profiles to be used for simulation. The data structure will be discussed further in Section 4.2.3 of this thesis.

4.2.2.2 Time-series data

The external data used by PAR to evaluate the capacity utilisation of the electrical network are the environmental conditions data surrounding the electrical components on the network. The data are gathered from the field monitoring devices using different communication methods, either through a file transfer protocol (FTP) server, distributed network protocol (DNP3), wireless mobile telecommunications (3G) technology or through periodic data download. The different data transfer methods are not discussed here and are based on the installed devices standard protocols for data transfer. As highlighted in Chapter 2, weather stations are capable of providing most of the environmental parameters that will have an impact to the electrical components that are above ground. For this research, nine weather stations have been used with each site having different sensors attached to it. All the weather station sites have been fitted with an ambient temperature sensor and wind sensors. The air temperature ranges from -7 degrees Celsius (°C) to 38 °C as seen in Figure 4.5. Apart from the weather station locations shown in Figure 4.2, air temperature sensors were also available for use at all the zone substations. The distribution for these sensors are marked with 'ZS' as its prefix in Figure 4.5.

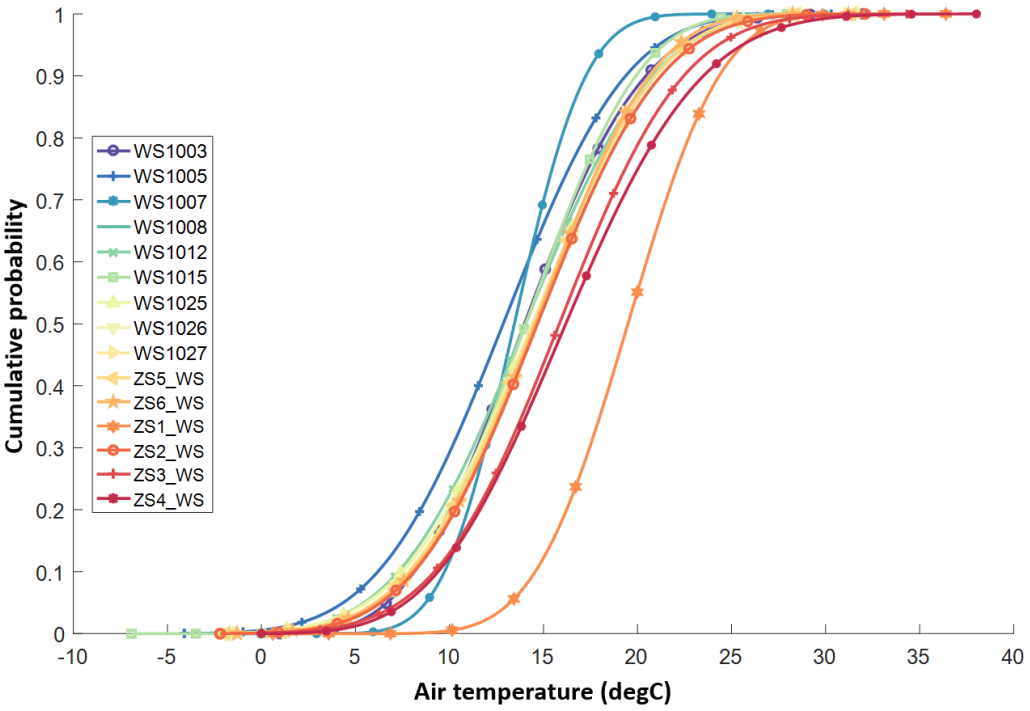

Figure 4.5 Distribution of weather station data (air temperature) from 2012 to 2017

The geographical area covered by the study is approximately 100 km^2. The air temperature between the different weather station averages to 18 °C in summer and 11 °C in winter. The maximum air temperature in summer is 38 °C and 31 °C in winter, where summer here is defined as the period between December to May and winter is the period between June to November. If the season is divided further to summer, autumn, winter and spring, taking December as the beginning of summer, the maximum air temperatures for the different seasons are 38 °C, 35 °C, 26 °C, and 31 °C, respectively from summer to winter. The months breakdown to represent the different season will be used interchangeably in this thesis to discuss ratings that are dependent on the season, from here on known as the seasonal maximum continuous rating (Season-MCR). The months used for the seasonal breakdown is arbitrary here, but will be refined by PAR when performing studies to better represent the rating values for the different time of the year.

The wind attributes captured are the wind speed and angle, its distribution shown in Figure 4.6. Some areas experience higher wind speed due to their location being at high altitude with no trees, such as the site at WS1015. It can also bee seen by the slope of the CDF that the likelihood

of getting a specific wind angle is approximately uniform.

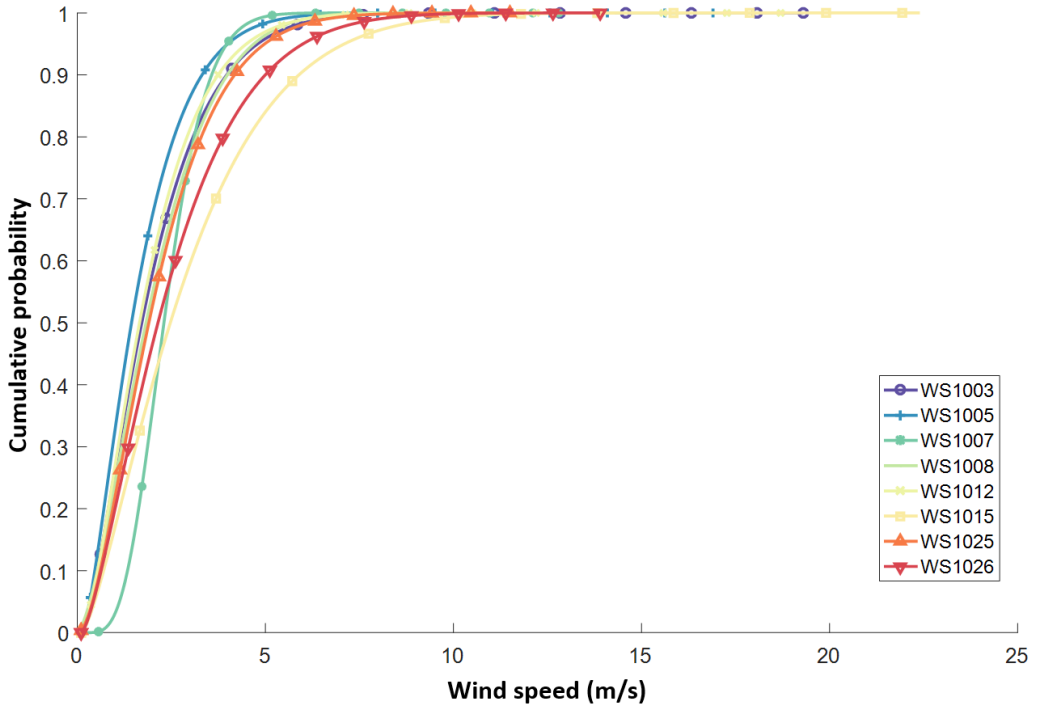

(a) Wind speed distribution

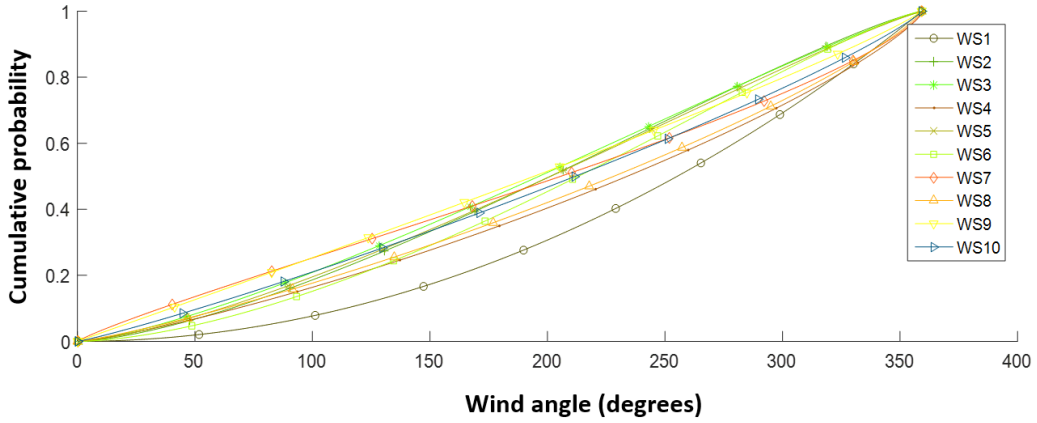

(b) Wind angle distribution

Figure 4.6 Distribution of weather station data (wind) from 2012 to 2017

The wind parameters are mainly used by the overhead line rating part of the PAR algorithm. It's use is of course not limited to overhead lines and can be used to be included in the heat transfer model across a power transformer. But as most transformers evaluated are either in an enclosed space or have wall barrier, the flow of the wind onto the power transformer body

and its impact have to be modelled either through a finite element method or through fluid dynamics and requires detailed design of the transformers spacing and its spatial points. Due to this the wind parameter is not considered for power transformers cooling in this research, the fan operation is however considered.

The weather station has also been installed with a solar radiation sensors, measuring the energy transferred by the sun on the Earth's surface, measured in Watts per metres squared (W/m^2). Only three sites were available for use and their distribution is shown in Figure 4.7.

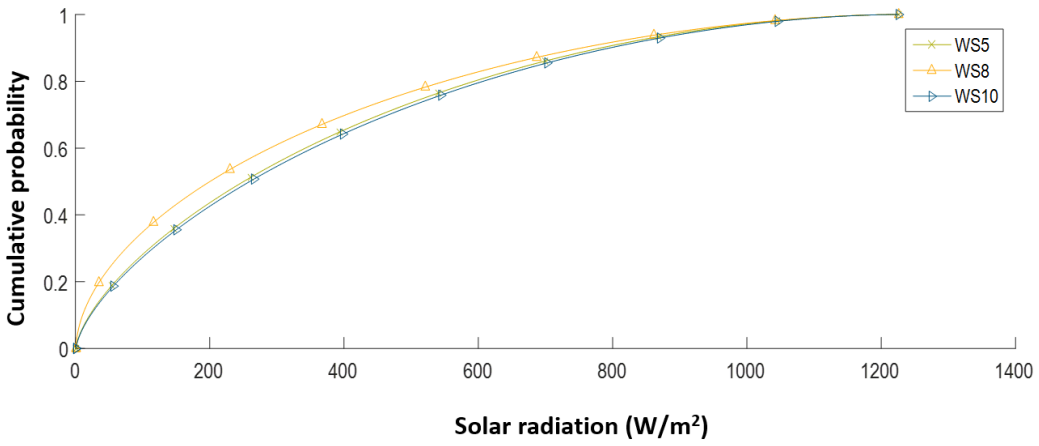

Figure 4.7 Distribution of weather station data (solar radiation) from 2012 to 2017

The maximum value possible for solar radiation is 1374 (1353 $\pm$ 21) W/m^2 [ASTM E490 2000] which varies depending on the distance of the Earth from the Sun. Not all of the solar radiation is able to reach the ground as it is absorbed or reflected by gases, clouds and dust in the air. Cloud has been identified as the most variable of these factors, changing with both time and location, reflecting approximately 20% of the solar radiation and absorbing around 4% [NIWA 2005]. For electrical components that are located on the surface of the Earth, heating through radiation is unavoidable and has been considered in this research. As the number of solar radiation sensors is limited, the solar radiation is interpolated at unmonitored areas. The solar radiation value at the unmonitored site will range from 0 (at night time) to the maximum value possible, 1374 (clear-sky).

For electrical components which are buried, such as underground cables, the PAR algorithm makes use of available soil information. Soil thermal pedestals were available for use at different

locations on the Unison distribution network. The thermal pedestals have been installed over different stages and some have data dated back to 2011, whilst some only have data from 2016 onwards. Each thermal pedestal has been located in close proximity to a high voltage (HV) cable as shown in Figure 4.2. The monitoring sites are capable of measuring the soil temperature and thermal resistivity at the thermal probe installed depth for a given point in time. The distribution of soil temperature and soil thermal resistivity are shown in Figure 4.8 and Figure 4.9 respectively.

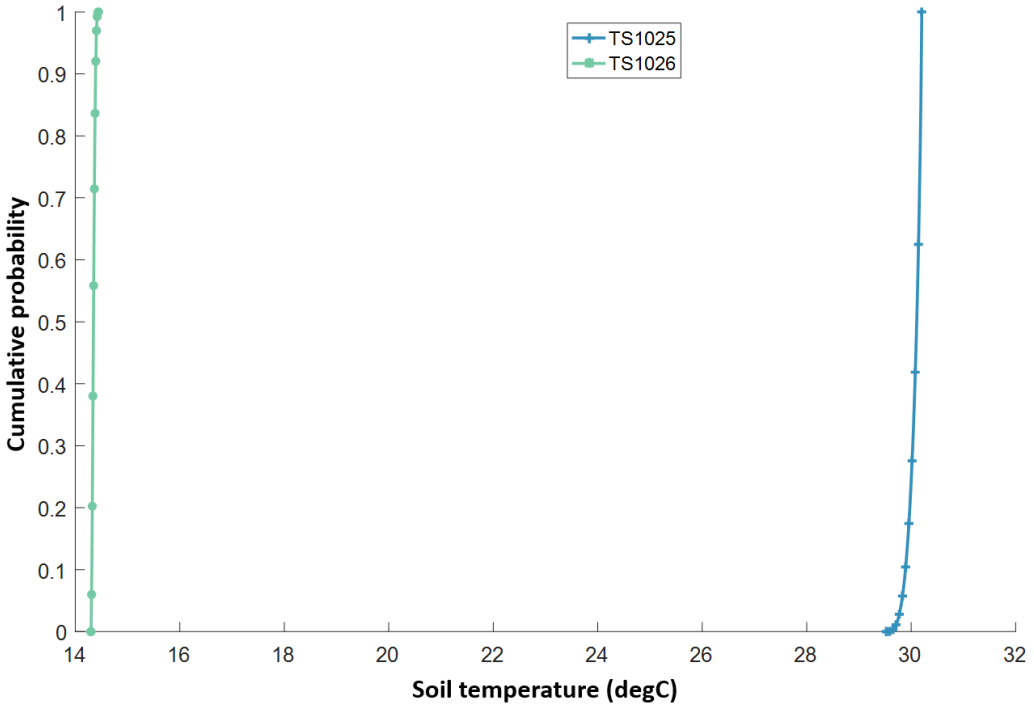

Figure 4.8 Distribution of soil monitoring site (soil temperature) from 2012 to 2017

The soil temperature distribution is similar to the air temperature distribution in Figure 4.5. The two environmental conditions are used interchangeably by the PAR algorithm for an underground cable's rating to determine the soil temperature at different depths based on the relationship discussed in Section 3.3. The soil thermal resistivity values can be seen to be uniform with a very steep change depending on the season. Higher thermal resistivity values relate to the summer period where the soil moisture content is likely to be lower and vice versa for winter. The thermal resistivity value is dependent on the type of soil as highlighted in Section 3.3. The type

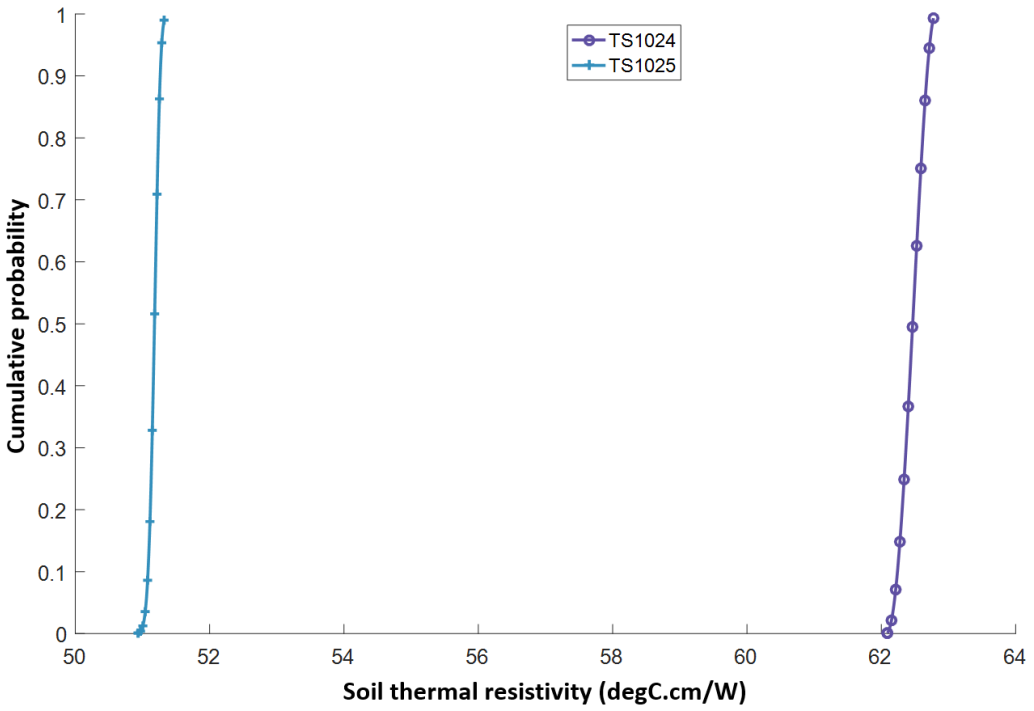

Figure 4.9 Distribution of soil monitoring site (soil thermal resistivity) from 2012 to 2017

of soil is identified based on the soil environmental survey data available from the local council and through site visits. The digital soil map for New Zealand has also been used to provide an overview of the type of soil and moisture content in the area as illustrated in Figure 4.10.

The overview is used to provide a relative soil boundary to the soil survey data. The surveyed data is then interpolated from known sampled soil sites at the soil monitoring sites based on the model discussed in Section 3.3.3.1 to the unknown sites. The soil survey data are mapped using key description of the soil such as sandy, clay, organic and rocky, each of which suggest the porosity of the soil and its ability to absorb and retain moisture. A soil laboratory based at Unison has been used to perform thermal dry-out test to obtain the thermal characteristic of the different soil types at varying moisture contents. The laboratory set-up is shown in Figure 4.11.

Soil sampled from thermal sensor sites shown in 4.2 are processed through the laboratory set-up to determine the thermal dry-out curve of the soil. This then provides a known measurement for interpolation. As the interpolation is approximate, a weighting factor, r that ranges between $0 < r < 1$ has been considered for the different environmental conditions. The weighting factor

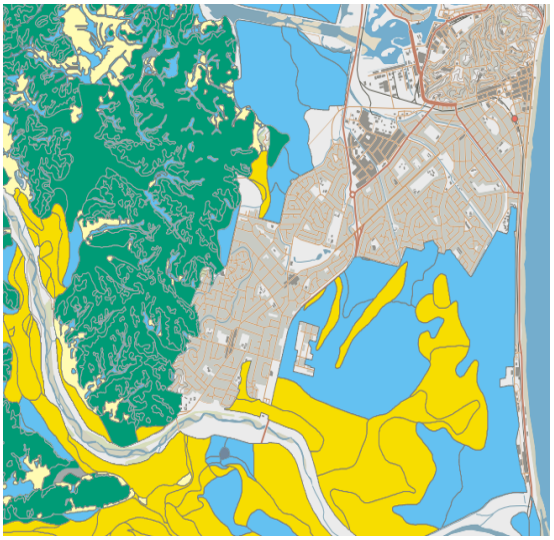

(a) Soil map for region under study, obtained from [Landcare Research 2016]

(b) Soil moisture map for region under study, obtained from [Landcare Research 2016]

Legend

Gley Soil	Very High (> 250 mm)
Pallic Soil	High (150 – 249 mm)
Recent Soil	Moderate to High (120 – 149 mm)
Raw Soil	Moderate (90 – 119 mm)
Unknown	Moderate to Low (60 – 89 mm)
	Low (30 – 59 mm)

* Based on New Zealand Soil Classification (NZSR) Soil Order definition

Figure 4.10 Soil map for region under study

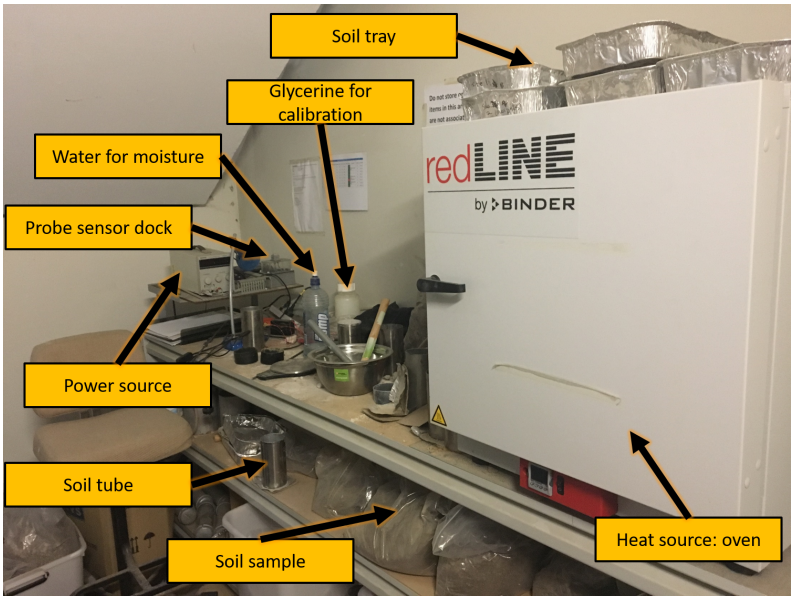

Figure 4.11 Soil laboratory setup

chosen depends on the confidence of the input data as discussed in Section 3.3.

4.2.2.3 Financial data

The last set of data is the financial data which relates to different decision making process in an EDN. To provide a generalised cost, the value compiled by six different EDNs in United Kingdom has been used as captured in the "Distribution Network Operator Common Network Asset Indices Methodology" report [WG DNO UK 2017]. In the report, the costs have been categorised into four different categories, all of which have previously been identified to capture the key issues affecting EDN. The cost is captured in Table 4.2 and categorised as:

(a) **Network performance**: cost related to loss of load and inability to provide a continuous supply of electricity.

(b) **Public safety**: cost related to impact on the safety of personal in the vicinity of the asset.

(c) **Financial**: cost related to the replacement of the asset.

(d) **Environmental impact**: cost related to the damages to the external environmental.

Table 4.2 Reference cost of electrical components by category (based on study by [WG DNO UK 2017])

Electrical component	Network performance[1]	Public safety[1]	Financial[1]	Environmental impact[1]	Total[1]
33kV Poles	114	358	6,188	150	4,728
33kV OHL[2]	1,666	2,672	29,622	160	34,120
33kV UGC[2]	5,144	4	52,680	1,210	59,038
33kV PTX	96,394	41,542	146,000	28,380	312,316
33kV Fitting	334	2,672	378	160	3,544
33kV Switch	24,548	41,542	17,074	5,178	88,342
33kV CB (air)	48,496	41,542	24,162	5,178	119,378
33kV CB (gas)	24,548	41,542	29,748	5,178	101,016

Note:
[1]Cost shown is in NZD, at an exchange rate of 2 NZD per 1 GBP.
[2]Cost shown for cables and lines is NZD per km.

The cost presented is a baseline value suggested by the study in [WG DNO UK 2017]. Additional factors would need to be applied to better represent the actual cost that's experienced by an EDN. Factors such as restoration time, number of customers supplied and asset location can be further considered to get a better representation of the cost per EDN.

4.2.3 Software architecture

The implementation comprises the use of different software to store, gather and process data as shown in Figure 4.12. The component's electrical characteristics and physical properties were gathered from the manufacturer's technical specification stored on a Microsoft SQL Server database. The physical location of the assets were obtained from a geographical information system (GIS) presenting the latitude and longitude based on World Geodetic System (WGS 84), a standard coordinate system used by global positioning systems (GPS). The different coordinate system is not discussed in this thesis as it has been discussed in GIS textbooks. The environmental conditions data are monitored remotely across the region and stored in a historian software package, OSIsoft PI. The inputs are then processed using a developed MATLAB graphical user interface (GUI) based on the rating models presented in Section 3.2 to calculate the rating of power transformers, underground cables and overhead lines.

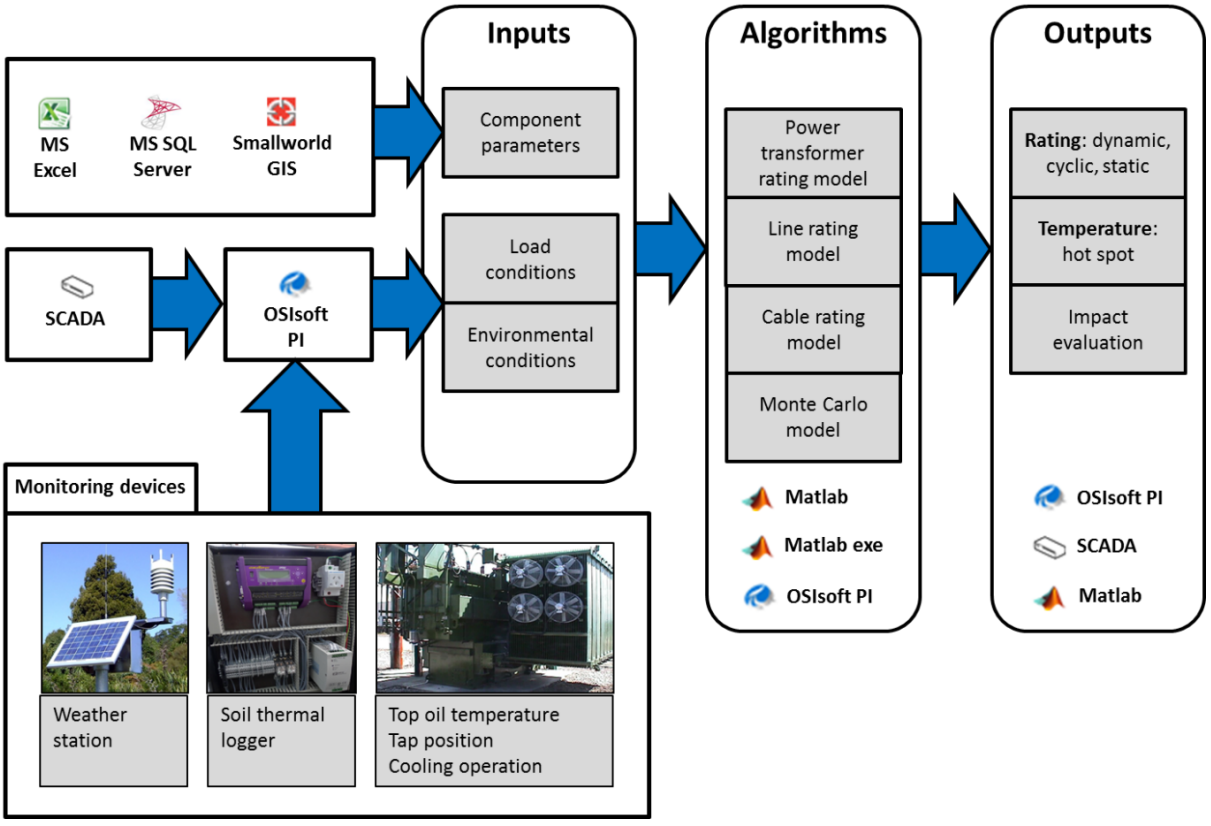

Figure 4.12 Software architecture of PAR tool implementation

The power system reliability of the components are then evaluated by carrying out a Monte Carlo simulation as presented in Section 3.4. The simulations populate the following indices for

the assets considered:

(a) **Rating probability**: evaluating operating range of the asset under specified environmental conditions.

(b) **Probability of constraint**: highlighting potential constraints and critical points.

(c) **Quantify risk**: evaluate risk based on the probability of an unwanted event and the consequences of the event.

The algorithm has been set-up to allow different layers of the network and period to be considered. The dataset are structured as circuitParam, loadParam and envParam containing the component parameters, load conditions and environmental conditions respectively. The data are assigned with a unique identification (ID) to allow selection of varying scenarios when running the simulation. The data model and its flow is illustrated in Figure 4.13.

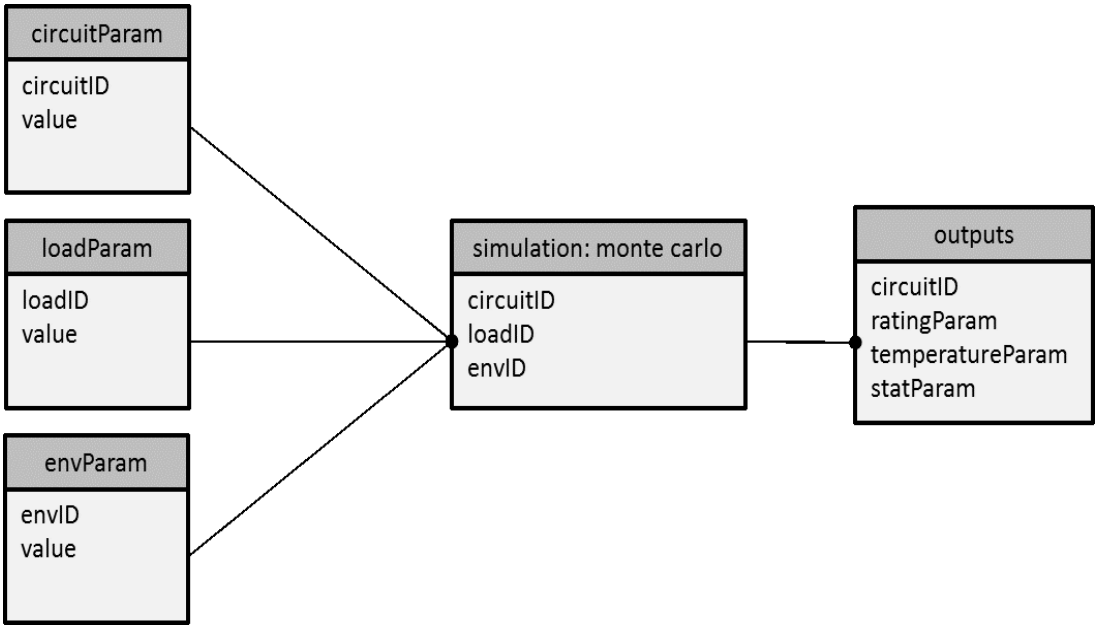

Figure 4.13 Data model of PAR tool evaluation

The circuitParam structure contains data of the components electrical and physical properties as discussed in Chapter 3.2. For power transformers: it consists of the transformer's thermal characteristics, for underground cables: it consists of the modelled cable's construction and for overhead lines: it consists of the line's survey measurements and mechanical properties.

The loadParam structure contains data of the components loading. Current transformers (CT) that have been attached either at the beginning or the end of the circuits termination are used

to monitor the current being carried by the overhead and underground circuit. Each of the CT's for the different circuits is assigned a loadID, which is used to carry out the simulation. For an unmonitored circuit, a load profile can be created, specifying either a 1-day, 7-day or a load based on a generic consumer profile. The GUI of the load set-up is as illustrated in Figure 4.14.

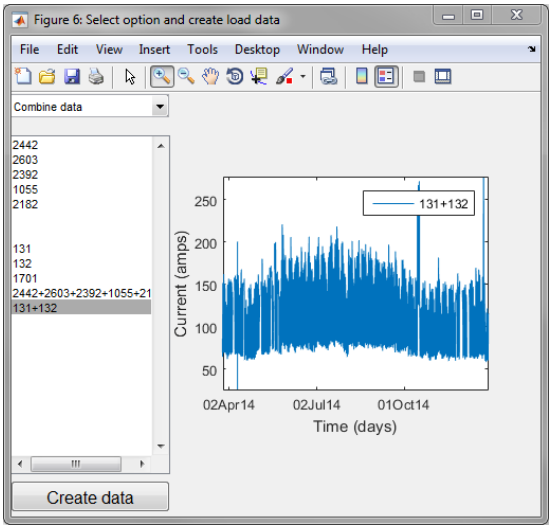

Figure 4.14 Selection and creation of load data for simulation

The GUI of the load set-up allows different scenarios of circuit loading to be established. If switching operation data is available, the algorithm has been set-up to approximate the expected loading on the circuit. This is useful as to consider only the base load of the circuit. Further modification can be made manually to the load profile to ignore any other known portion of the load that's not part of the base load.

The envParam structure contains data of the environmental parameters that can be used by different electrical components to evaluate the heat transfer model as discussed in Section 3.2. The power transformers uses the ambient air temperature, cables uses soil temperature and soil thermal resistivity and lines uses air temperature, wind speed, wind angle and solar radiation data.

A GUI interface shown in Figure 4.15 was developed to house the PAR algorithm, allowing set-up, simulation and evaluation of the circuit's capacity utilisation based on the different operating conditions.

The dataset available can be reviewed under the "Review data" tab which provides a view of

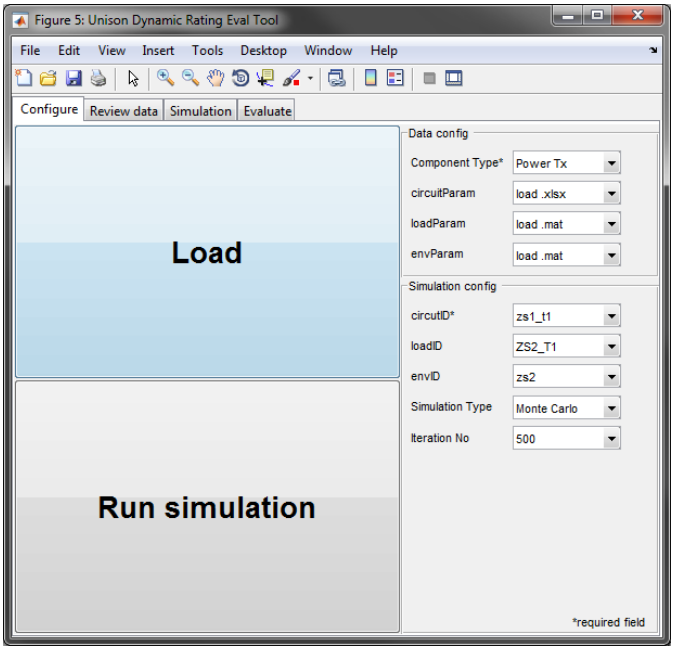

Figure 4.15 Graphical user interface of Predictive Asset Rating tool

the distribution that will be used as an input to the Monte Carlo simulation. Depending on the display option selected, the plot will be updated to either show, time-based plot, histogram, probability density function (PDF) or cumulative distribution function (CDF). The different options available from the GUI are discussed in Section 4.4. The envParam structure captures the latitude and longitude of the monitoring site based on the World Geodetic System (WGS) 1984 geographical coordinate to perform spatial interpolation at unmonitored site where an electrical component exist. It has been found that although the soil boundary provides an overview, the soil type at the actual site can very due to other work carried out by the land owner and also potential backfill that may be used at site. The next section discusses the validation steps taken to ensure the PAR tool worked as designed by comparing against the manufacturer's rating and measurable criteria. At the end of this chapter, the tool's ability to satisfy the following requirements set out in Chapter 3 will be discussed:

(a) *Ease of implementation*: the models are able to easily integrate with common data that EDN operators have.

(b) *Flexible*: the models are able to consider different operating scenario and environmental conditions.

(c) *Modular*: the models are developed as a building block which can be simulated on its own

or combined.

4.3 VALIDATION OF PREDICTIVE ASSET RATING MODEL

Validation has been carried out throughout the development stages. The models discussed in Chapter 3 have been published in peer reviewed proceedings of national and international conferences as part of this research as listed in the pre-amble of this thesis. The development of base rating model for the three electrical components as per the international standard presented in Section 3.2.1, 3.2.2 and 3.2.3 has been developed by the author of this thesis and the Asset Intelligence team at Unison. This research further develops and extends the base rating model to enable a predictive rating based on probabilistic methods. The next section discusses the validation steps taken for the different models used by the PAR tool. The rating of electrical components, environmental model and reliability assessment model will be covered.

4.3.1 Electrical Components Model: Power Transformers

As presented in Chapter 3, the hot spot temperature of a PTX is located in its windings, normally close to the top terminal where the oil temperature is at its highest. The high electric potential of the winding makes it difficult to install a sensor to measure the hot spot temperature directly through-out the windings on older transformers. New transformer design, such as the work performed by [Das *et al.* 2015], where sensors can be embedded at the winding for temperature measurement allows for improved input data for the evaluation of the PTX rating. For this research, the only measurement point available at the transformer winding is from the winding temperature indicators (WTI). Some of the PTXs in Unison's network have been retrofitted with indicators which calculate the winding temperatures based on the transformer load and top oil temperature as illustrated in Figure 4.16.

The pocket at the transformer top cover contains a sensing bulb filled with liquid which expands and contracts to measure the top oil temperature. The current used by the WTI is directly proportional to the current flowing through the transformer winding which then allows an indirect measurement of the winding temperature. Comparing the measured value by the WTI and

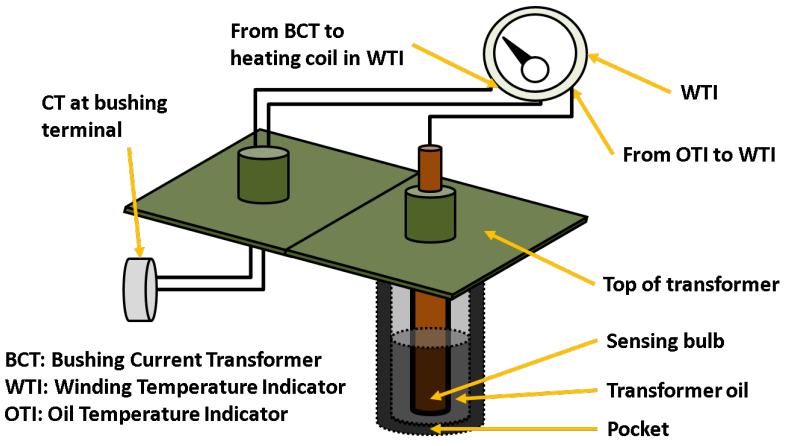

Figure 4.16 Winding temperature indicator set-up

the calculated value by PAR model for PTX shows that the two are very similar as shown in Figure 4.17.

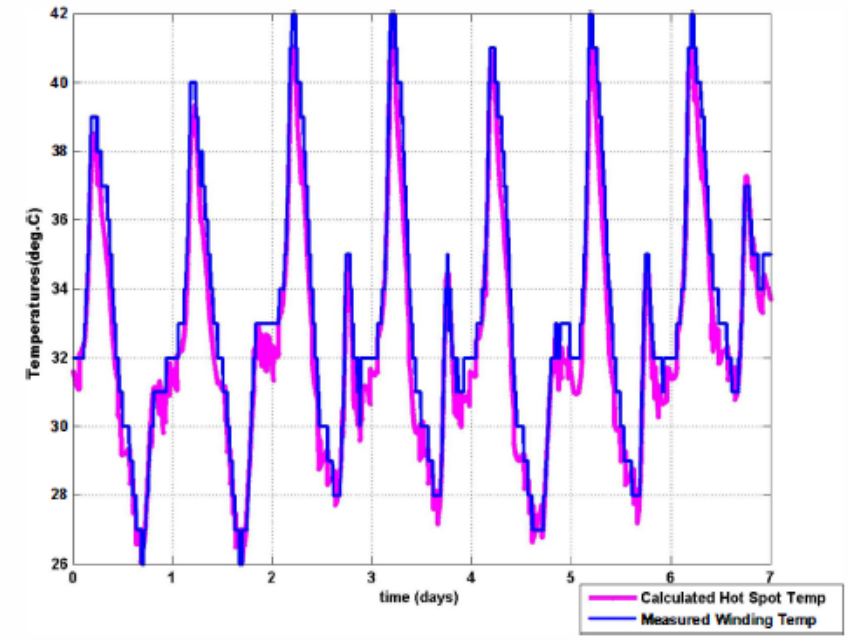

Figure 4.17 Comparison of measured and calculated values of hot spot temperature of a power transformes

The real-time hot-spot calculation is performed at a higher interval than the sampling of the measured winding temperature. The calculation takes on average 30 seconds to complete. The calculation time given includes the time taken to query the input parameters, extracting the transformers thermal properties, environmental and operating conditions. The methodology developed to query and select the calculation time interval will be discussed at the end of this chapter.

The rating and loss-of-life evaluation model has also been compared against the model used in [AS/NZS TC EL-008 2013b] applying the same parameters and conditions. The results presented in Figure 4.18 can be seen to be similar to the output found in Annex E of [AS/NZS TC EL-008 2013b]. The comparison is shown without reprinting of the figure from the standard.

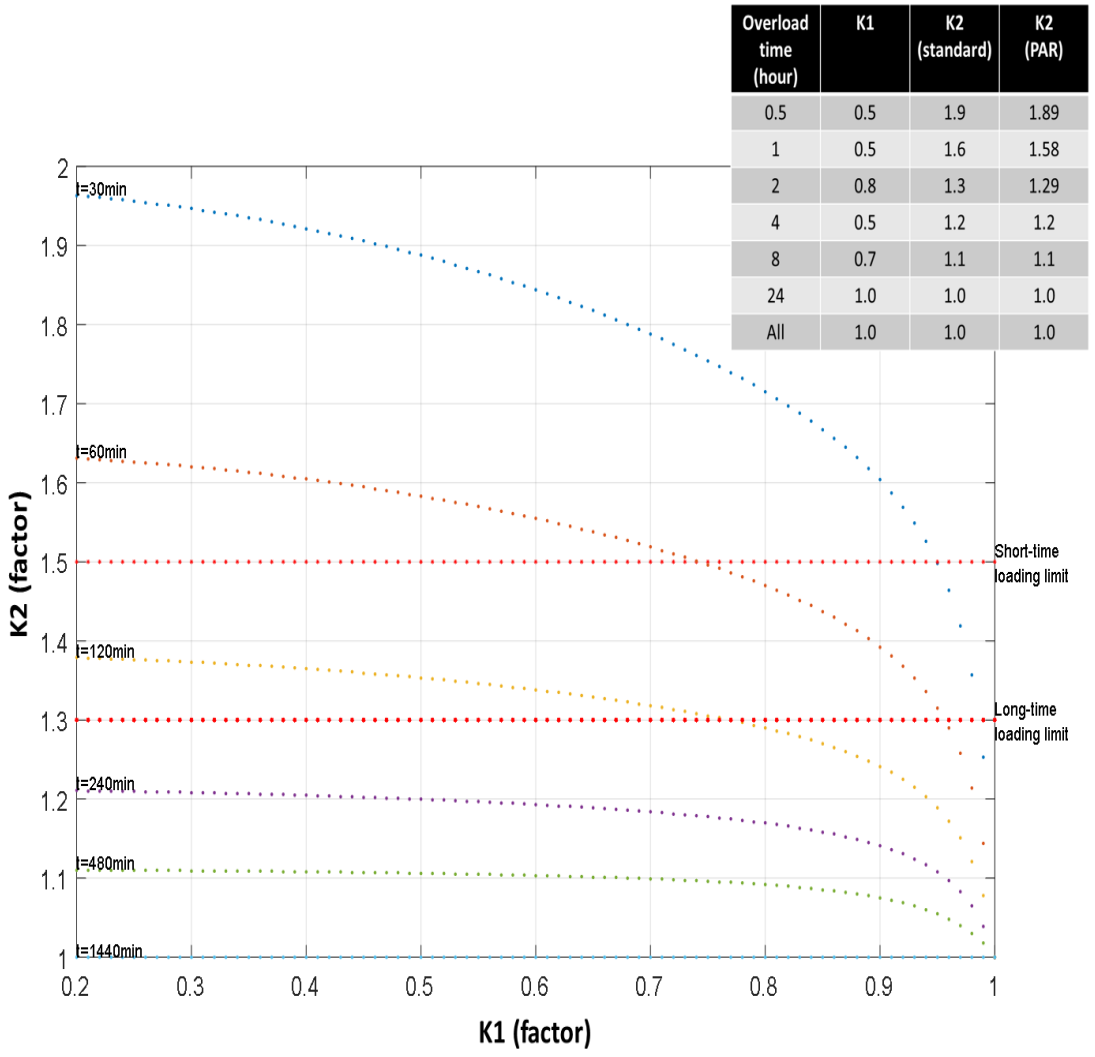

Figure 4.18 K1:K2 curve for varying overload time at unity loss-of-life

The exact value was not given in the standard, but the relative comparison between the figure in the standard and Figure 4.18 shows similarity as tabulated. The comparison provides validation in both the loss-of-life model used and the rating model used. The result shows expected loading (K2) over a duration (t) for a given pre-loading (K1) conditions such that a unity loss-of-life is achieved.

4.3.2 Electrical components model: Underground cables

A commercial rating software was available at Unison, CYMCAP developed by CYME International T & D [CYME 2012]. It also uses the IEC 60287, solving cable rating based on analytical techniques. The thermal resistance model used by PAR tool is also based on the IEC 60287 as discussed in Section 3.2 solving based on a finite element method. A comparison of the PAR algorithm output for cables and the commercial software available is shown in Figure 4.19.

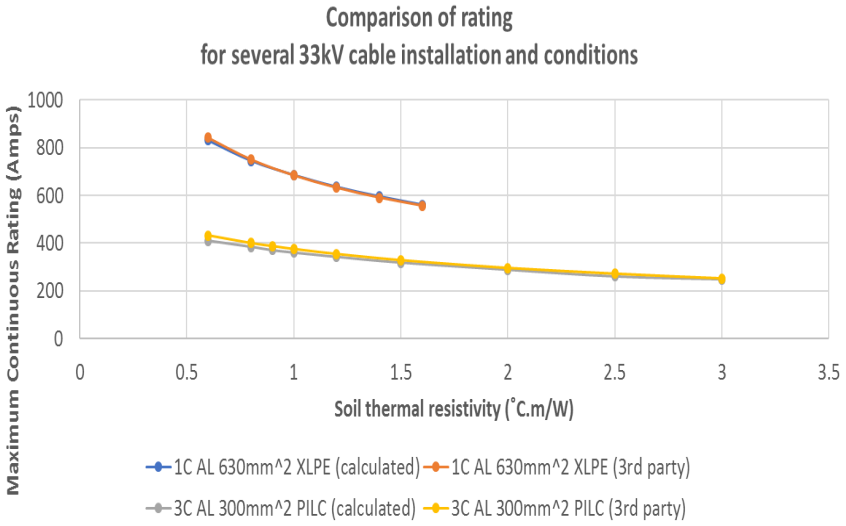

Figure 4.19 Comparison of outputs of PAR algorithms and a commercial software

Two distinctly different cable types were chosen for illustration, evaluating the cable rating for different thermal resistivity values. Similar cable properties and thermal resistance were used to compare the two models, and the result is approximately the same for XLPE cables with root mean square error (RMSE) of 5.7. The two models has slight difference at lower thermal resistivity for paper insulated lead covered (PILC) cables with root mean square error of 29.3. The difference is likely due to the difference in the way soil thermal resistivity is being mapped between the two models. The PAR tool applies different weightings to the soil surrounding the cable based on the finite element method (FEM), with weightings relative to the soil distance from the cable. Taking this into account, the PAR tool approximated a higher rating that could be achieved.

Some of the circuits on Unison's network have been installed with distributed temperature sensing (DTS) fibre along its route. As part of the validation process for the PAR tool, a cross

section of a circuit on a Unison's network has been selected and modelled at TS1095, as marked in Figure 4.20. The site consists of a 33kV circuit, a thermal pedestal that's connected to a thermal probe installed 5cm above the 33kV circuit and a DTS fibre that has been laid in the same duct as one of the circuit's phase.

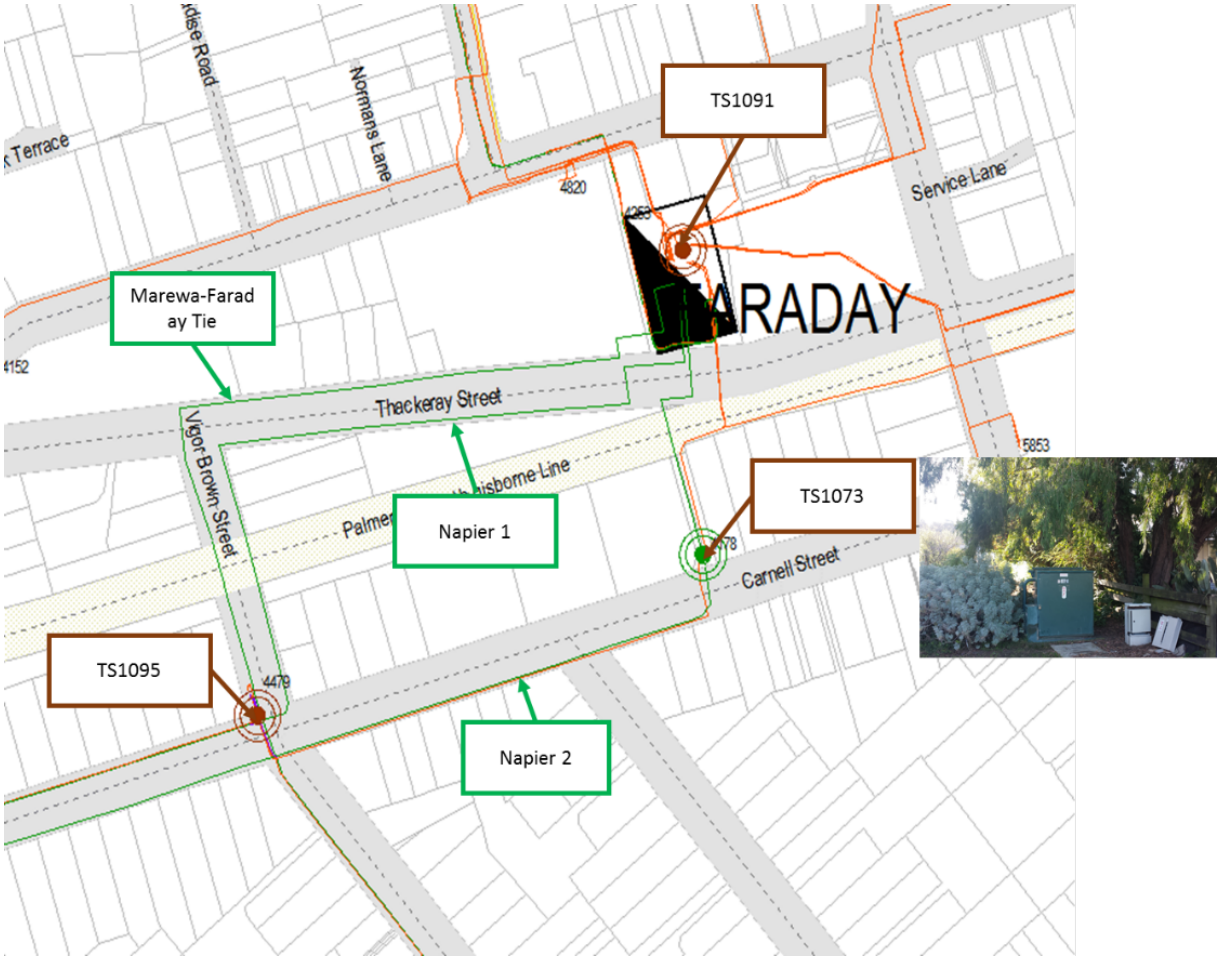

Figure 4.20 Validation site for DCR showing information of circuit and DTS fibre

The DTS equipment is located at the zone substation and wired up to send data to Unison's historian database. The equipment and wiring are as shown in Figure 4.21. The orange wire is the multi-mode fibre required to perform temperature measurement and is connected to the Sensortran Gemini HSI DTS equipment [Halliburton 2011]. The fibre cable is laid along the circuit under study and is used for validation.

Along its route, the DTS fibre goes through different terrain as summarised in Table 4.3. The cross section selected for validation is located approximately 356m from the Faraday ZS, which is the location of thermal pedestals, TS1095.

(a) Distributed temperature sensing equipment

(b) Wiring of DTS fibre and communication patch panel

Figure 4.21 DTS set-up at the zone substation

Table 4.3 Landmark along DTS fibre route

Distance (m) from ZS3	Description
50	Street crossing #1
270	Railway line
356	TS1095
586	Cable joint #1
708	Street crossing #2
1161	River crossing #1
1192	Cable joint #2
1380	Stree crossing #3
1817	Switching station

Comparison of the calculated values from PAR tool and the measured temperature from the DTS hardware over time in Figure 4.22 shows similar trend between the two measurements as the feeder load changes over time.

The data sampled looks at some of the peak period on the feeder. The feeder is utilised at 25% of its rated value. The comparison shows the hot spot temperature on the cable calculated based on FEM and the temperature of DTS fibre which is located in the cable duct. The DTS equipment provides temperature sampling for every 0.25 meters along the DTS fibre. The sampled value is then averaged every 1 meter to pin-point to the cross-section at TS1095. The FEM hot-spot measurement relies on how often the temperature indices gets updated for each change in load,

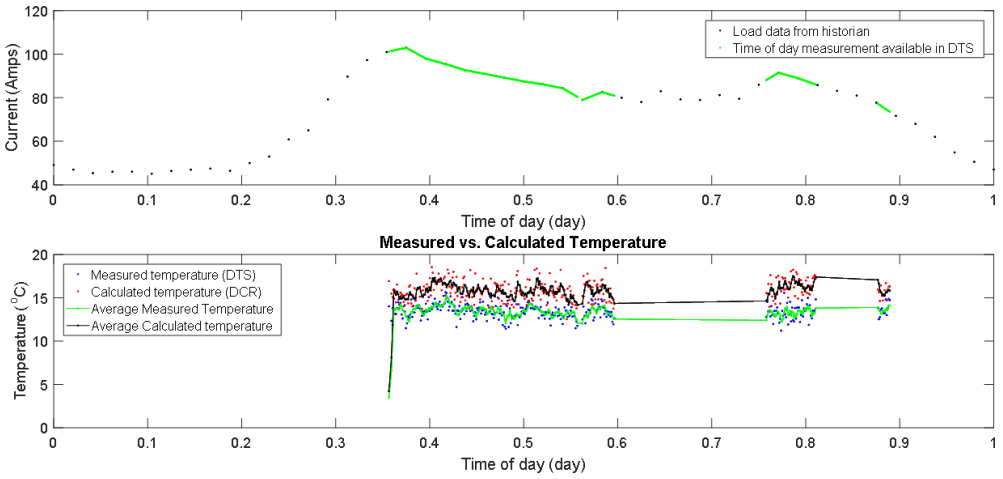

Figure 4.22 Comparison of calculated hot spot temperature of an underground cable and measured ambient temperature of a DTS fibre

every 10 minute was used for the comparison. As the two calculations have different sampling rate, a moving average has been used to compare the two. The measurements can be seen to fluctuate over time and there's no distinct relationship between the temperature inside the duct and the actual temperature of the cable when looking it the dispersed value. When looking at the moving average, the difference between the two temperatures is approximately 2 °C. Additional comparisons can be made by using the latest technology in cable construction which have an in-built DTS fibre at the screen wire layer and has been recorded as future work for the research. In regards to rating evaluation which considers the maximum operating temperature of the conductor, the PAR tool matched well with commercially available software and manufacturer's recommended rating as shown earlier in Figure 4.19.

4.3.3 Electrical components model: Overhead lines

The validation work for overhead lines looks at the calculation of the sag model presented in Section 3.2.3. The sag-tension calculation was compared against the line tension sensors that have been installed on a selected span on the Unison 33kV OHL network. A comparison between the calculated and measured span tension for different conductors is shown in Figure 4.23.

The comparison shows close agreement between the measured and calculated tension values. The rating and sag calculation model applies the same principle as the model developed by

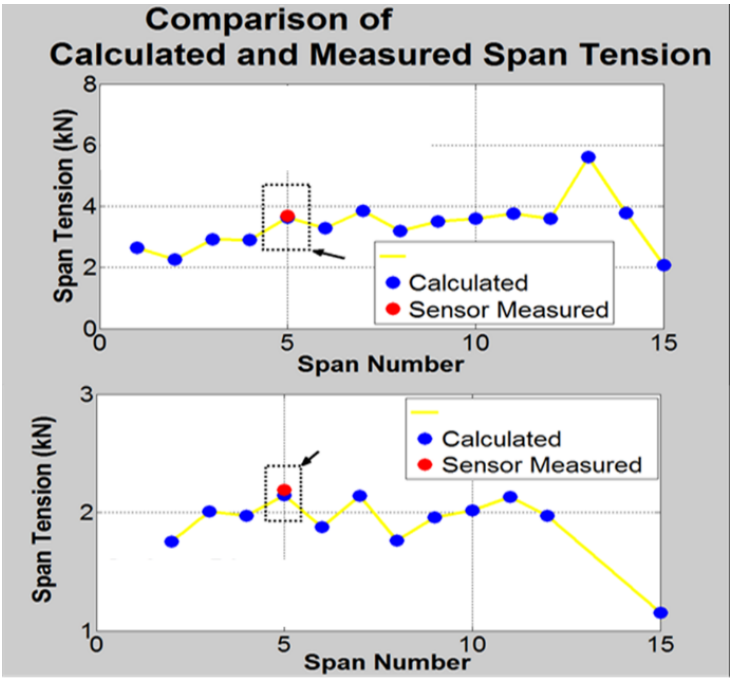

Figure 4.23 Comparison of calculated and measured tension of an overhead line

[IEEE 738 2013, CIGRE WG B2.12 2002] and applying clearance limit suggested by [AS/NZS 7000 2016].

4.3.4 Environmental conditions model: Interpolated site

The spatial interpolation model based on the study by [Shepard 1968] has been implemented in the PAR tool as discussed in Section 3.3.3. To validate the accuracy of the model, data from several soil thermal pedestal sites were gathered. The criteria for site validation was that detailed survey data must be available and the site is monitored. The area selected for validation is shown in Figure 4.24 with soil layer obtained by request from the local regional council [Hastings District Council 2015].

Based on the detailed survey data of the top soil, the soil was found to be made up of sandy and loamy material. The sites labelled 3 and 4 also contained limestone. Based on the compilation of different soil types by [IEEE 442 1996], a moist soil with a mixture of these soil types will have thermal resistivity values that range between 0.5 °C.m.W^{-1} to 1.5 °C.m.W^{-1}. Using the inverse distance weighting (IDW) model, it can be seen that the interpolated region closely follows the surveyed soil boundary as shown in Figure 4.25.

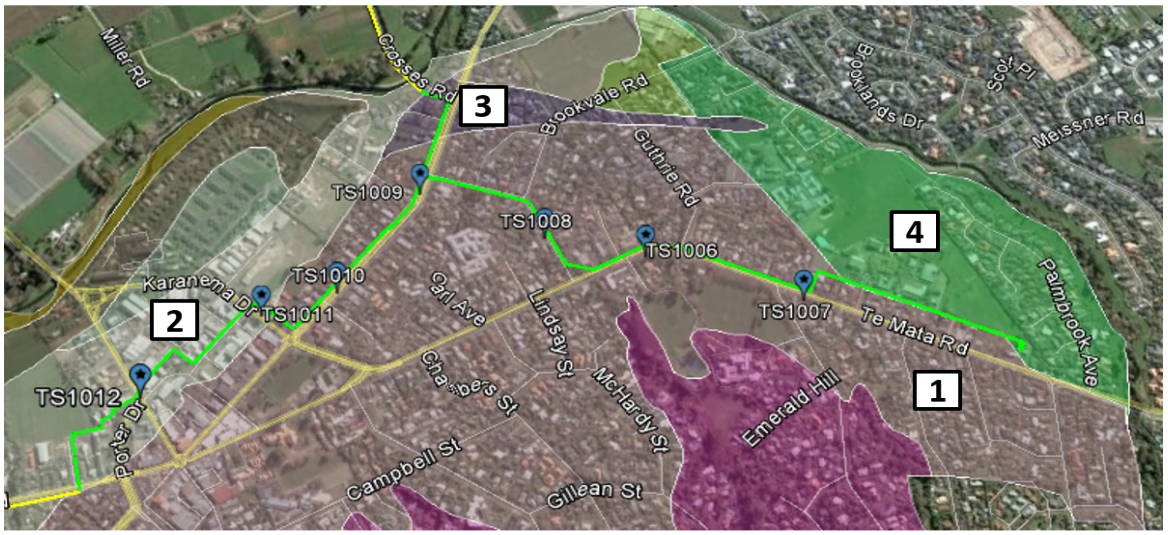

Legend

Label No	Boundary	Soil description
1		30-45cm ashy sandy loam on sandy loam on pan over gravel >60cm (poor water table (WT) on pan)
2		>60cm silt loam on sand (imperfect WT 30-60cm)
3		12 - >45cm sandy loam from sandy limestone >60cm (good WT)
4		12 - >45cm sandy loam from sandy limestone >60cm (good WT)

Figure 4.24 Spatial interpolation validation site

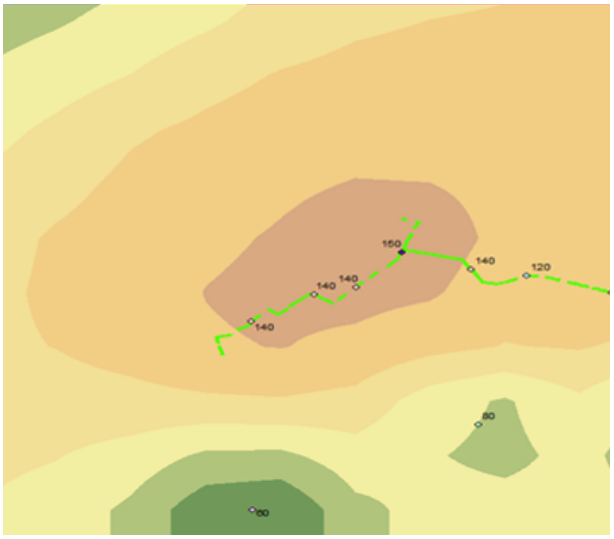

Figure 4.25 Interpolated soil thermal resistivity region

As the interpolation is an approximation and only considers the soil type and thermal resistivity values, site visits are still carried out to lookout for possible material that could cause the thermal resistivity to increase along the underground cables. This include items such as trees, shrubs and roadways. Safety factors are applied for such cases to account for the different items based on its likelihood to cause changes to thermal resistivity values.

4.4 DISCUSSION

With the vast developments in sensor and communication technologies, there were many potential investment and development options that could have been made to study the capacity utilisation of electrical components. To carefully select the relevant development path for the PAR tool, the desired features to be included are built upon benefit scoring which was used to determine the key area and features that would benefit an EDN in the area of capacity utilisation. The framework used was presented in the case study by [Jalal *et al.* 2015] to rank the benefit realisation for power transformers. Figure 4.26 shows an extract from the smart grid benefits that were anticipated for power transformers.

			ALGORITHMS					EMBEDDED FUNCTIONS (DISTRIBUTION MANAGEMENT SYSTEM)			SMART GRID TECHNOLOGIES (DIRECT IMPACT)	
Category of Benefit	Benefit Realised	Benefit Weight	Power Transformer Dynamic Rating (DR)	Power Transformer Aging Calculator (due to DR)	Power transformer remaining life expectancy (RLE) calculator	Power transformer health index calculator	Power transformer asset management advisor	Remotely determined fault location	Automated feeder restoration (Automated Sectionalisation and Restoration)	Load management	Ground Fault Neutralisers	DTS (Fibre in the Windings)
Increased asset utilisation	Enhanced asset capacity (rating)	0.25	◕	◑	○	○	○	○	○	○	○	◔
Increased asset utilisation	Extended asset life	0.2	○	○	◑	◕	◕	◔	◔	○	○	○
Enhanced operational efficiency	Optimisation of planned maintenance	0.15	○	○	○	○	◕	○	○	◔	○	○
Improved power quality	Avoiding faults	0.1	○	○	◔	◑	○	○	○	◑	○	○
Improved power quality	Faster restoration of supply post-fault	0.05	○	○	○	○	○	◔	◔	○	○	○

	LEGEND
○	Benefit not supported at all
◔	Benefit supported in a minor or incidental fashion
◑	Benefit supported moderately
◕	Benefit supported strongly
●	Benefit completely achieved

Figure 4.26 Benefit-feature framework for power transformers, reprinted from [Jalal *et al.* 2015]

To represent the framework and putting it into perspective, the features offered by the different technologies are grouped together and stacked based on the scoring of the technology's individual benefits which then provides a clear mapping of the benefits that can be realised by the different technologies as illustrated in Figure 4.27. Similar scoring of the framework was performed for cables and overhead lines which leads to the mapping as shown in Figure 4.28 and Figure 4.29 respectively.

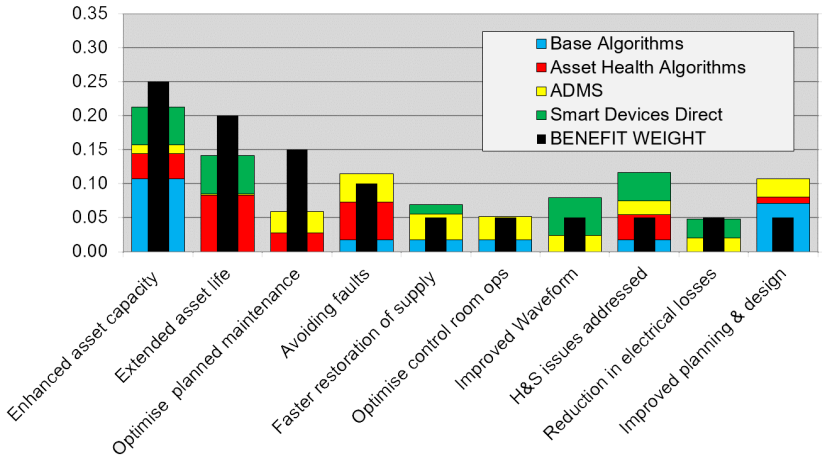

Figure 4.27 Benefit-technology alignment for power transformers

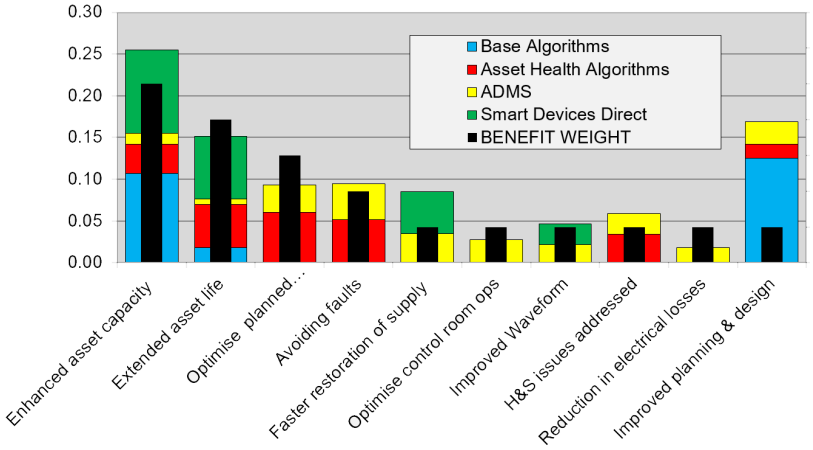

Figure 4.28 Benefit-technology alignment for underground cables

Based on the mapping, it can be seen across the electrical components that the immediate feature required to be developed, is the ability to enhance asset capacity utilisation and the different technology that can be utilised to realise the benefit. The benefit-technology alignment mapping provides a stock-take of the different technology available to then decide on the features to be developed. As part of the criteria for development, the PAR tool is designed; to ensure

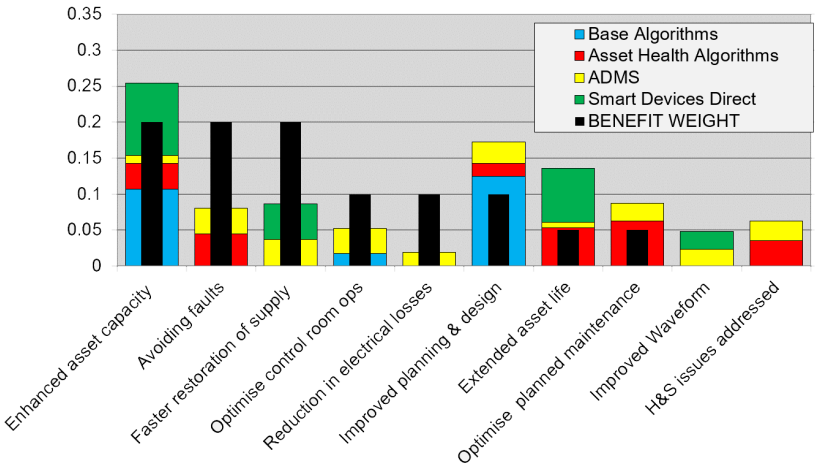

Figure 4.29 Benefit-technology alignment for overhead lines

ease of implementation, to be flexible to simulate different scenarios, and that the algorithm is modular in the way it is executed. The criteria set out for the development are important to solve the following challenges faced when implementing an intelligent computational algorithm for an EDN as discussed in the next section.

4.4.1 Challenges in Implementing Algorithms for EDN

4.4.1.1 System interoperability

Similar to other utilities, Unison faced the challenge on interoperability of various proprietary Information Technology (IT) systems which complicates the implementation of any computational framework throughout the company. Figure 4.30 shows the various IT platforms required to run various business processes within Unison.

There are layers of IT systems to be considered in order to extract the data required for an intelligent computational algorithm. An example of an interoperability problem faced in the past was when the base rating algorithm from the PAR tool was to be implemented on the wider network. The first algorithm that was rolled out in 2012 was the Dynamic Power Transformer Rating (DTR) algorithm. The data that describes the asset is stored in an asset management system, such as Activa. However, most of the data required for the algorithms were sampled at the substations and remitted via the remote terminal units (RTU) to OSISoft PI system at a

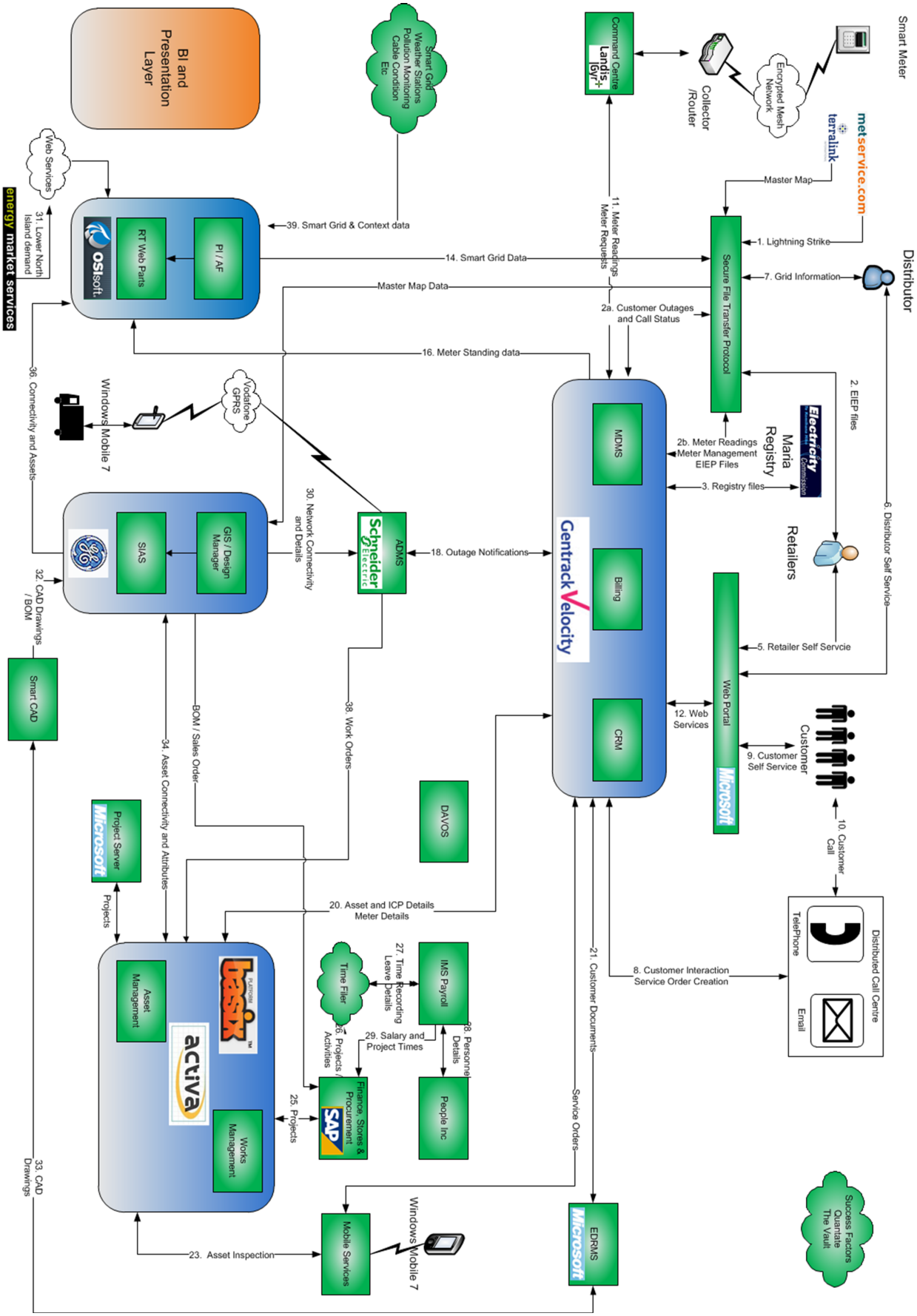

Figure 4.30 Various IT system in operation in Unison as at 2015

central location. The PI system also collects the ambient temperature data from weather stations through an external server owned by the service provider. PI ACE (the calculation module of PI) performs the DTR calculations and stores the outputs into the PI historian database which can then be extracted using the relevant PI tags. An example of a tag from PI system and its data is shown in Figure 4.31.

Tagname	CHURCH_T1_MVA
Start Time	1/01/2017
End Time	2/01/2017

Time of day	Apparent Power (MVA)
01-Jan-17 00:00:00	1.491417765
01-Jan-17 00:30:00	1.4125016
01-Jan-17 01:00:00	1.34307531
01-Jan-17 01:30:00	1.273649021
01-Jan-17 02:00:00	1.204222731
01-Jan-17 02:30:00	1.134796442
01-Jan-17 03:00:00	1.110392484
01-Jan-17 03:30:00	1.131227188
01-Jan-17 04:00:00	1.152061958
01-Jan-17 04:30:00	1.172896728
01-Jan-17 05:00:00	1.193731498
01-Jan-17 05:30:00	1.214566268
01-Jan-17 06:00:00	1.235401037
01-Jan-17 06:30:00	1.263664667
01-Jan-17 07:00:00	1.396449567
01-Jan-17 07:30:00	1.593592302
...	...

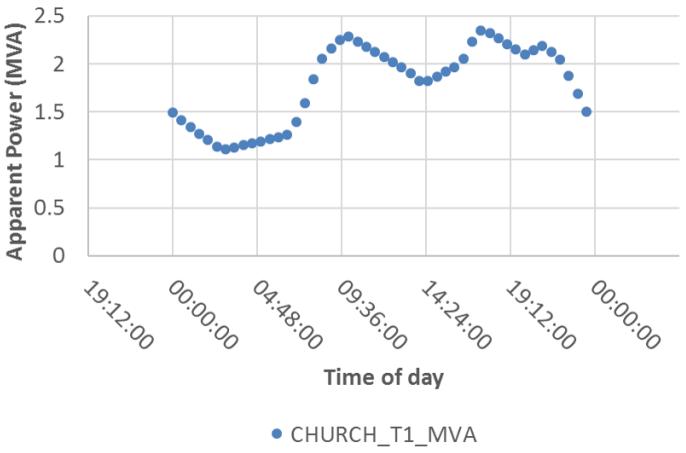

Figure 4.31 Data extracted from PI Tag for a transformers

Using the PI tags, a snapshot in time of the data are then linked to Supervisory Control and Data Acquisition (SCADA) tiles to allow the outputs to be accessible by the control room operators. During the DTR algorithm development phase, the algorithms in its Matlab codes format have already been tested rigorously. However, since all the sampled real time data collected for the algorithms were stored in the OSISoft PI system, the initial solution for algorithm implementation was to utilize the PI system computational module, in a Visual Basic (VB) language. Hence, the DTR algorithm was re-coded into VB language. This step took another several months of development work because the code had to be rigorously tested again to ensure that it works under all circumstances such as communication failures. Due to the significant amount of time spent duplicating similar tasks, an alternative solution is proposed here. Rather than re-coding whole algorithms, the option of placing Matlab on a server and getting PI to schedule the Matlab code to run periodically was explored as shown in Figure 4.32. By understanding which data

needed updating regularly, both the Matlab and the VB code were optimized to ensure that each program was executed in sequence and provided the relevant outputs in a timely manner.

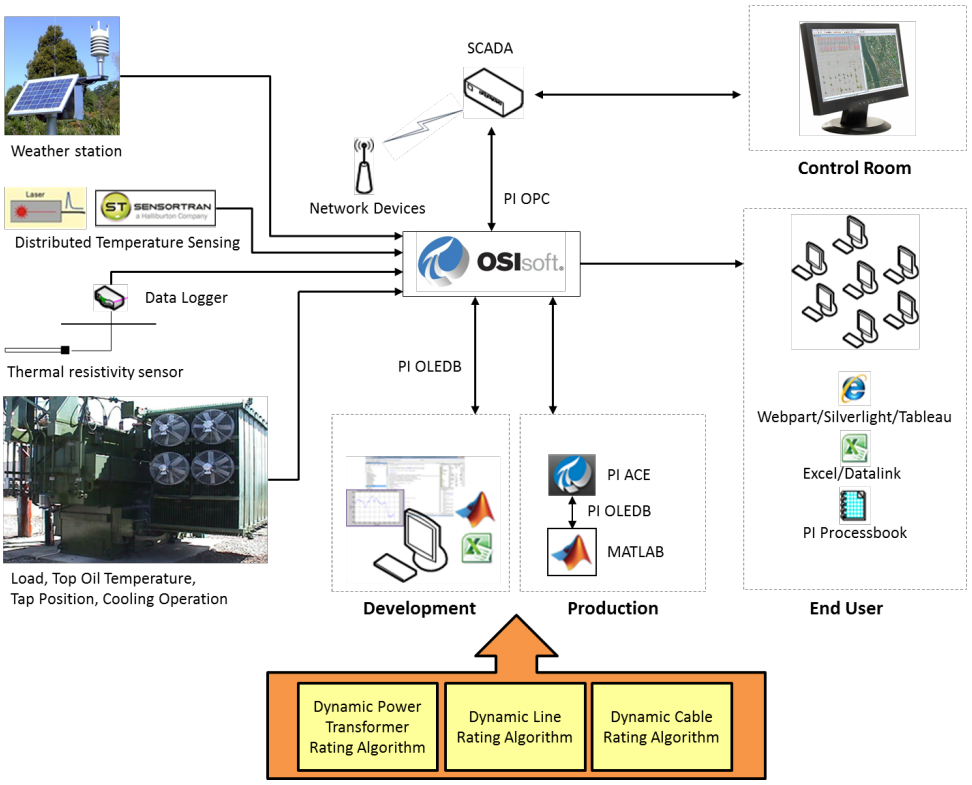

Figure 4.32 The dynamic rating algorithm implementation using OSISoft PI system

4.4.1.2 Output Visibility

The algorithms developed for capacity utilisation involve complex formulae and computations. In order to increase the usefulness of the algorithm's outputs to various users across the business, it was important to visualize the data in an effective manner. The user requirements from different groups of an EDN were captured to determine the calculation that needs to be triggered and the different set of outputs required as shown in Table 4.4.

Based on the summary, the algorithm's outputs are utilised differently by different teams in an EDN. The development has been implemented based on this requirement set-out and the challenges faced by EDN to process a growing list of data, and using it for decision making.

Table 4.4 Algorithms user communities and their business needs

User communities	Business applications
Control room operators	Real time network operation decisions e.g. how much to load a line?
Asset managers	Asset condition and utilization e.g. how many times has a transformer's tap changer operated?
Network planners	Asset long term loading capability e.g. can an investment be deferred by optimizing an asset in a better manner?

4.4.1.3 Data Availability and Quality

For any intelligent computation to produce an accurate result, its inputs have to be correct and available when required. For example, without a good sensor validation and re-calibration regime, the computation results can be wrong without any warning. At the same time, the need for dependable hardware and communication systems could also be justified as hardware that lacks the required accuracy can easily introduce round-off errors during computation. The lack of a reliable communication system can lead to expensive hardware not able to send data when required. The data quality varies for the different data set as it depends on the technology and its communication system. A set of rules have been developed as part of this research to identify the key triggers of a data quality issue in the area of capacity utilisation and can be used to alert for possible errors in the data. This will be discussed further in Chapter 5.

4.4.2 Predictive Asset Rating Tool

As a solution to solve the challenges discussed and to provide EDN the capability of evaluating rating utilisation as a real-time solution, constraint management and decision support, the PAR tool is developed. The tool has been made generic, flexible and modular, allowing easy integration for different EDN. The algorithms are broken up into three different stages as shown in Figure 4.33.

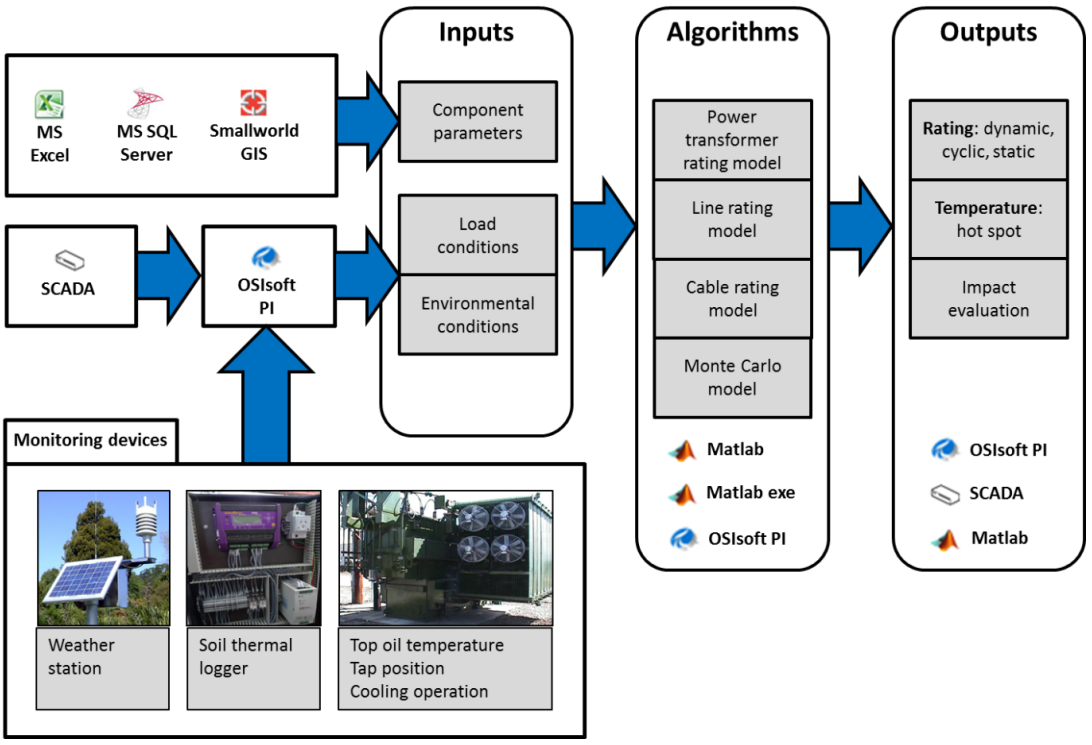

Figure 4.33 Software architecture of PAR tool implementation

4.4.2.1 Input data consideration

During the input gathering stage of the algorithm, three key information needed to evaluate the capacity utilisation are specified: the component parameters, load conditions and environmental conditions. As the components parameters needed to be extracted from various IT systems, key fields are first mapped to the PAR tool. Depending on the type of IT system specified, different fields are mapped to the PAR tool as a MATLAB structure data type. The data gathered from the field are mapped in a similar fashion using MATLAB structure data type, leading to three separate input variables as input to the PAR tool: circuitParam, loadParam and envParam. By doing this, the tool is not constrained to a proprietary IT system and new mapping can be easily set-up to consider a different IT system. Once the inputs are specified, its data can be reviewed using the GUI as shown in Figure 4.34.

The review data is limited to show data in time-domain and as a histogram. If an anomaly is identified, the brush tools can be used to mark the data points for removal as shown in Figure 4.34b. The different data set used for the research was shown earlier in Section 4.2.2 and can be displayed into the review tab in time-domain or as a histogram. The review provides an

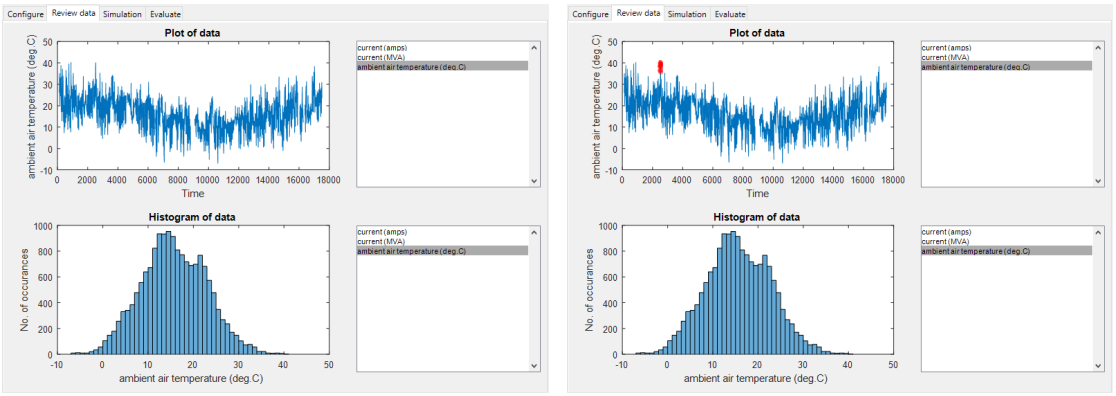

(a) Review of air temperature data

(b) Review of air temperature data with marker to remove anomaly

Figure 4.34 GUI for data review pre-simulation

illustration of the different set of data available. Once the data are set, different combinations of simulation can be performed as shown in Figure 4.35.

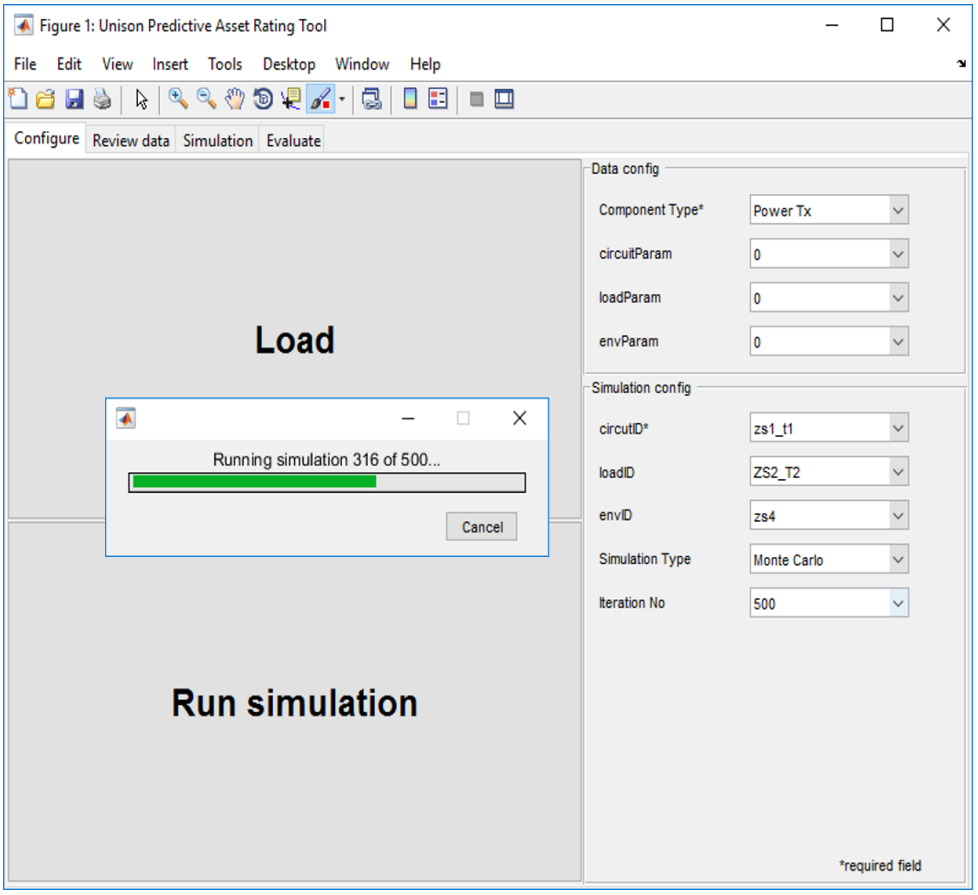

Figure 4.35 Simulation configuration for PAR tool

The circuitID represent a collection of asset that will be simulated and can be made of either

power transformers, underground cables, overhead lines or combination of the three. The assets that are linked to circuitID are populated from a table. Microsoft Excel was used in this research for simplicity but a database would have provided a more robust solution as it provides security and control over different versions of the table. The option of moving the tables into a database is part future work for this research. Depending on the component type within the circuitID and the simulation mode selected, either: "Rating", "Standard", "Monte Carlo" or "All", different functions will be executed. The simulation of "Standard" represent the maximum continuous rating evaluation based on the international standard and "Rating" based on the model applied in the PAR tool as discussed in Section 3.2. The two can be run independently and are mainly used to provide a quick check and comparison on the rating profile over time for a given loadID and envID. The results from the different simulation will be discussed further in Chapter 5 of this thesis. The data flow model for a "Monte Carlo" simulation type is re-printed in Figure 4.36 and shows the link of the different data structure from the input, then recombined within the PAR tool to perform a different calculation module to provide the requested output to the user.

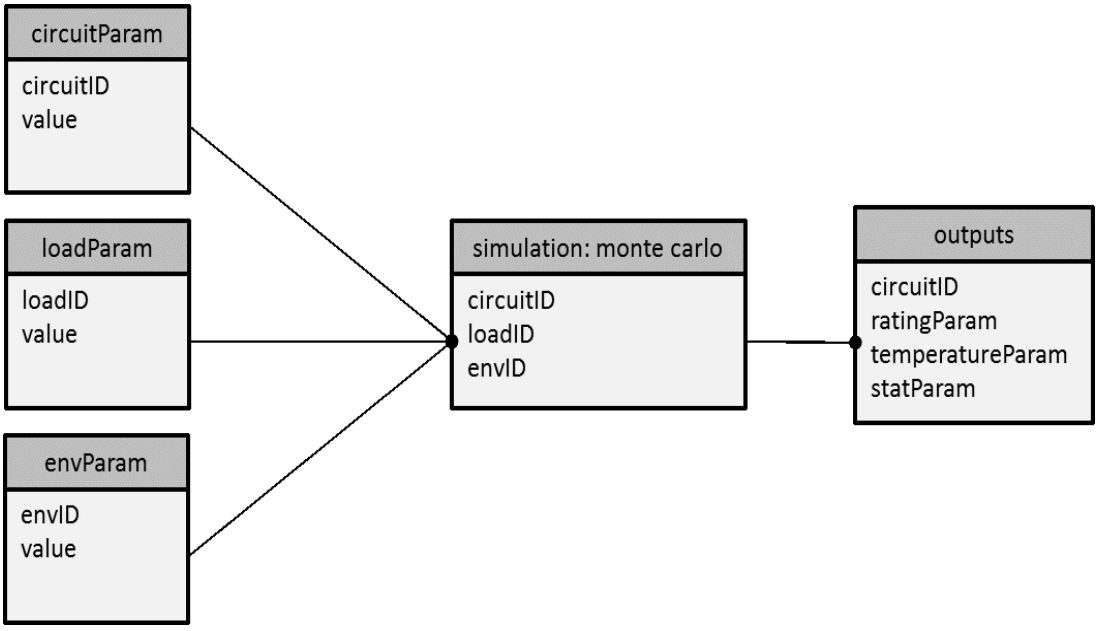

Figure 4.36 Data model of PAR tool evaluation

A mixture of overhead and underground electrical components have been studied looking at its capacity utilisation for varying environmental conditions. The datasets from installed field monitoring devices and meteorological stations in the vicinity of these sites were limited. It is important to arrive at an appropriate distance of separation that would strike a balance between

cost and accuracy. For overhead lines; wind speed, wind angle, ambient temperature, and solar radiation are parameters that strongly impact the dynamic line rating (DRL) calculations. The ambient temperature and solar radiation exhibit low variation with localized distance as it depends mainly on the sun location, coverage and time of day. It does however vary significantly for wind speed and angle depending on local terrain and vegetation. To investigate the appropriate distance of separation for the environmental parameters that vary significantly, the correlation between wind speed readings between every pair of weather stations installed were determined. Statistically, the magnitude of correlation ranges from 0 to 1. Correlation values above 0.5 would indicate that the two weather stations involved have strongly correlated readings, while those below 0.5 indicate weakly correlated readings. A weather station that is located in the forest area are expected to have poor correlation with neighbouring weather stations with an increase in distance compared to flat terrain, as found in Figure 4.37.

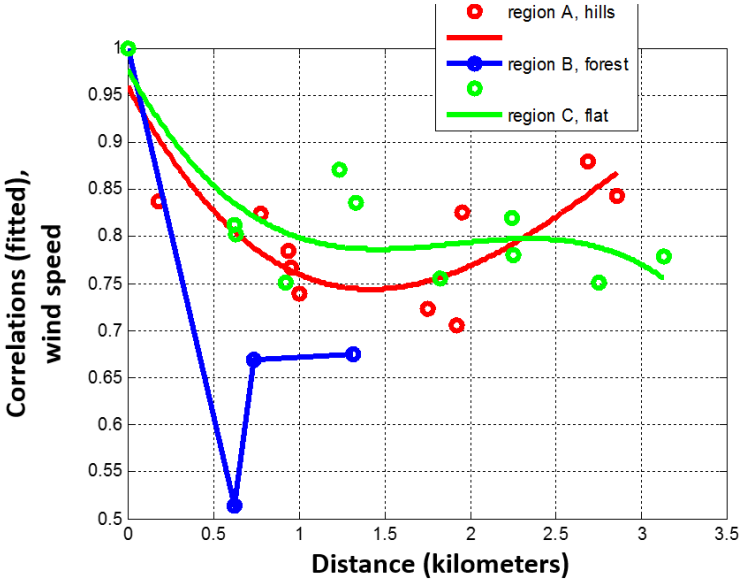

Figure 4.37 Correlation of wind speed value for varying distances and terrain

The second approach was through the use of the rating algorithm to carry out a sensitivity study of the wind speed readings that are interpolated from relatively nearby weather stations instead of an on-site weather station. The error in the current rating is recorded and grouped based on the distance between the circuit and the interpolated weather station's location. The error in rating values when choosing a monitoring site located 1.32 km away from the circuit is shown in Figure 4.38. It can be seen that the error has an almost Gaussian shaped distribution with

mean error of 24.2 A and standard deviation 101.6 A. This indicates a 95% confidence interval of almost ±200 A.

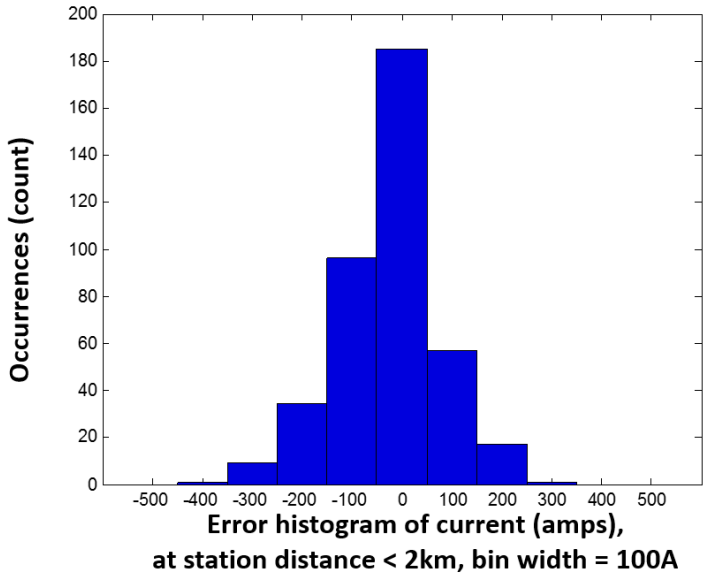

Figure 4.38 Histogram of line rating evaluation error for monitoring site within 2km distance

If the interpolation values are found to be unrealistic, a conservative approach is employed, defaulting back to the recommended environmental conditions for the different electrical components as per the values from IEC international standards discussed in Chapter 3.2.

4.4.2.2 Simulation consideration

Operation research is concerned with determining the maximum (of profit or utilisation) or minimum (of loss, risk or cost) of a real-world objective, in this case in operating and managing an electrical distribution network. Operation research provides a detailed study on decision making process from initiation all the way to implementation, identifying the wastes and benefits. This research looks at some of the aspects utilised in operation research to provide quantitative indices for management decisions, mainly in the area of cost-benefit identification. The application of the developed PAR in a 33kV electrical distribution network are evaluated. Several simulations are carried out based on the criteria outlined in Figure 4.39. The results of the simulation are collated to determine the indices to make management decision for an EDB.

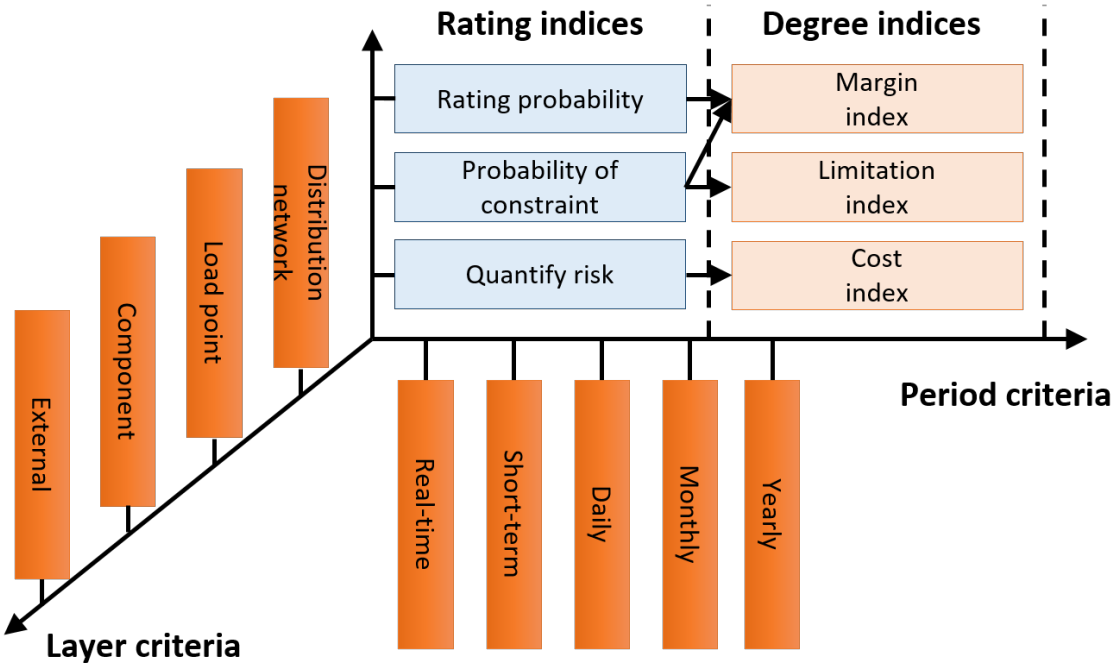

Figure 4.39 Simulation criteria and indices

The simulations are separated into two management decision criteria, decisions that are required to be provided in real-time and detailed analysis for constraints management and network planning. The applications of the PAR tool for simulation consideration are discussed here and the results of the simulation carried out for each of the management decision are discussed in Chapter 5.

4.4.2.3 Real-time network evaluation

The application of the PAR tool for real-time network evaluation focuses on providing decision support capability in the area of capacity utilisation for network operators. The tool has been developed with the following features to perform real-time analysis of electrical components:

(a) *Network operators: Monitoring of assets.*

(b) *Network operators: Capacity utilisation headroom planning.*

(c) *Network operators: Constraints identification.*

As the first step, for a given circuit, the PAR tool collate the data from the database and extract all the information required into the circuitParam structure. The PAR tool then export

the minimum amount of data required to perform real-time simulation into a table. This step is called moving from development to production seen in Figure 4.32 and the detailed step for cables as an example shown in Figure 4.40.

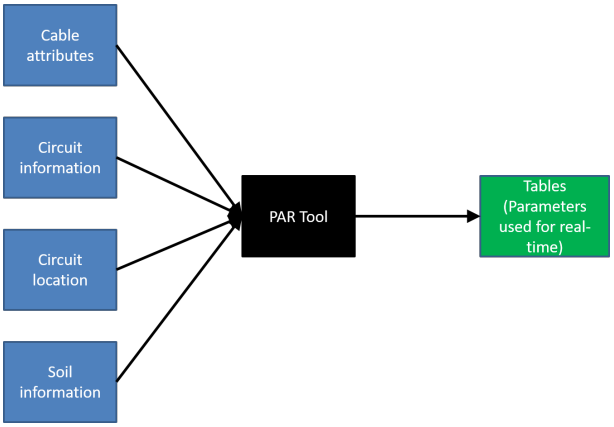

Figure 4.40 Steps for processing data into table for real-time (cables)

The tables used for real-time evaluation are the thermal parameters discussed in Section 3.2. Key parameters that have an impact to the rating of the electrical components are calculated by the PAR tool. For cables this includes the layers of the cables which reflect the rate of the heat dissipation from the cable's core to the external environment. The circuit location and soil information are also captured and represent the measurement point for interpolation. With the base algorithm of the PAR tool deployed onto the server, the rating calculations reference this table and are scheduled by the PI ACE system. This was possible with the help of the System Integrator at Unison. A similar concept has also been employed for power transformers and overhead lines. The parameters selected are based on its sensitivity to the rating evaluation model and will be discussed further in Chapter 5.

4.4.2.4 Detailed network evaluation

The application of the PAR tool for detailed network evaluation focuses on providing scenario analysis and decision support capability in the area of network planning and constraint identification for network planners and asset managers. The tool has been developed with the following features to perform detailed analysis of electrical components.

(a) *Network planning: network expansion.*

(b) *Network planning: capacity utilisation.*

(c) *Asset management: loss of life due to circuit loading.*

(d) *Asset management: asset design specification.*

As discussed in Section 3.4, different reliability assessment methodologies have been investigated. Based on an extensive literature review and evaluation, Monte Carlo simulation has been found to provide the best methodology for scenario analysis and reliability assessment. The tool developed utilises the same data for real-time however with additional ability to specify varying location and conditions for reliability assessment as shown in Figure 4.41.

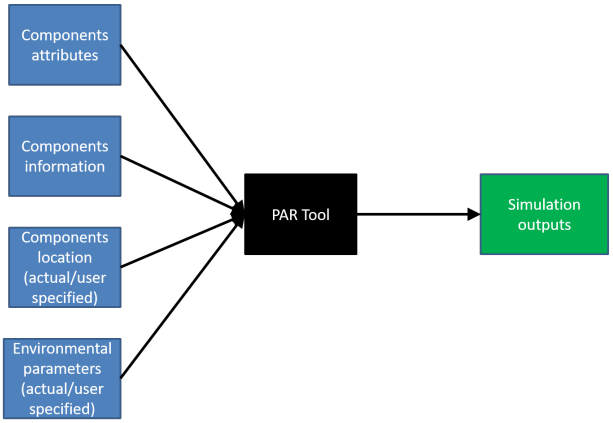

Figure 4.41 Steps for processing data for detailed network evaluation

The component's attributes and information provides a baseline on the expected rating. Then using the evaluation model proposed in Section 3.4, the electrical components are evaluated considering the component's location and the expected environmental parameters. Based on the simulation, the optimal components are ranked and provide quantitative indices for decision making considering the capacity utilisation margin, expected limitation and costs.

4.5 SUMMARY AND CONCLUSIONS

This chapter presented the application and implementation of the developed system for an electrical distribution network. The service area under study and the electrical components on Unison's network have been presented. The available datasets and its distribution has been presented, extracted from available monitoring devices. Validation steps taken to evaluate interpolated environmental conditions at unmonitored location have been discussed. Where uncertainty of the

environmental condition data exist, a weighting factor relative to the rating has been applied. The manufacturer's rating has been used as the base rating for component's thermal rating model evaluation. The evaluation then looks at the percent increase or deficit from the base value. To provide a holistic evaluation for the network considered, the utilisation of the assets were measured as a probability and scored against the decision indices covering rating margin, asset limitations and cost. The development ensures the tool is flexible and modular to carry out different types of simulation required by EDBs. The evaluation of the network using the PAR tool is discussed further in Chapter 5.

Chapter 5

RESULTS AND DISCUSSION

5.1 OVERVIEW

In this chapter, the results of the research are presented. This chapter highlights the key deliverables of the research, looking at the pattern observed when using predictive asset rating model under different challenges faced by distribution network. The results are presented focusing on the model's ability to optimise the utilisation and planning of power transformers, overhead lines and underground cables. The findings are then discussed to provide electrical distribution networks opportunities to improve decision making process in the business using the developed model.

5.2 INTRODUCTION

The model and its validation have been discussed in previous chapters. This chapter covers the model's ability in solving challenges experienced by a modern network due to consumer technological shifts. Network companies are constantly looking for an opportunity to reduce expenditure on the network to keep electricity prices low. Increased pressure from the government and consumers ability to choose an alternative secondary source of electricity also plays a role. The developed model will be used to predict a suitable rating for distribution assets under the following scenario:

(a) *Ability to provide rating predictions during load transfer*,

(b) *Ability to provide an optimised selection of assets for network expansion*,

(c) *Ability to account for distributed generation,*

(d) *Ability to predict capacity utilisation of the network and provide decision support.*

To provide context to the discussion of the different scenarios, three possible events under each category has been selected. Other scenarios that can also be considered are highlighted in Chapter 5. The next sections will make reference to the algorithm developed, outlining how the individual steps are used to solve the different challenges for a distribution network. The network under study was discussed in Section 4.2.1 and will be used again throughout the next sections.

5.3 PREDICTIVE ASSET RATING FOR ELECTRICAL DISTRIBUTION NETWORK

The data gathered from distribution assets will be used with the developed model throughout this chapter to collectively evaluate the capacity utilisation of the assets and tackle challenges experienced in an electrical distribution networks. The data processing were discussed in Section 4.2. The algorithm discussed in Section 3.4 is outlined here again for quick reference as shown in Figure 5.1. The interface shown in Figure 5.2 will also be mentioned throughout the section to provide context of the simulation carried out.

To compare the results produced by the developed model, the probability density function (PDF), cumulative distribution function (CDF) and quantile-quantile (q-q) plot will be used throughout this chapter. The PDF and CDF are used compare the simulation results and its distribution whilst, the q-q plot is used to test for equality between the PDF produced. A linear q-q plot suggests equal distribution whilst a variation towards negative suggests a reduced probability and vice versa for positive variation [Thas 2010].

5.3.1 Network control and operations

This section looks at how the PAR models were used to solve daily challenges faced in the industry to transfer load from one circuit to another due to an abnormal condition on the network. The main challenge discussed here will be focused on optimising capacity planning during contingency events and how the developed models are used to solve the challenges involved.

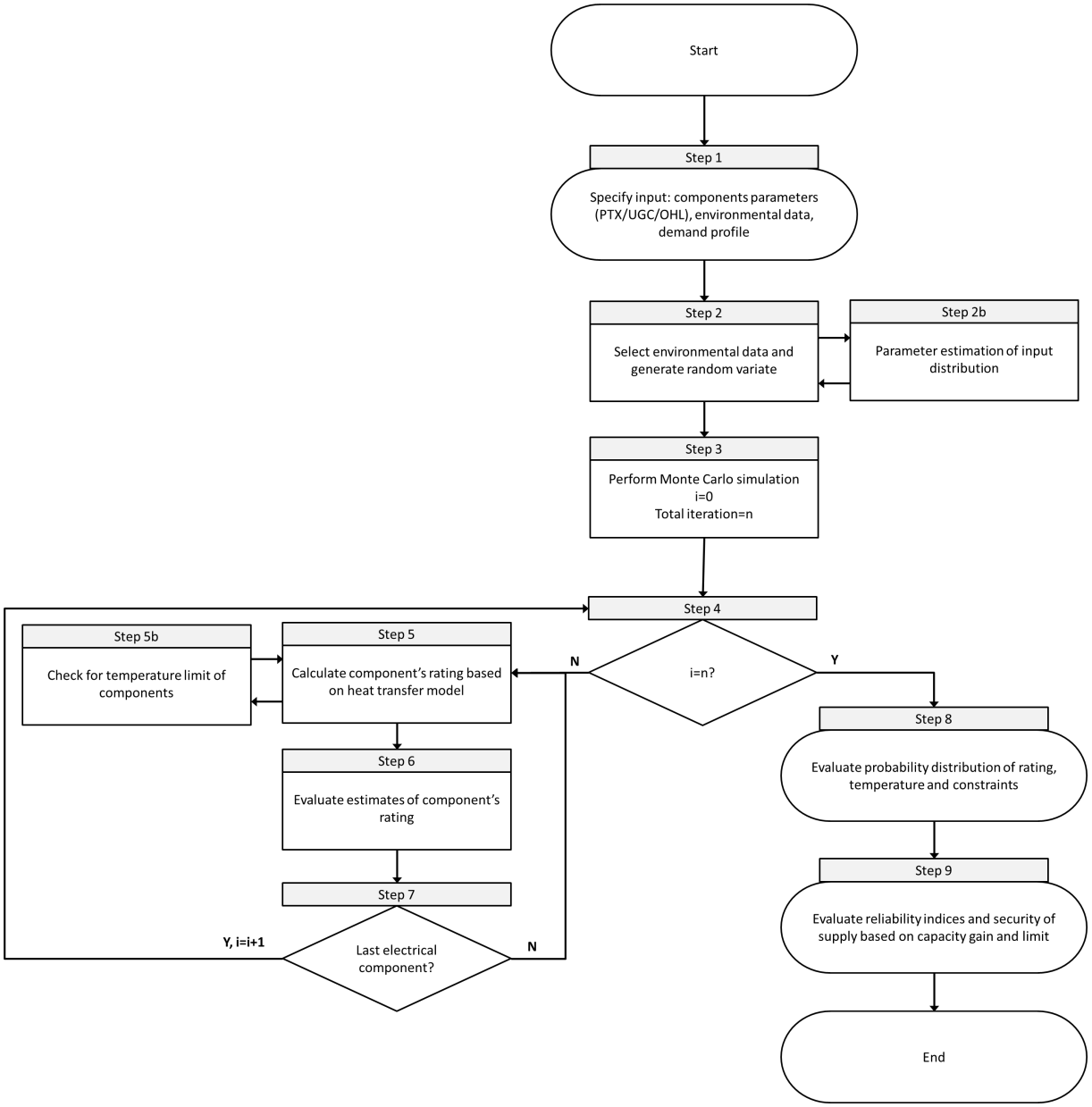

Figure 5.1 Predictive asset rating model

The circuits considered supplies an area with a total load demand of 60 MVA in winter and 46 MVA in summer. The network single line diagram is shown in Figure 5.3. Different scenarios of load transfer were studied and the PAR model's were used to identify the optimal circuit to be used during load transfer. The asset ratings are modelled in Step 6 of Figure 5.1. The load transfer scenarios (LTS) considered are outlined in Table 5.1.

The results from the simulation will be discussed in the next subsections to demonstrate how the results from PAR model can be used in network control and operations.

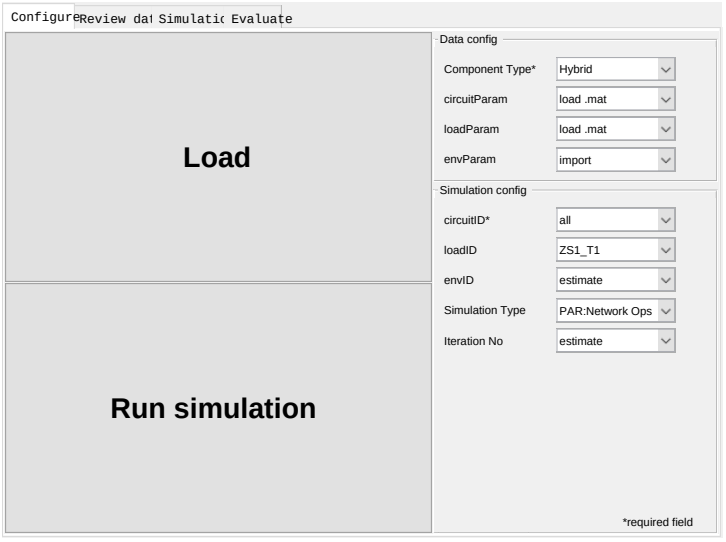

Figure 5.2 User interface for predictive asset rating tool

Table 5.1 Load transfer scenarios (LTS)

Scenarios number	Description
LTS000	Normal condition - comparing observed and PAR outputs.
LTS001	An outage on one circuit.
LTS002	One source of supply - simulating supply sourced from only one grid exit point.

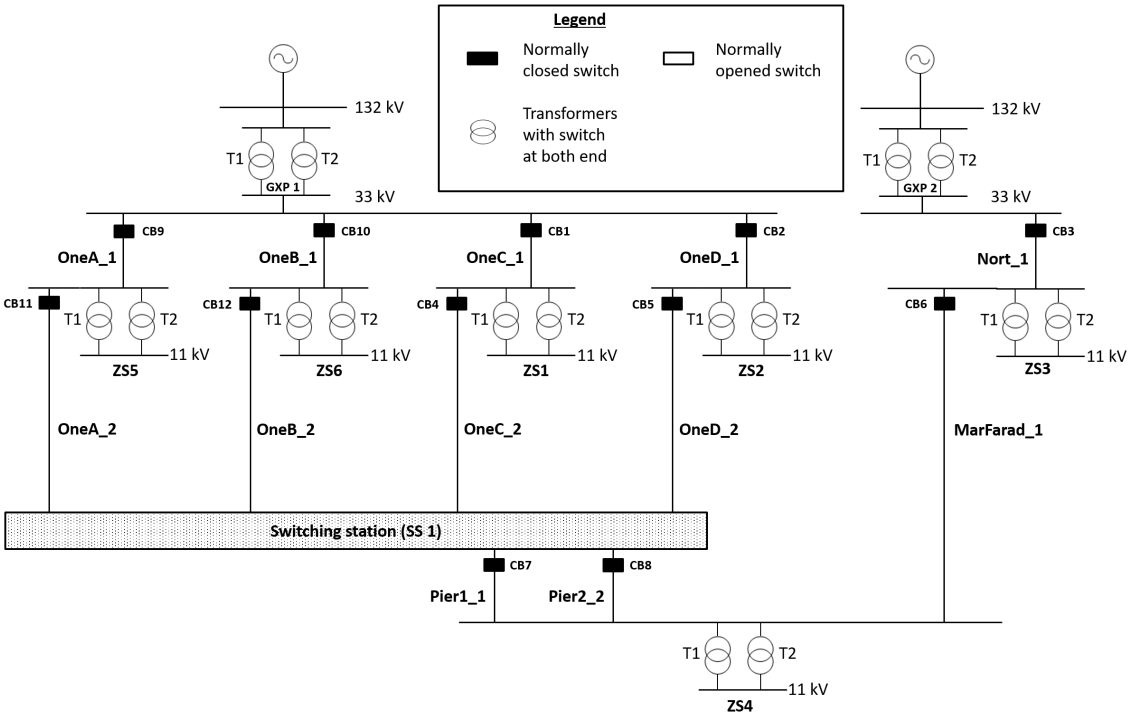

Figure 5.3 Single line diagram of network under study

5.3.1.1 Available capacity during load transfer

The circuits with prefix *ONEC* and *ONED* are analysed in this section. These circuits were selected as they're commissioned as a double circuit requiring the two working in parallel. The breakdown of the circuit has been discussed in detail in Table 4.1, consisting of mainly XLPE underground cables and ACSR overhead lines. It was found that in all of the cases considered, the limiting factor for the circuits is the power cable with a maximum continuous rating of 704 *amps* when based on the manufacturer's design condition. The simulation results in Figure 5.4 shows the predicted rating under the different scenarios described in Table 5.1 with the circuit loading shown in Figure 5.5.

The results in Figure 5.4 presents the estimated circuit rating when considering the environmental conditions experienced by the asset with data dated back to 1985. *LTS002* are simulated by assuming there was an outage at *CB3* in Figure 5.3 thus requiring the power to be routed from *CB1*, *CB2*, *CB9* or *CB10* through to *CB6* to ensure the consumers connected to *ZS3* remains with power. *LTS001* are simulated by assuming the adjacent circuit has an outage

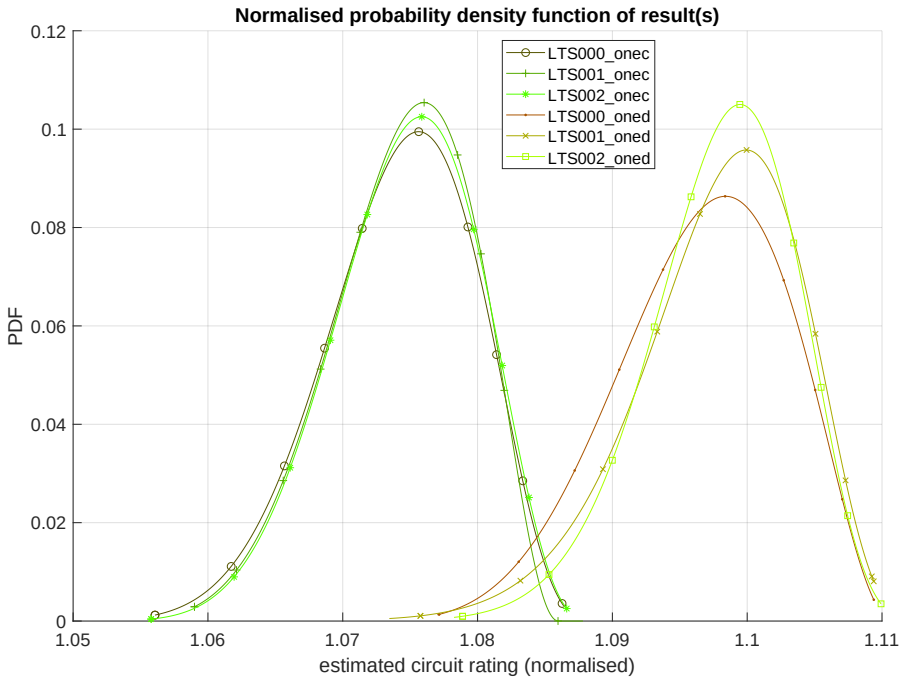

Figure 5.4 Probability of rating for varying load transfer scenarios

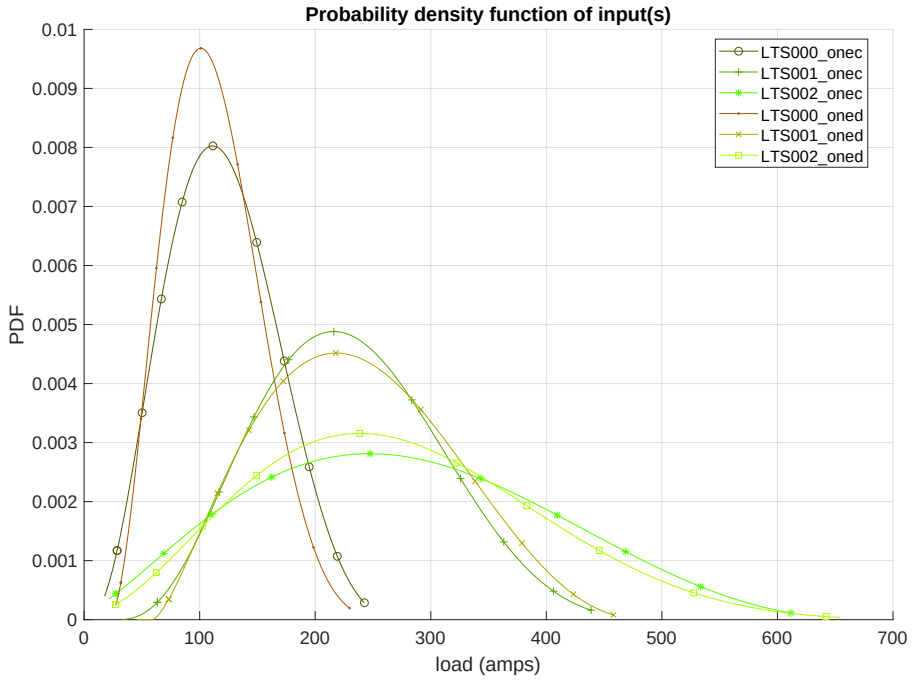

Figure 5.5 Distribution curve of load for varying load transfer scenarios

thus requiring circuit to be back-fed to ensure continuity of supply. The estimate circuit rating has been normalised against the manufacturer's design conditions to present the relative difference. One would expect the available capacity to be higher than the manufacturer's rating when the observed environmental conditions is favourable such as lower air temperature, higher wind speed and improved soil thermal diffusivity since the equations that relates this conditions to the heat transfer across the electrical components leads to a lower $\Delta\theta$ in (3.1), (3.16) and (3.37), a reduction in the overall temperature. The developed model provides the ability for network operators to collectively consider past and present operating conditions to estimate the circuit rating. It can be seen in Figure 5.4 that when the observed environmental conditions is considered, the expected available capacity can be up to 1.11 higher than the manufacturer's rating as seen for the *ONED* circuit. From the result, it can be identified that the circuit *ONED* is the best path to use under any contingency event based on the higher expected rating under different load transfer scenarios, up to 3.5% higher as seen in the q-q plot shown in Figure 5.6. The circuits *ONEC* and *ONED* also have an equal probability of getting the expected value of 1.073 and 1.095 rating factor respectively based on the linear trend.

5.3.1.2 Operate based on risk and performance

The PAR model provides the ability to rapidly evaluate the available capacity of the network under varying loading and environmental conditions. Through Monte Carlo simulation, samples of the conditions are selected at random to determine the expected value of the asset ratings. When the *PAR:Network Ops* simulation is selected, the model focuses on calculating the ability of interconnected electrical components: power transformers, overhead lines and underground cables to carry out load transfer scenarios. Each simulation allows the network risk to be evaluated based on the likelihood of achieving a rating for a given operating limits of the network such as maximum operating temperature and protection settings, given as,

$$F(x|a,b) = \frac{1}{B(a,b)} \int_0^x x^{a-1} (1-x)^{b-1} \, dx \tag{5.1}$$

where, a and b are the shape parameters of the distribution and $B(a,b)$ is the beta function

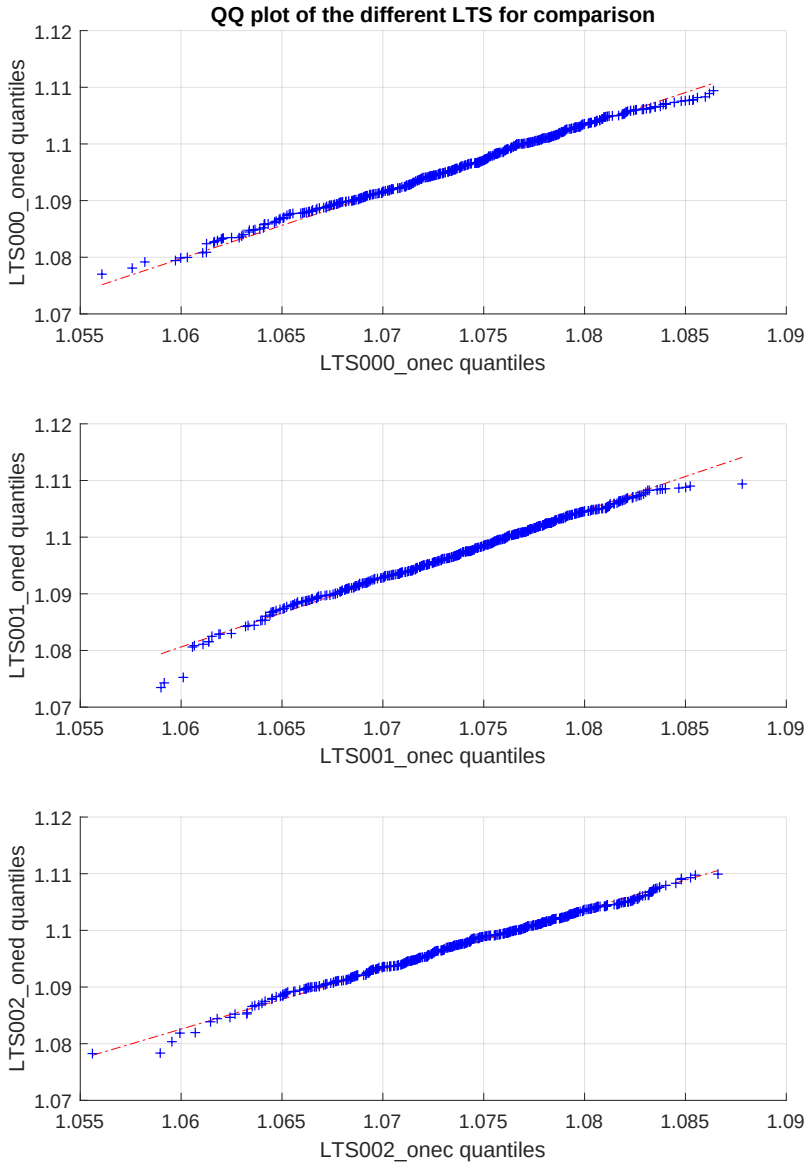

Figure 5.6 Comparison of ONEC and ONED circuit rating PDF

that's fitted to the expected rating. In a network outage scenario, x will be the rating estimates when exposing the electrical components to different operational and environmental scenarios. Simulating for the different scenarios allows network operators better control over the choice of expected rating for the circuits, balancing the operation based on improved rating whilst maintaining the network risk. Choosing a higher rating while knowing with some certainty the risk involved and vice versa. Consider one of the present practice where in the event of abnormal conditions, load flow studies are carried out to determine whether the electrical components are overloaded. In the past and to-date, these studies have been carried out using static environmental conditions such as the seasonal value, thus, not reflecting the conditions experienced by the asset on a day-to-day basis. Comparing the rating of cables commissioned in different operating conditions and normalising it against the static rating, it can be seen in Figure 5.7 that the estimated rating are consistently higher, suggesting that the assets have been installed in relatively better environmental conditions than the conditions suggested for static value.

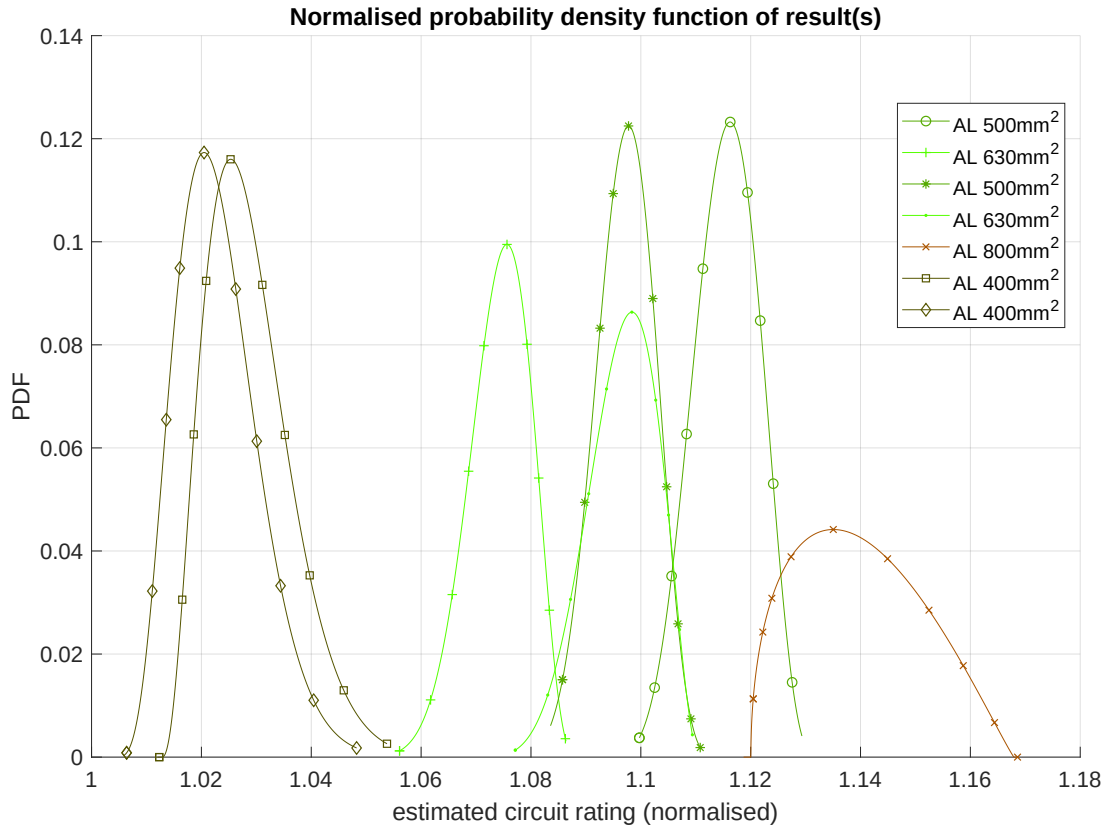

Figure 5.7 Comparison of in-situ rating as a factor against static

If the asset were commissioned in a poor environment, a factor less than one would be expected. Stacking up the results looking at the risk of overheating, it can be seen in Figure 5.8 that the circuits can be operated comfortably between 27 and 35°C. The circuit with the highest risk of overheating is *NORT* with 39°C of headroom to the 90°C limit of XLPE cables.

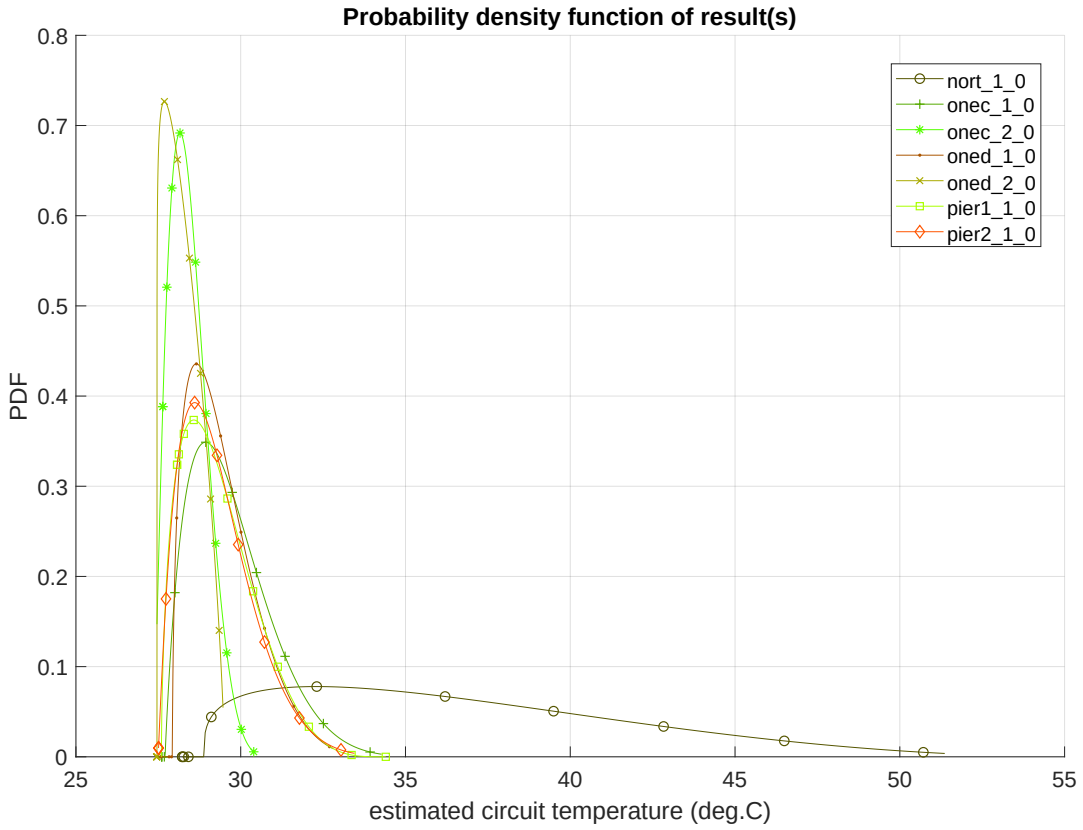

Figure 5.8 Probability of overheating on the circuit

5.3.2 Asset health and constraints

This section looks at the constraints model focusing on thermal and mechanical constraints. The circuit constraints are modelled in Step 5 and 5b of Figure 5.1 whilst still ensuring the capacity are optimised through the predictive rating model. The results of the constraint model will be demonstrated in this section.

The thermal constraints are modelled based on the heat transfer equation of the three elec-

trical component discussed in Chapter 3, consisting of power transformers, overhead lines and underground cables, where their thermal constraints were given as,

$$\theta_{ptx} = \theta_a + \Delta\theta_{oil} + \Delta\theta_h \tag{5.2}$$

$$m \cdot c_p \cdot \frac{d\theta_{ohl}}{dt} = W_{gen} + Q_{sun} - Q_{radiation} - Q_{convection} \tag{5.3}$$

$$\frac{1}{\alpha}\frac{\delta\theta_{ugc}}{\delta t} = \frac{\delta^2\theta}{\delta x^2} + \frac{\delta^2\theta}{\delta y^2} + W_{gen,n} \cdot T_n \tag{5.4}$$

while θ_{ptx}, θ_{ohl} and θ_{ugc} is less than their respective maximum operating temperature, θ_{max}. The design temperature of the components were used and gathered from the manufacturer's technical specification. The temperature limit under normal continuous operation for the different electrical components as discussed in Chapter 3 are summarised in Table 5.2.

Table 5.2 Temperature limit of electrical components

Electrical components (type)	**Max operating temperature ($^\circ C$)**
PTX (oil-immersed)	105
OHL (ACSR)	75
UGC (XLPE)	90
UGC (PILC)	75

For mechanical constraints, only OHL are considered looking at the sag-tension model. The constraints are determined by ensuring the clearance of objects surrounding the OHL are within the specified standard safety limit as illustrated in Figure 5.9. The clearance limit for different objects are summarised in Table 5.3. As mentioned in Chapter 3, the limit given are based on New Zealand application and will vary for different countries based on local regulations.

The OHL clearance constraints covered in this research only look at a subset of objects in the proximity of the OHL. For other objects such as near houses and refined clearance limit, readers

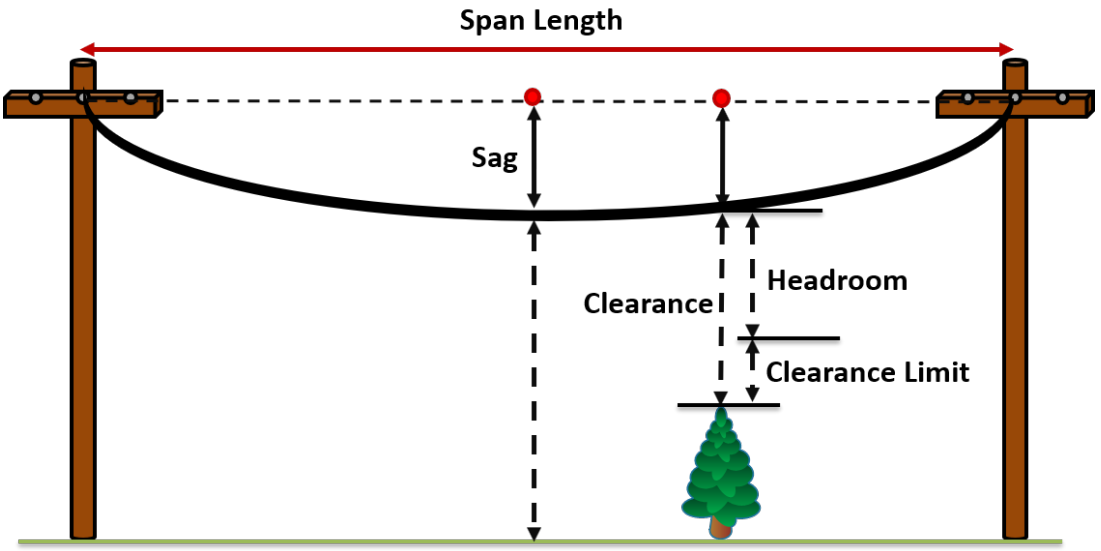

Figure 5.9 Illustration of span clearance limit

Table 5.3 Clearance limit of 33kV OHL in New Zealand

Object	Minimum clearance (m)
Ground	6.5
Non-electrical	4.5
Non-electrical (non-traversable)	3.7
Electrical (11kV)	1.2
Electrical (400V)	1.5

can make reference to the "AS/NZS 7000 - Overhead Line Design" [AS/NZS 7000 2016] which will not be discussed in detail here.

Performing the simulation with mode "PAR: Constraint Management" determines the likelihood of constraints on the network and suggests an optimised solution to resolve the issues. This is achieved in the algorithm by sampling the operating conditions of the assets, determine the expected constraint of the asset by evaluating (5.2), (5.3) and (5.4) solving for temperature, θ. Once evaluated, the location of the constraint at each iteration are captured and finally scored.

To demonstrate this, the NORT circuit has been selected as it has the highest percentage of overhead with 87% and the remaining of the circuits are made up of three different types of

underground cables, AL 500mm^2, CU 500mm^2, and AL 800mm^2. The output in Figure 5.10 shows the result of a single constraint simulation showing the overall span's height profile of the NORT circuit at the sampled condition. Zooming in to span 130, it can be seen in Figure 5.11 that the clearance headroom is 1 m which is 0.2 m lower than the required clearance limit of 1.2 m seen in Table 5.3. The critical clearance location to an object (other conductors, crossing line, shortpole, trees, fence or ground) are also captured as marked and labelled in Figure 5.11. These metrics are captured at each iteration to determine the probability of constraints occurring under different operating conditions. Constraint management simulation were carried out on the same part of the network for *NORT* based on the scenarios outlined in Table 5.4.

Table 5.4 Constraint analysis scenarios (CAS)

Scenarios number	Description
CAS000	Baseline - simulated at an arbitrary time for each component type
CAS001	Introduce conditions that increases constraints for each component type
CAS002	Introduce conditions that reduces constraints for each component type

The scenario *CAS000* looks at the constraints of electrical components based on the environmental conditions experienced throughout the year. For *CAS001*, the simulation will prominently use the distribution of environmental conditions in summer where higher temperature and longer exposure to solar radiation are observed. The opposite is selected for *CAS002* by choosing environmental distribution fitted during the winter period. The results of the constraint analysis scenarios are shown in Figure 5.12 showing the expected monthly rating value. It is observed that January is the worst performing month for this circuit, able to only achieve 229 amps due to constraints on the network. Whilst July provides a lot of opportunity for load transfer if remedial work needs to be performed on either of the circuit, OneA, OneB, OneC and OneD supplied from GXP1 in Figure 5.3.

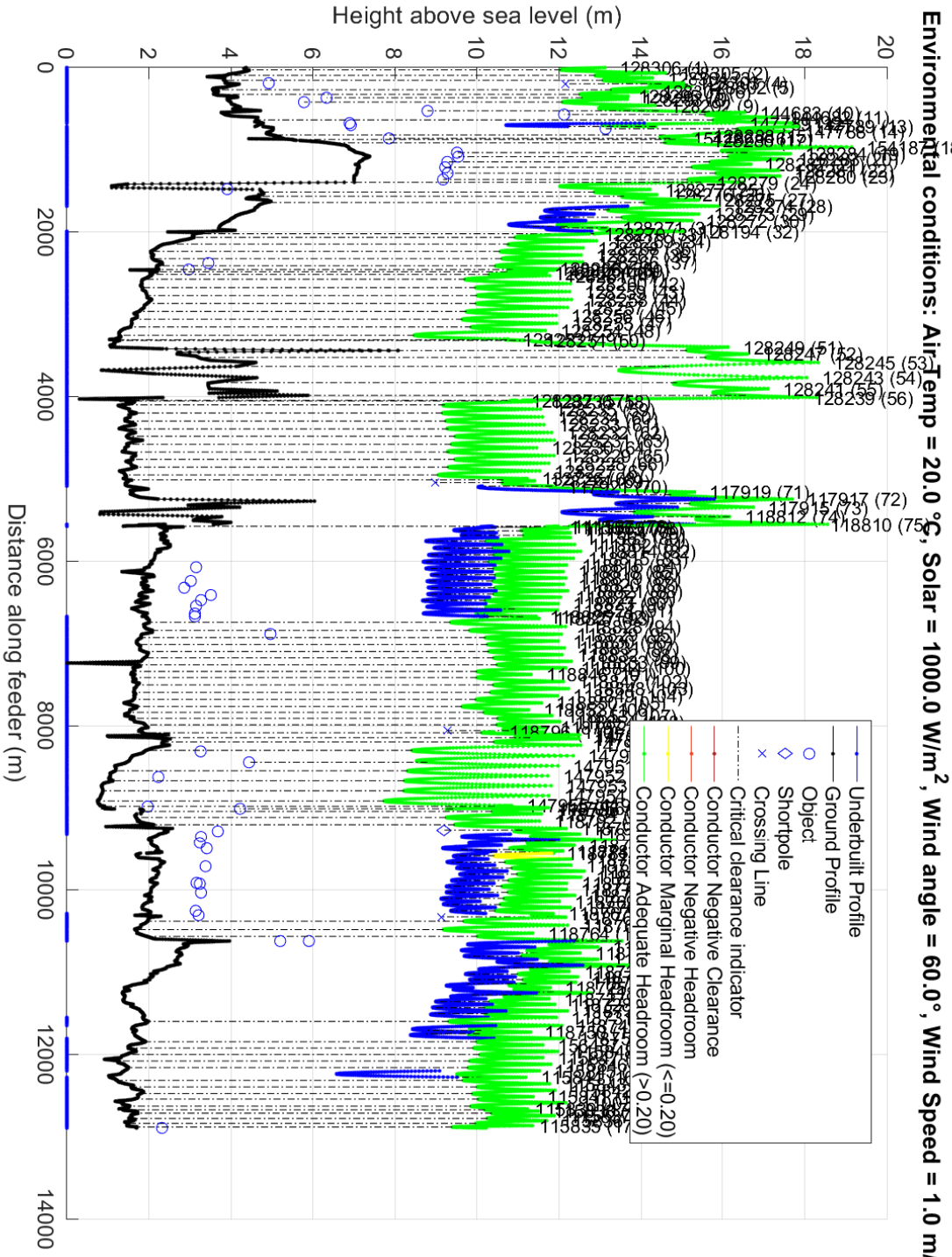

Figure 5.10 Constraint analysis at observed environmental condition

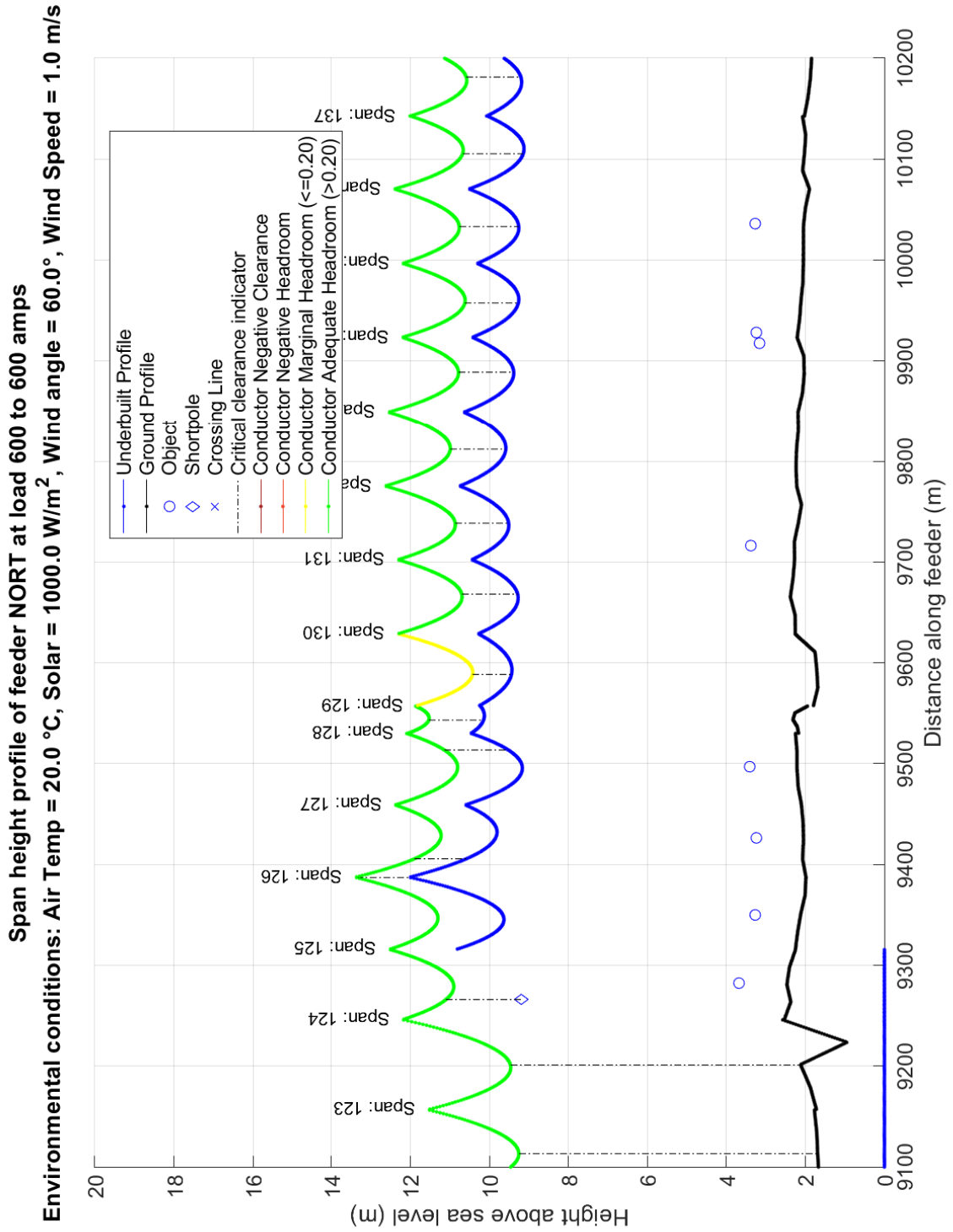

Figure 5.11 Constraint analysis at observed environmental condition (span 123 - 137)

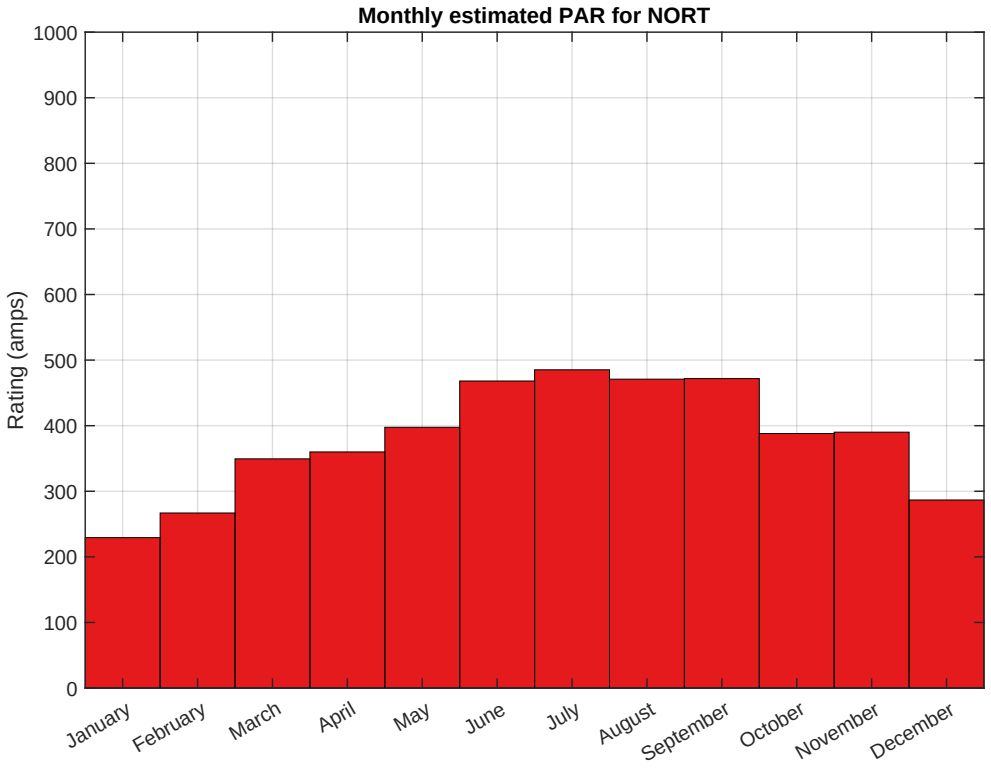

Figure 5.12 Predictive asset rating for NORT circuit

5.3.3 Network expansion planning

Consumer behaviour on energy use varies due to seasonal and uptake of technologies as discussed in Chapter 2. This is demonstrated in Figure 5.13 which shows the breakdown of load demand at different parts of the network, with *CB1* containing the simulated technology uptake, showing a slight increment in the overall current. As the capacity headroom decreases, the decision to upgrade or redistribute the load needs to be made. The algorithm in Step 9 of Figure 5.1 was developed to provide network expansion decision support capability. This is achieved by utilising the load demand and consumer behaviour data to identify potential constraints and expected headroom of the network. The different inputs are considered in Step 1 to Step 3 of the algorithm. The result of determining the optimised electrical components to meet the desired load demand and consumer behaviour are presented in this section.

It can be seen that the circuits studied are lightly loaded with the highest value off 400 amps recorded on *CB3*. Under installed conditions there are no immediate requirements for network

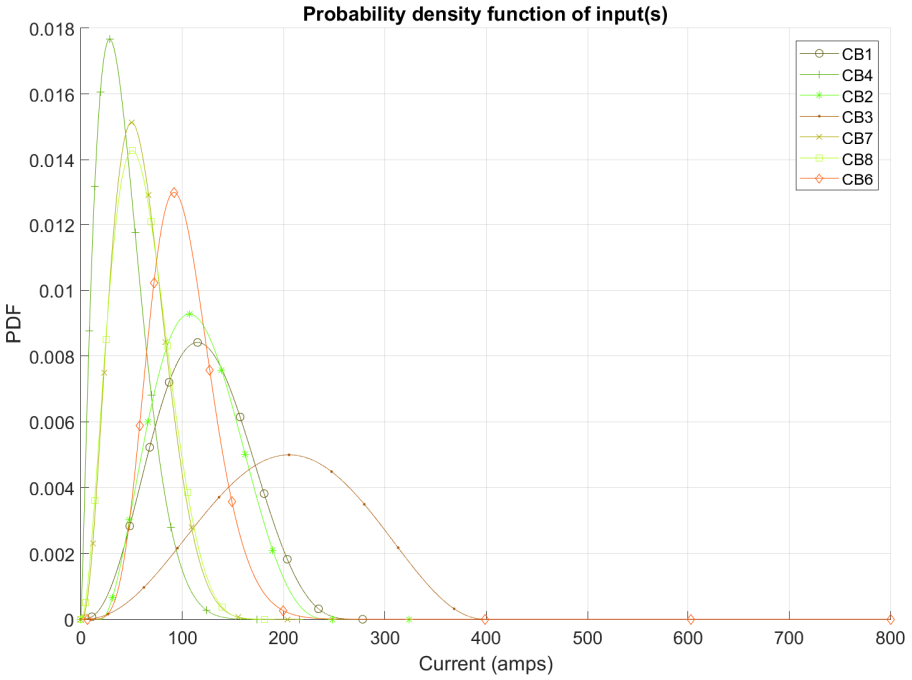

Figure 5.13 Collection of load demand and consumer behaviour data

expansion. To simulate possibilities of network expansion, the scenarios outlined in Table 5.5 were carried out. The simulations were performed to highlight the model's ability to score and rank different parts of the network based on the capacity headroom and identify areas on the network that can be optimised to meet load demands.

Table 5.5 Network expansion scenarios (NES)

Scenarios number	Description
NES000	Baseline - load demand with no back feeding
NES001	Introduce load variation based on forecasted load demand

The scenarios will be focusing on the load center at *ZS4* which can be supplied by *MARFARAD*, *PIER1* and *PIER2* as per Figure 5.3. The distribution circuits are made up of purely UGC with type and size of AL 300mm^2 and AL 400mm^2. To provide context to the scenarios, two approaches to tackle network expansion are compared first in this section, deterministic and probabilistic. The later approach is the methodology used by the developed algorithm.

Deterministic approaches in network expansion are still practised by most utilities where a criteria for replacement is determined up-front. A common approach is to assume the forecasted load demand to be linear and replacement are required when network capacity reach a pre-set capacity utilisation, for example 80%. Given the load demand of *ZS4* between the year 2012 to 2015 shown in Figure 5.14, the absolute peak load were selected. In an ideal scenario, the peak demand needs to be based on the base load of the zone substation not accounting for back-feeding as this period often occurs for a short period of time and does not lead to thermal stress on the network. Raw load are used throughout this chapter to allow consistent comparison. Based on the yearly peak for *ZS4* and interpolating the data until 2021 based on least square regression, it can be seen that the circuits supplying *ZS4* needs to be upgraded in 2019 to meet the deterministic criteria of 80% capacity utilisation. The down side of deterministic approach is that the likelihood of the capacity constraints are not measured which introduces a higher error if the operating conditions changes as the scenarios are not accounted for.

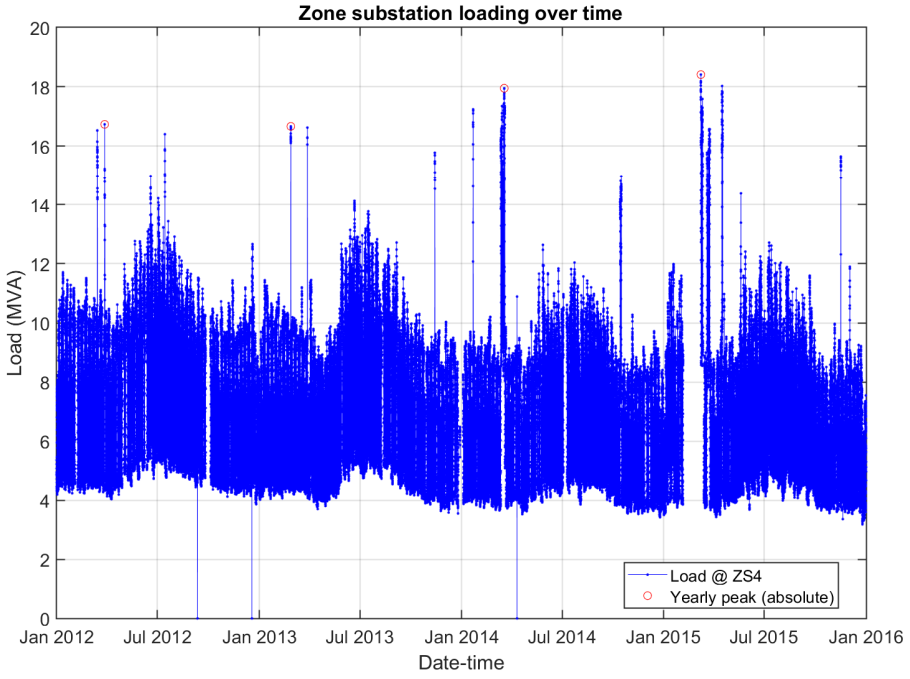

Figure 5.14 Half-hourly load profile for ZS4

Looking at the same problem in a probabilistic manner, other than just looking at the load for each year, conditions that can likely change the capacity headroom of the circuit are also

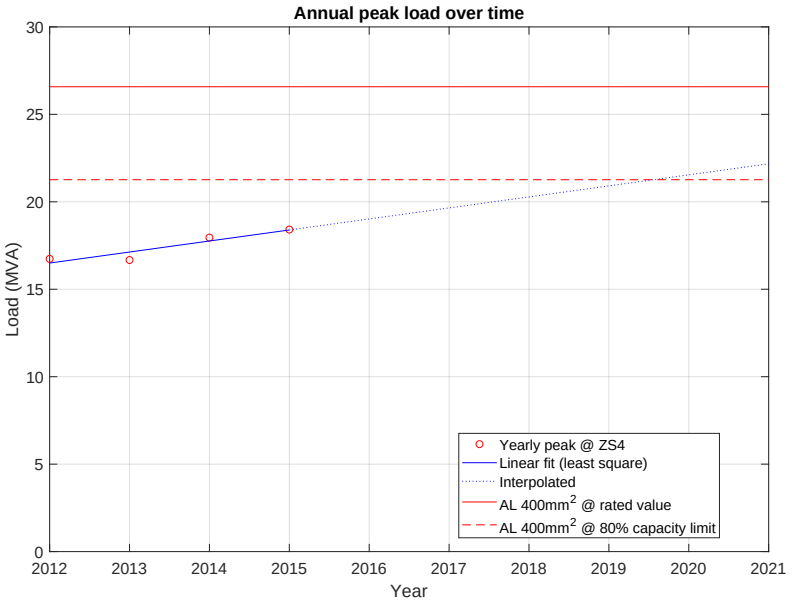

Figure 5.15 Load forecast for ZS4 based on linear trend with deterministic capacity limit

considered. As an example, it is known from the collected data that the air temperature of the region ranges from 5°C to 30°C with an average temperature of 18°C as shown in Figure 5.16.

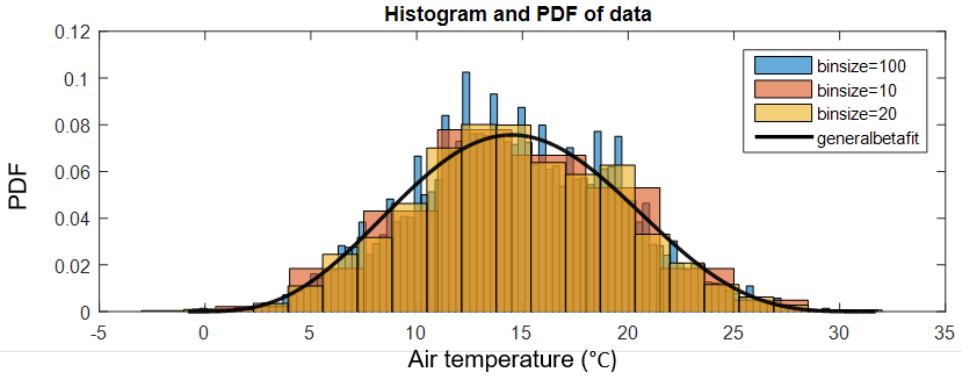

Figure 5.16 Air temperature at ZS4

It can be seen that the likelihood of the air temperature to be at the maximum value of 30°C is low. Using the dataset to evaluate the predictive rating of the circuit, it can be seen in Figure 5.17 that at 95% confidence interval, the likely capacity available on the circuit is higher than the rated value. Based on this information the network expansion can be delayed and wouldn't need replacing in 2019.

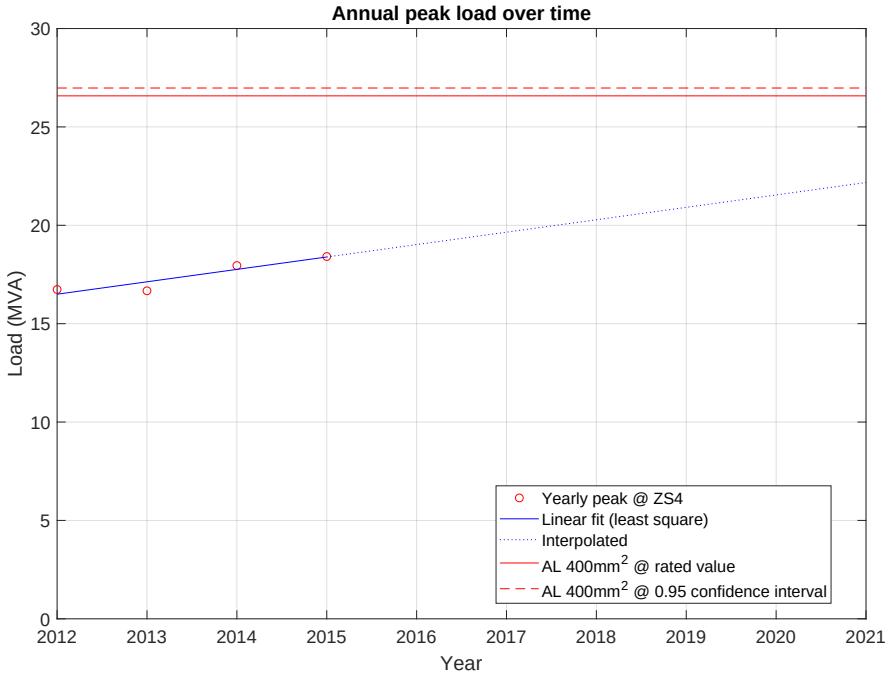

Figure 5.17 Load forecast for ZS4 based on linear trend with probabilistic capacity limit

As the probabilistic capacity evaluation considers past and the likely weather going forward, there is a higher certainty of the calculated available capacity. To demonstrate the use of PAR in network expansion studies, the scenarios listed in Table 5.5 were considered. The *NES000* scenario focuses on providing a point of reference on the capacity utilisation of the network with the load demands as shown in Figure 5.13. The impact of increased demand to the capacity utilisation of the network expansion is simulated in *NES001* scenario. The forecasted load demand based on linear regression shown in Figure 5.17 is factored year-on-year to generate a forecasted load distribution.

In an electricity distribution service where price-quality regulation exist, profits are limited and investment needs to be optimised to ensure consumers demands on service quality are met. Through a centralised decision making processes it is hypothesised that requirements for network investment can be highlighted through distinct criteria. This is the basis of this research which looks at day-to-day decision making process that occurs within an electrical distribution network. One of the main topic this research focuses on is the capacity utilisation of electrical components, which is seen as the main backbone of the network needed to ensure quality of

supply. This topic is discussed in Section 5.4.3.1. The developed model looks at the impact of different environmental conditions to asset rating, then aggregates and quantifies the impact for different decision making processes in an electrical distribution network which will be discussed in the next section.

5.4 DISCUSSION

The results presented have demonstrated how different steps of the algorithm shown in Figure 5.1 can be used to solve challenges faced by network operators. Used collectively it provides a new capability for decision making in an electrical distribution network. The steps utilised in the simulations will be discussed in the following sections to highlight how the developed model provides an improvement in the industry over past practices. The steps will be discussed in three parts:

(a) *Processing raw data*,

(b) *asset rating computations*,

(c) *decision making process*.

5.4.1 Processing raw data

The processing of raw data for the simulation made references to Step 1 to Step 3 of the PAR model shown in Figure 5.1. Step 1 of the model provides the ability to specify the input. The inputs are imported as either one of the following file extensions: MATLAB (.mat), Excel (.xls) or JavaScript Object Notation (.json). It was decided to support these file types as they are seen as the most commonly used in the industry other than a raw text file. The use of a raw text file, such as .csv, .txt and similar file format were also considered. It was however decided for this to be pre-processed prior to importing it into PAR. Doing so allows better exception handling if the user selected an unrecognisable file format. Raw text files are parsed to a .json using the MATLAB built in function, $jsonencode()$. The generated .json can then be imported for processing in PAR.

The data required to run the model were gathered using existing infrastructure available at

Unison. The three parameters needed are the circuit, load and environmental data as discussed in Chapter 4 and reprinted in Figure 5.18 for reference.

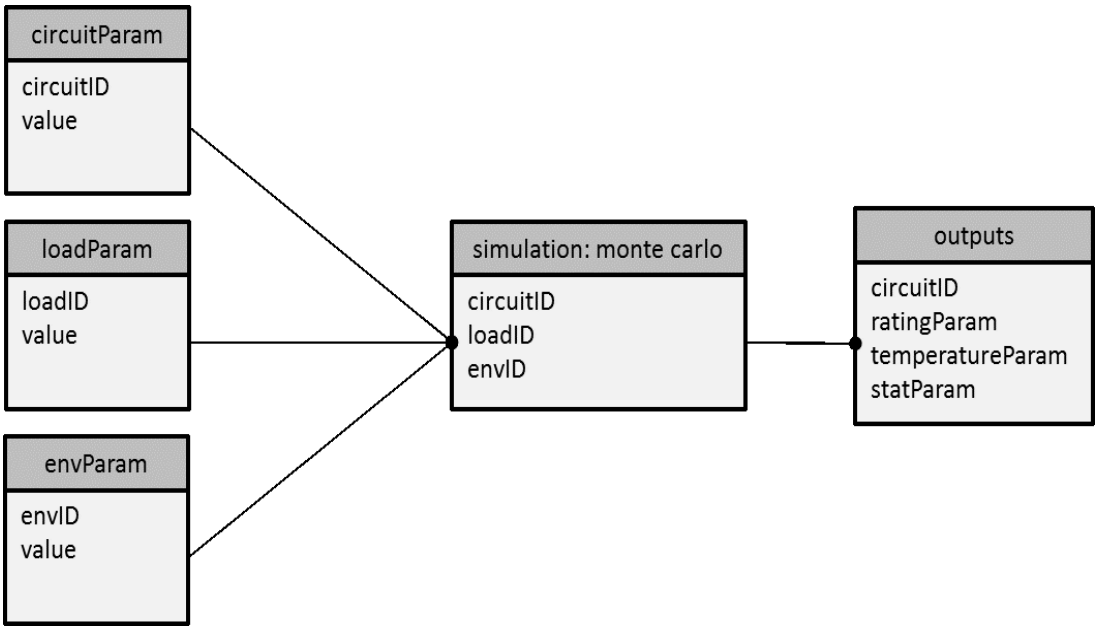

Figure 5.18 Data model of PAR tool

At this stage of the algorithm, the raw inputs are fitted to the generalised beta distribution (GBD). As highlighted in Section 3.3.2, the GBD is appropriate since the distribution allows for the shape of the probability density to change depending on the fit to the observed data. These characteristics of GBD are seen as a good fit to the model since even if the probability density of the raw data are not known in advance, a good distribution fit can still be determined by estimating α and β of the beta distribution function. For this particular case, utilising GBD provides a refined probability distribution compared to just using the Rayleigh distribution which has been used extensively for the probability density function (PDF) of wind speed data.

The input data are transformed by a series of operations to clean up the data, a step mentioned in Chapter 3 and Chapter 4 as data curation. The operations are selectively used by the model looking at stale data, impossible rate of change and errors in data capture. For stale data, data curation is performed in the model by looking at periods where the second derivative of the data is zero for more than a specified stale period. Based on known sampling rate and to remove incomplete data from the monitoring stations, the stale period threshold for the different environmental conditions shown in Table 5.6 are used. During this step, outliers are also removed

by looking at the gradient of the data that's above or below an abnormal value.

Table 5.6 Stale period threshold

Environmental conditions	Duration
Air Temperature	2 hours
Wind Speed	3 hours
Wind Angle	3 hours
Solar Radiation	16 hours
Soil temperature	6 hours
Soil thermal resistivity	6 hours

Consider the raw air temperature data from a weather station shown in Figure 5.19. The trend in Figure 5.19a shows an extreme value that's very unlikely for an air temperature. For the same set of data looking closely at period shown in Figure 5.19b, a stale data can be identified at 16 Dec. Likely caused by a lost of communication to the monitoring station which is very common for field devices. Without evaluating the raw data through Step 1 to 3, a poor distribution fit is observed as shown in Figure 5.21. The curation process leads to the result shown in Figure 5.20.

After identifying and filling the anomalies where possible, an improved fit was achieved as shown in Figure 5.22a. The curation step is important to ensure a representative distribution fit to the data is achieved. The process built into Step 1 to 3 of the algorithm can be applied to different sets of data used by network operators.

This step was applied to every environmental data considered to determine the shape parameters of the distribution. The parameters are reused to generate random variate that's applied to different scenarios of network evaluation such as the scenarios listed in Table 5.1, Table 5.4, and Table 5.5. The monthly distribution of the different environmental data are shown in Figure 5.22 and Figure 5.23, each of which has a distinct shape. The shifting of the expected value for the different seasons can be easily identified through this approach as seen for air temperature in Figure 5.22a and wind speed in Figure 5.22b.

5.4.2 Asset rating computations

When comparing the rating model, the manufacturer's rating has been selected as a baseline. Manufacturers use a common set of environmental conditions based on industrial standards

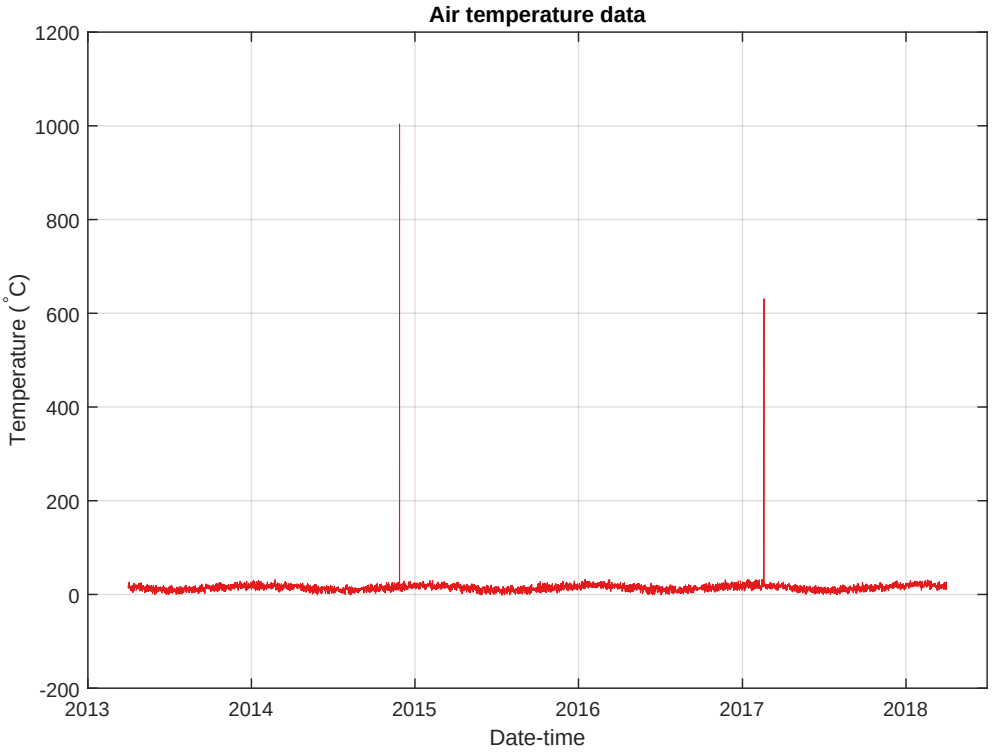

(a) Outliers

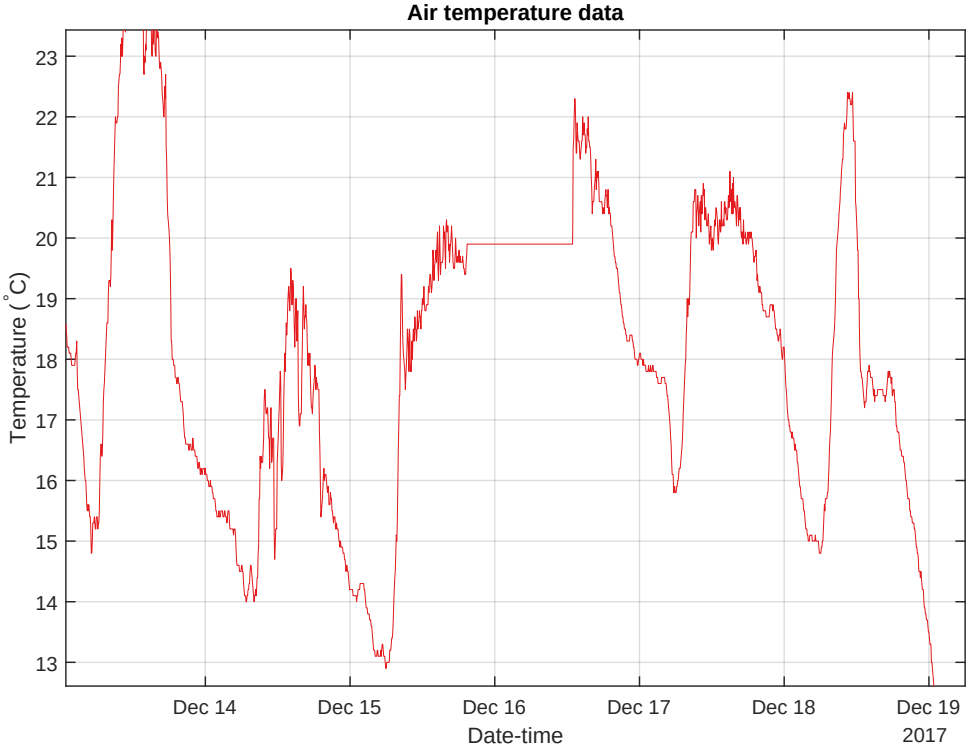

(b) Stale data

Figure 5.19 Raw air temperature data

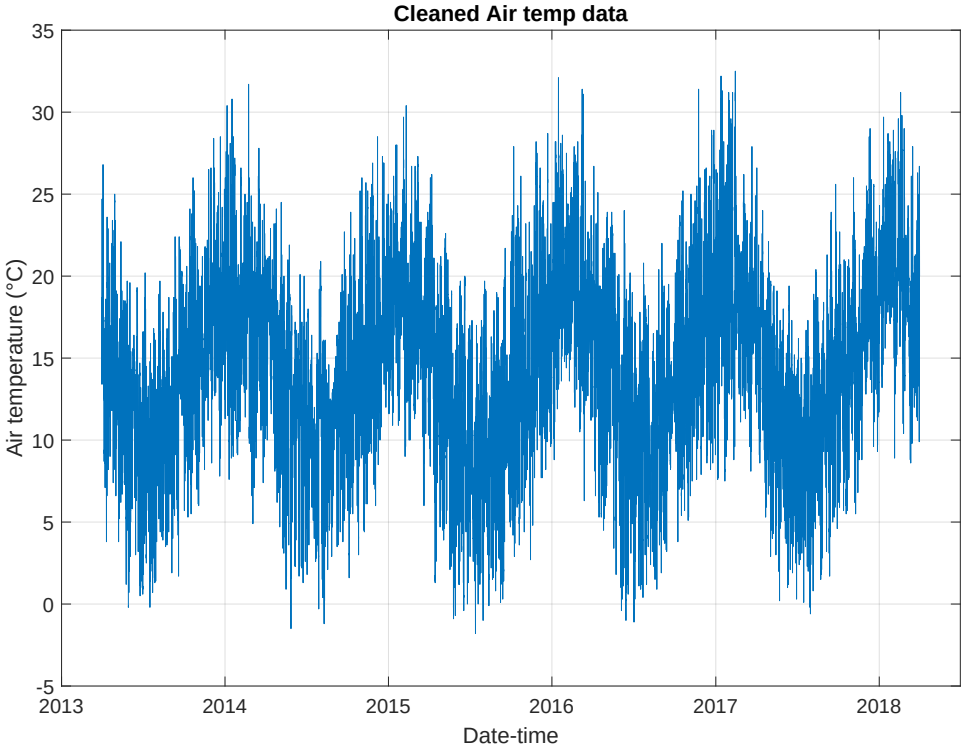

(a) Outliers identified and removed

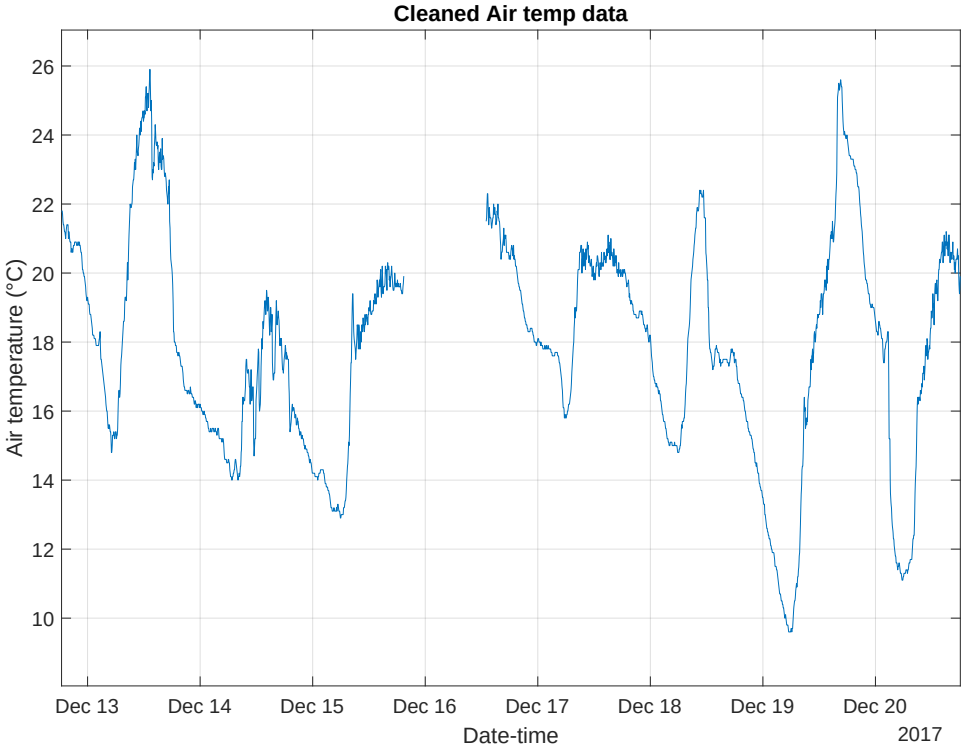

(b) Stale data identified and removed

Figure 5.20 Cleaned air temperature data

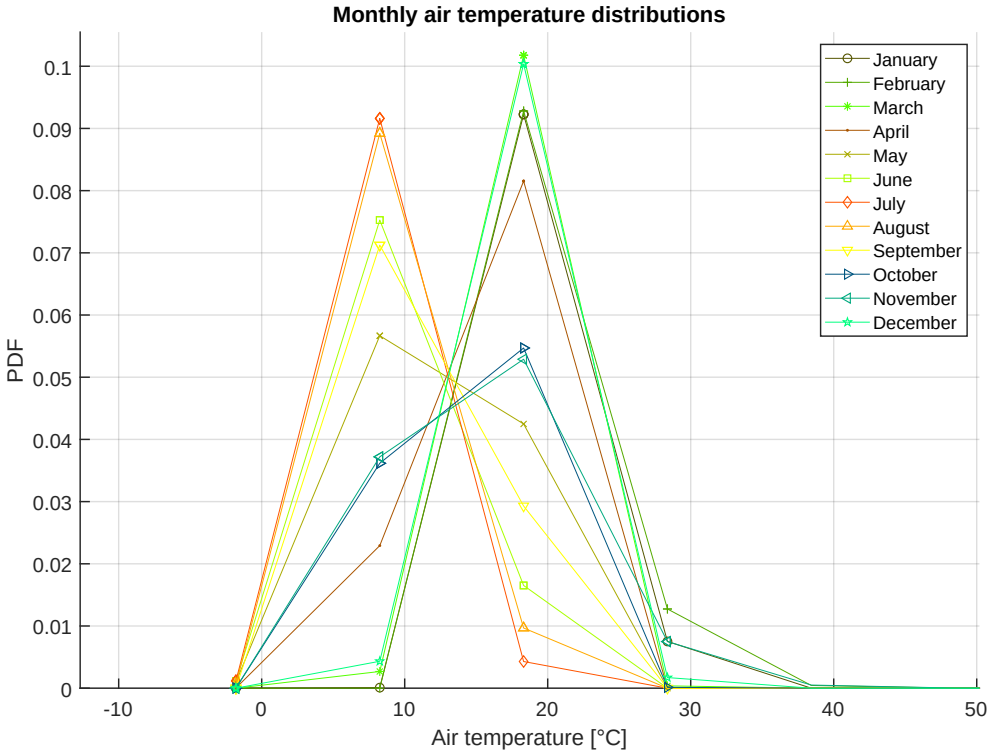

Figure 5.21 Poor fit of probability density

across their products. The environmental conditions considered for the base rating is given in Table 5.7.

As highlighted in Chapter 3.2, the heat transfer across electrical components have varying impact to its rating. It is immaterial to the rating values to consider environmental condition with low sensitivity score. Due to this, it can be seen in Table 5.7 that not all environmental conditions are considered by manufacturers or industrial standard when evaluating the rating of an electrical component. For discussion, different types of rating used in the industry are highlighted. Network operators have historically relied upon static ratings to define the maximum allowable current (ampacity) passing through electrical components which are set as the operational limits. Many of the input values that are used to calculate these limits (such as ambient temperature, soil temperature, wind speed, solar radiation and environmental conditions) are assumptive in nature. Typically, network operators select values that represent the worst-case scenario based on historically observed conditions in the service area. This leads to static ratings

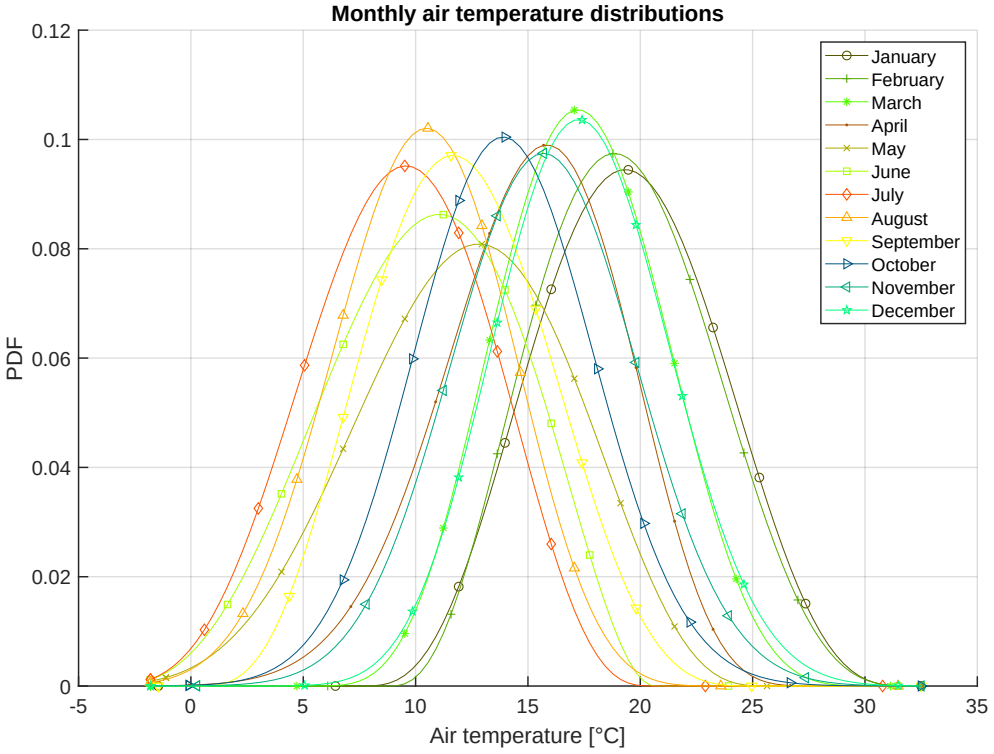

(a) Air temperature

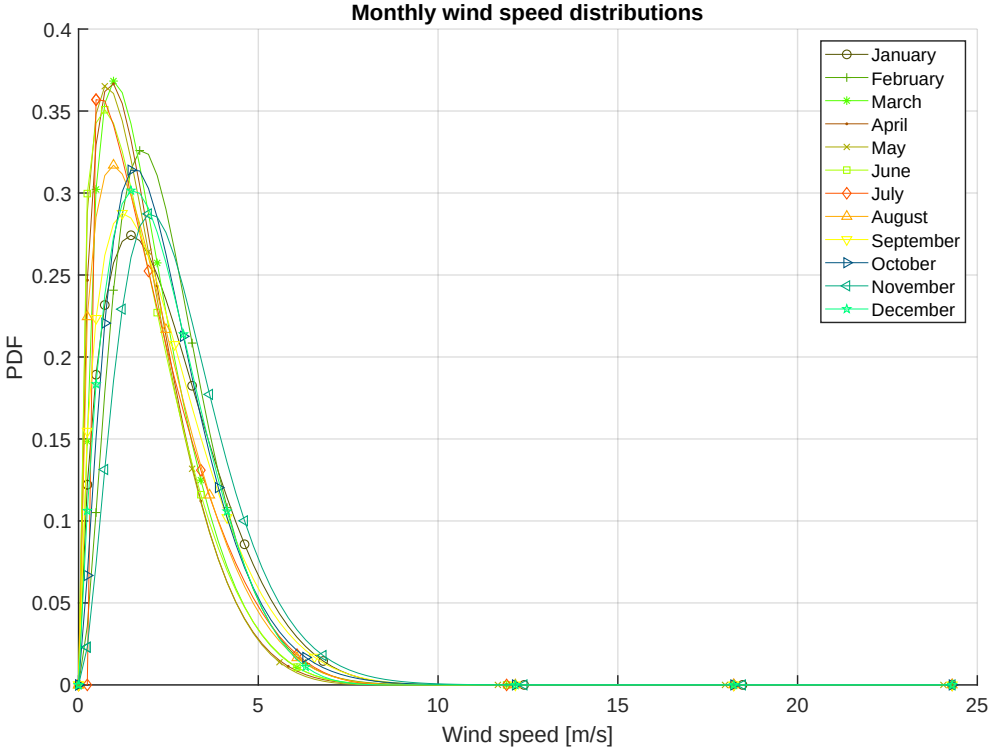

(b) Wind speed

Figure 5.22 Probability density of environmental data

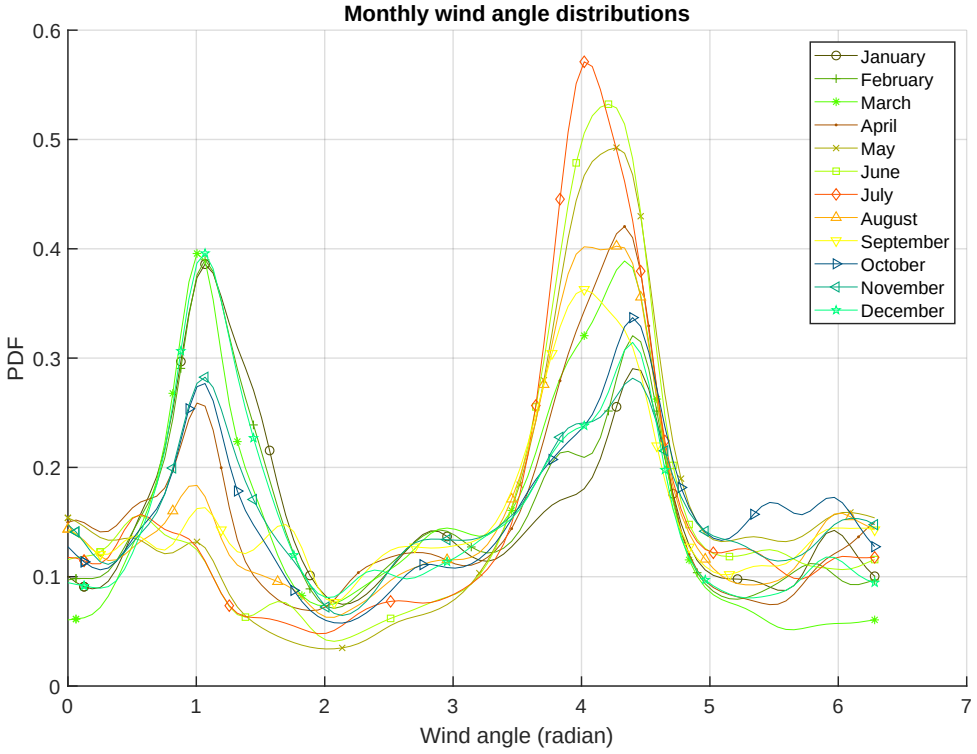

(a) Wind angle

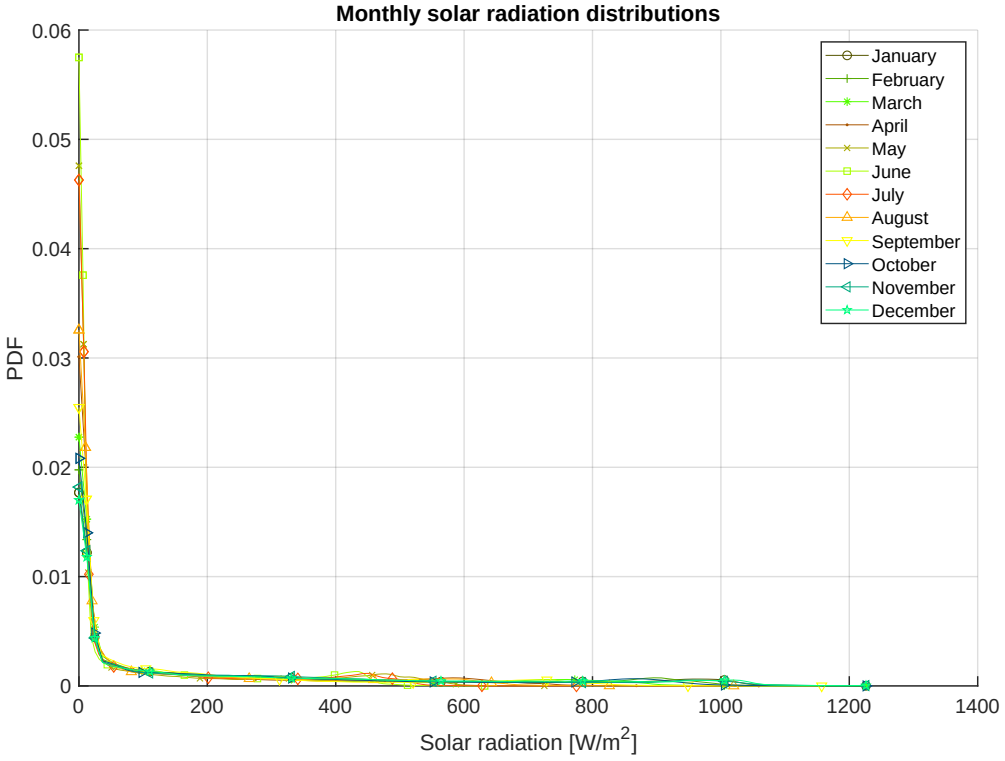

(b) Solar radiation

Figure 5.23 Probability density of environmental data

Table 5.7 List of environmental conditions used for base rating

Environmental parameters	**Static values used for different electrical components**		
	PTX RF	**UGC RF**	**OHL RF**
Air temperature (°C)	-	30	30
Wind speed ($m.s^{-1}$)	-	-	1
Wind direction (degrees)	-	-	60
Solar radiation ($W.m^{-1}$)	-	-	1000
Soil temperature (°C)	-	15	-
Soil thermal resistivity ($°C.m.W^{-1}$)	-	1.2	-

(SR) that are conservative for most conditions but could potentially exceed the true ampacity during unfavourable conditions. The next section discusses varying types of rating used in the industry followed by an evaluation of how the developed model are used to support the decision making process for EDN in Section 5.4.3.

5.4.2.1 Evaluation of rating model

The predictive asset rating (PAR) model that has been developed during this study suggests an advancement in the rating model over what's currently available in the industry. The different type of rating model presently used in the industry were discussed in Chapter 3.

The advancement suggested for power transformers (PTX) looks at substituting additional variables relating to the PTX state of operation such as the tap position and fan modes when evaluating the differential equation discussed in Chapter 3. The inclusion allowed one rating model to be used for multiple power transformers configuration. This is especially beneficial if an oil-natural-air-natural (ONAN) were retrofitted with a fan, the model are able to adapt to the changes when evaluating the rating to ensure the correct thermal constants are used. A month trend of thermal rating of the PTX at ZS3 is shown in Figure 5.24 comparing the calculated ONAN and ONAF rating. The period of a month is chosen here to allow clearer trend compared to showing 5 years worth of data. Depending on the frequency of fan's operation status, the

estimated rating will consider ONAN and ONAF computation.

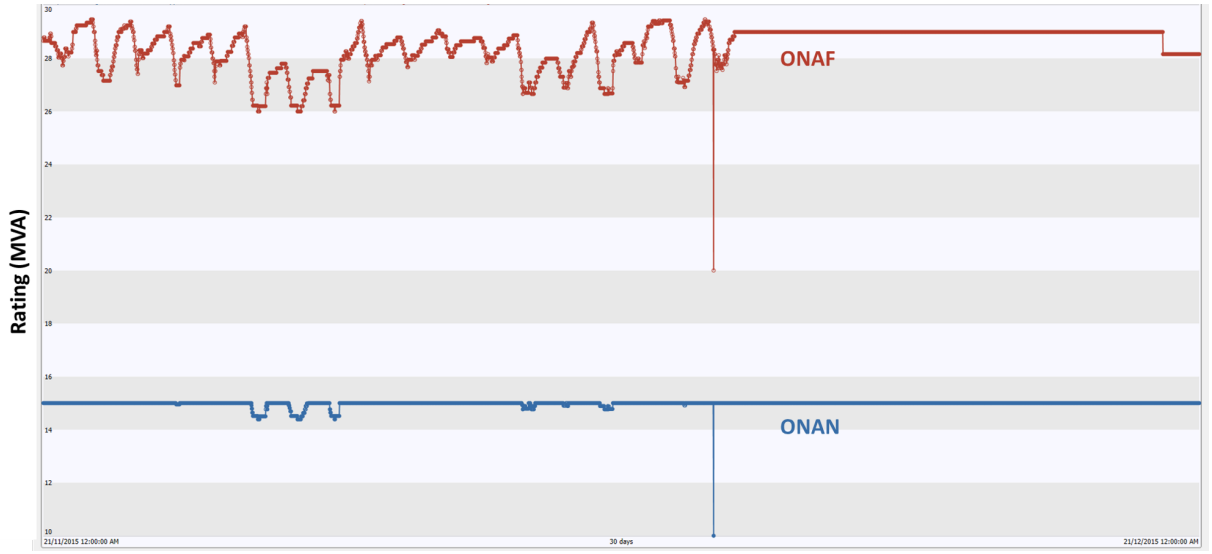

Figure 5.24 Trend of power transformer rating with additional variable considered

For overhead line, it is suggested in Chapter 3 to substitute the temperature variable, θ_f in the tension calculation (3.36), shown again here for reference,

$$1 + \frac{F_{t,hi}}{E \cdot A} + x_{lexp} \cdot \theta_i + \varepsilon_i = S_0 = \frac{S_f}{1 + \frac{F_{t,hf}}{E \cdot A} + x_{lexp} \cdot \theta_f + \varepsilon_f} \tag{5.5}$$

with the thermal model in (3.36), given as,

$$m \cdot c_p \cdot \frac{d\theta}{dt} = W_{generation} + Q_{sun} - Q_{radiation} - Q_{convection} \tag{5.6}$$

The result of the substitution allows improved flexibility when carrying out network constraints for overhead line allowing the rating evaluation to consider both the line clearance and thermal evaluation. It is advised the two should be evaluated together to ensure health and safety risk are mitigated. This was utilised when carrying out the constraint analysis scenario (CAS) listed in Table 5.4 for the overhead lines.

For underground cables, the finite element model were proposed and developed as discussed in Chapter 3. Generating the mesh network impose the biggest challenge as detailed information of the cable layer and configuration were needed. Information needed includes the thickness of

individual layer, the thermal resistivity of those layers, automatically arranging the position of screen wires and order of the layers from a external environment to the core of the cables. This was achieved by building in rules from manufacturer's data. Key information looked at were cable diameter, layer info such as oversheath material, insulation material, number of screen wires (if any). Doing so then allows placement of individual layers for the cable mesh. The nodes of the mesh and its layers are shown in Figure 5.25.

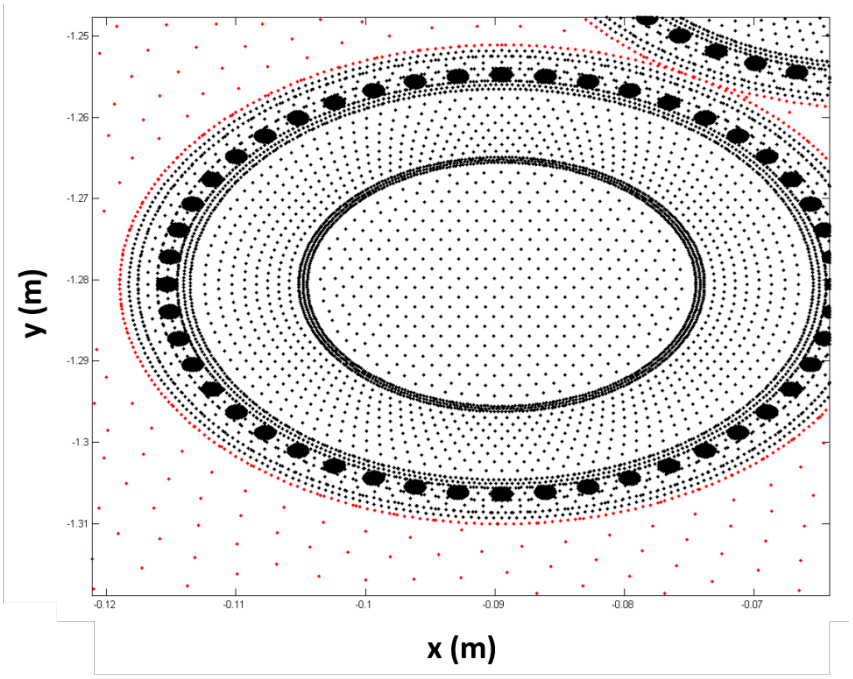

Figure 5.25 Nodes for cable mesh showing circular uniform layers

Comparing the rating calculation against 3rd party application, CYMCAP which uses FEM shows similarity between the two calculation as shown in Figure 5.26. The root mean squared error (RMSE) for the environmental and installation conditions comparison is 5.7 and 5.86 respectively.

5.4.3 Decision making process

5.4.3.1 Decision making in electrical distribution network

A distribution network consist of a series of electrical components that are connected together to make a complete circuit. A bottleneck in a part of the network affects the overall supply.

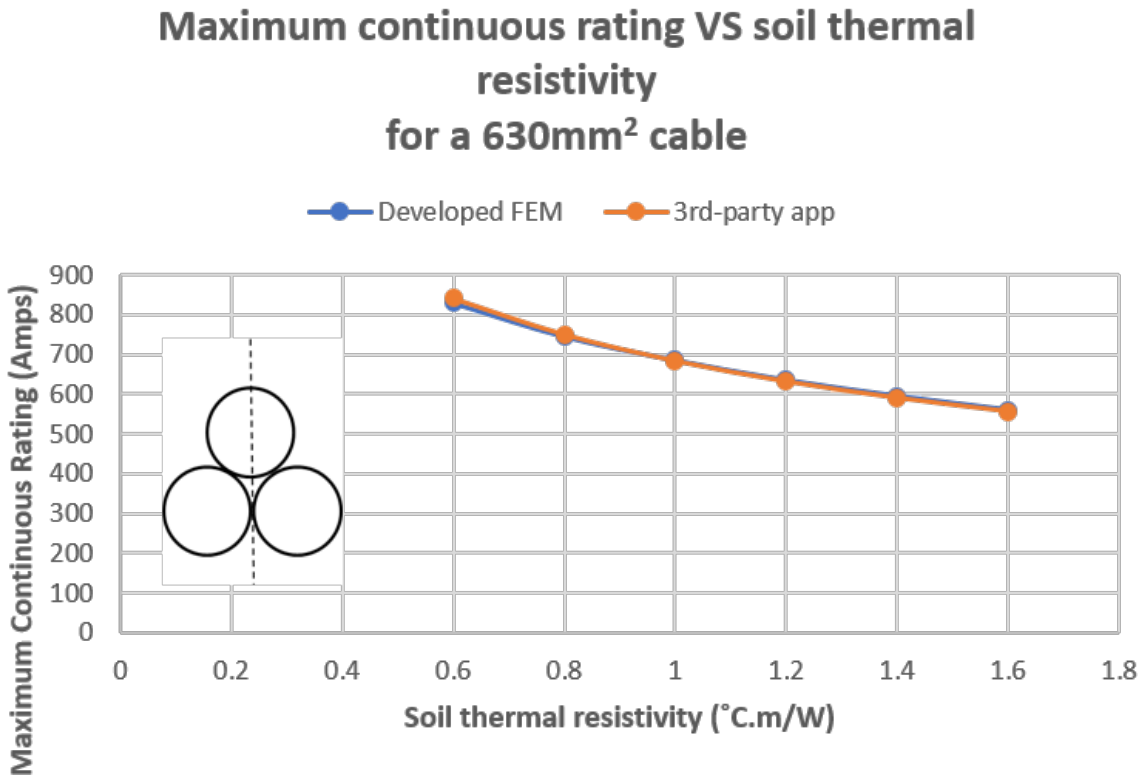

(a) Comparing 3xsingle core cables in trefoil formation

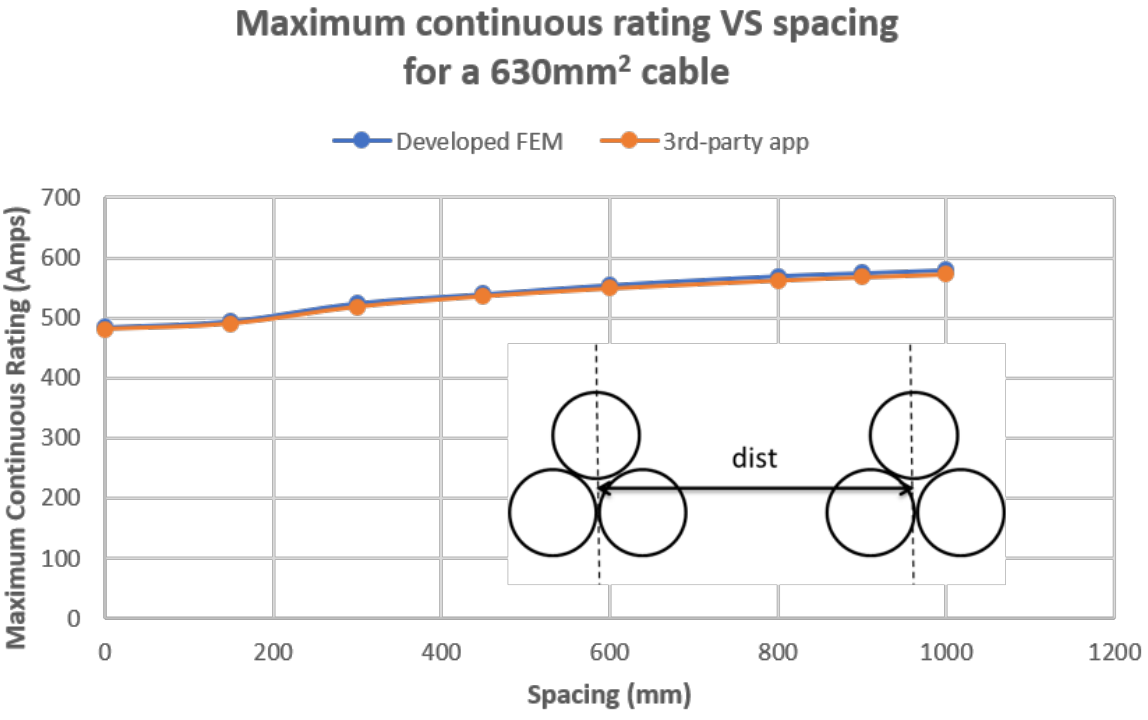

(b) Comparing parallel 3xsingle core cables in trefoil formation

Figure 5.26 Comparison of maximum continuous rating calculation

It is then important to identify operationally the impact of environmental conditions on these circuit throughout its operational life. A circuit in a distribution network comprises of assets with similar ratings to maximise the capacity utilisation. It can be seen in Figure 5.27 that a bottleneck in one section, *NT-Section 3* which has a dynamic feeder rating of 571 amps prevents the higher rated section, *NT-Section 1* with a dynamic feeder rating of 760 amps to be fully utilised as doing so will lead to overheating of the *NT-Section 3* section.

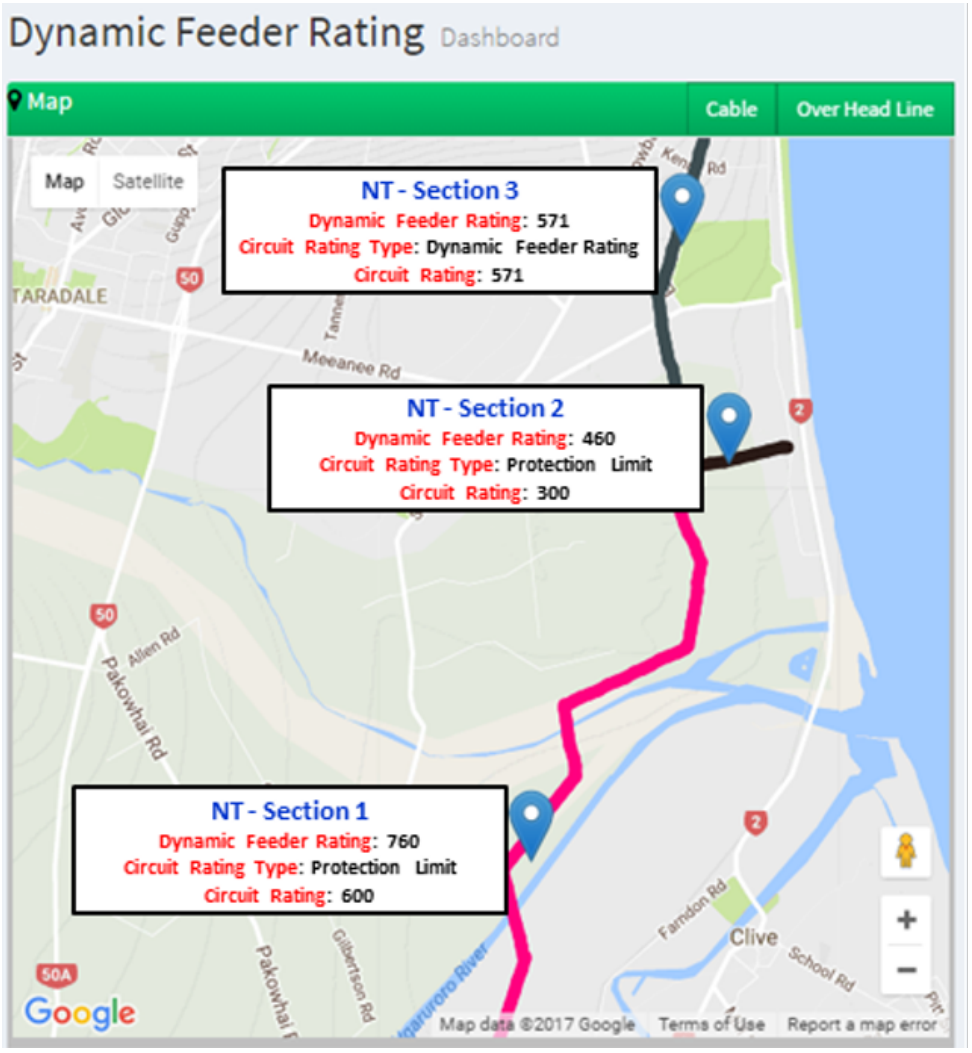

Figure 5.27 Dynamic feeder rating dashboard implemented at Unison

The circuit is also capped to the protection limit, with the final rating labelled as circuit rating as shown in Figure 5.27. This ensures that the network operator does not accidentally trip the circuit by loading the circuits higher than the protection settings. The rating values on the dashboard shown in Figure 5.27 is the output of Step 5 to Step 7 of the PAR model given in

Figure 5.1. The steps evaluates all the electrical component along the section of the circuit consisting of overhead lines and underground cables and report the likely value as a rating per section. The likely value here is the estimated rating, $E[y(X)]$ from Monte Carlo simulation, such that the evaluation of the asset operating temperature, θ is estimated by performing multiple calculation of θ_n from large number of samples, that is $\hat{\theta}_n \xrightarrow{\text{a.s.}} \theta$ when $n \to \infty$ as discussed in Section 3.4.1.3.

Simulations were carried out to evaluate the rating and temperature of the electrical components based on the circuits load profile shown in Figure 4.3 and the environmental conditions shown in Figure 4.5, Figure 4.6a, Figure 4.6b, Figure 4.7, Figure 4.8 and Figure 4.9 as discussed in Chapter 4. The circuits selected here is to compliment the capacity evaluation carried out in Section 5.3.1.1 which looks at circuit *OneC* and *OneD*. The simulation for rating and constraint were evaluated to identify the rating and degree indices described in Figure 4.39. The summary of the results is shown in Table 5.8 and Table 5.9 respectively.

Table 5.8 Rating evaluation and degree of indices for selected circuits

Circuit	PAR range (Min - Max)	PAR	SR	Margin ratio (PAR:SR)
OneC_1	780 - 807	798	664	1.2
OneC_2	640 - 655	647	590	1.1
OneD_1	758 - 781	772	664	1.16
OneD_2	782 - 817	797	726	1.1

*PAR: predictive asset rating, SR: static rating.

Table 5.9 Temperature evaluation and degree of indices for selected circuits

Circuit	Temperature range (Min - Max)	EC	C_{max}	Limitation ratio (EC:C_{max})
OneC_1	30 - 35	31	90	2.9
OneC_2	27 - 30	28	90	3.2
OneD_1	28 - 33	30	90	3
OneD_2	27 - 29	28	90	3.2

*EC: Expected constraint, C_{max}: Max limit of constraints (either thermal or mechanical).

The margin ratio represents the factor of potential capacity gained/reduced with the implementation of PAR. It was found that the environmental conditions considered on the network prior to this study has been over estimated and the capacity margin can be as high as 20% more than

initial assumptions. Over estimation is aligned with industry practice of using near-extreme value to exercise caution when planning the network. A reduction in available capacity is possible if the initial environmental condition based on static rating has been under estimated and assumed to have better environmental conditions.

The limitation ratio represents the factor of potential constraint on the network due to capacity utilisation of the circuit. For these circuits, the headroom available were found to be up to 3.2 times lower than the limit. It was also found that the limiting components along the circuit does not experience a lot of variation in its environmental conditions based on the narrow PDF shown in Figure 5.28, with the only exception being the *OneD_2* circuit.

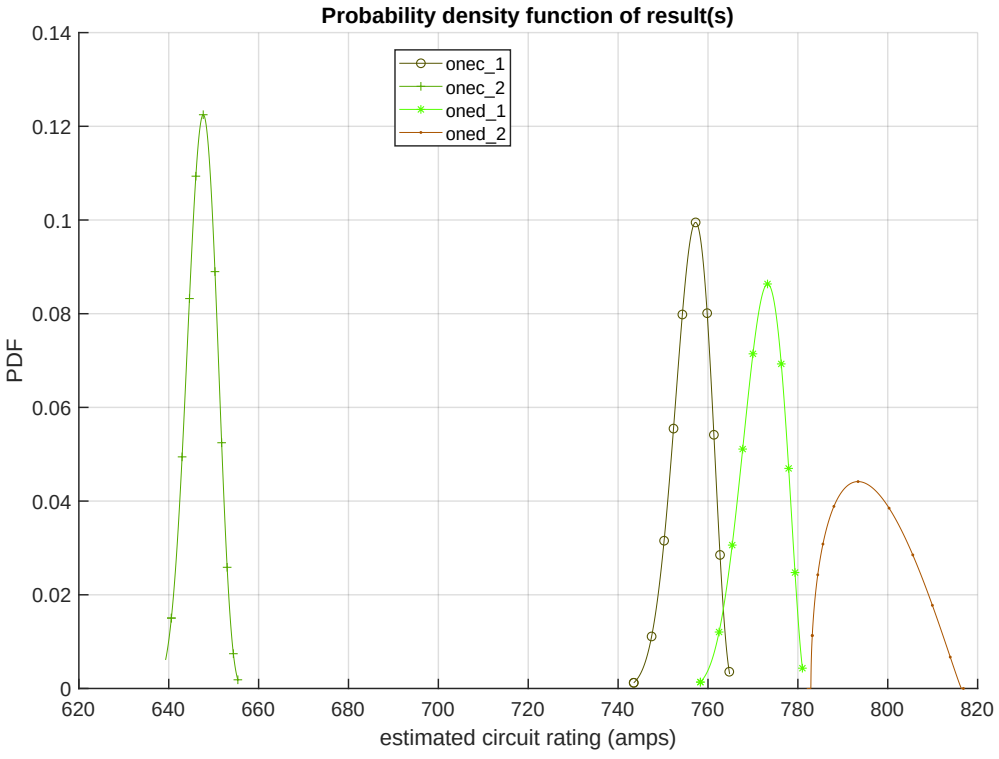

Figure 5.28 PDF of cables dynamic rating

Under normal loading condition, the probability of loading the circuit *OneC* and *OneD* above the cable thermal limit of 90 °C is low as shown in Figure 5.29. Based on this evaluation by looking at the margin and limitation ratio, the two circuits can be safely used to meet the expected load demand without overheating or breaching constraint on any part of the circuit.

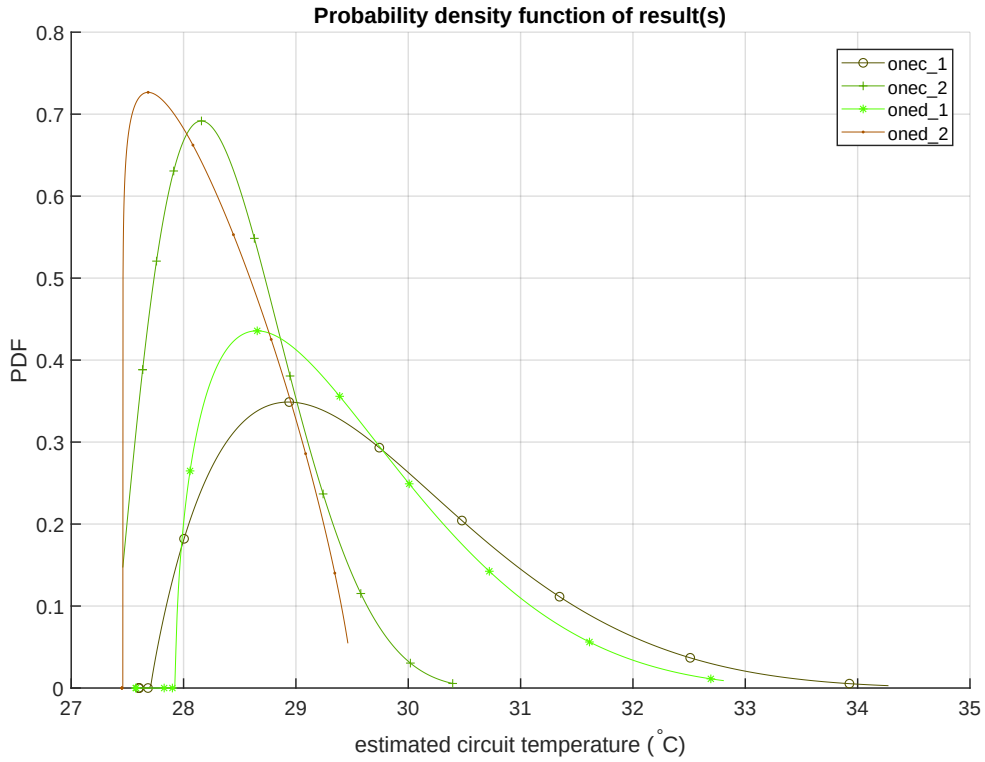

Figure 5.29 PDF of cable's operating temperature

5.5 SUMMARY AND CONCLUSIONS

The results and discussion of the model presented in this research demonstrated how network operators are able collectively consider different network configurations and environmental conditions to make decisions based on probabilistic method. The model provides a better understanding in the operation and limitation of the electrical components on the network by carrying out multiple scenarios based on Monte Carlo simulation. This is made possible through the added ability to fit distribution of environmental data and considerations of parameters such as circuit loading, fan operations, clearance data and others discussed in this chapter which has been demonstrated to have an impact to the overall asset utilisation. The results presented has shown that the model can be used but not limited to evaluating the available capacity during load transfer, selection of asset for network expansion and evaluation of capacity margin thus covering the criteria set for this research.

Chapter 6

CONTRIBUTIONS, FUTURE WORK AND CONCLUSIONS

6.1 OVERVIEW

In previous chapters the developed model were discussed and the research findings were presented. In this chapter, the summary of each chapters are first presented. The research contributions are then highlighted. The tasks to be considered for future improvement of the predictive asset rating model are then discussed. The final section concludes this thesis.

6.2 INTRODUCTION

The predictive asset rating (PAR) model and the results of the model's implementation across asset management, planning and network operation at Unison Networks Ltd have been discussed in previous chapters. The summary of each chapter are discussed below:

Chapter 1 has presented the background, problem statement, objective and structure of the thesis.

Chapter 2 has provided the concepts, data structure and asset parameters that are relevant to determine the assets' capacity utilisation. Different research on capacity utilisation were discussed. Finally, the chapter presented the current shortfall of existing method and the proposed solution to develop an aggregation model for rating evaluation to solve the technical challenges.

Chapter 3 has detailed the modelling used for rating evaluations. The chapter highlighted the available industrial standards and the work adopted into the PAR model. The aggregation

model were discussed, outlining the model requirements to be flexible: being able to be fitted to different input data, accurate: able to measure confidence, fast and simple: ability to update the underlying model. These requirements were met by demonstrating the model's ability to perform a range of simulation for different type of electrical component, load profile and operating conditions as discussed in Chapter 3 and Chapter 4.

Chapter 4 has presented the application and implementation of the developed model in an electrical distribution network. The datasets and network model used for the study demonstrated a range of technical challenges faced by the industry and highlighted ways the developed model can be used to simulate and provide a measure of rating and constraints on the network.

Chapter 5 has discussed the results of predictive asset rating tool implementation in an electrical distribution networks. The simulation of varying environmental conditions and their impact to different electrical components were presented. It was found that the developed model were able to support decision making by providing suggestion of circuits to use during abnormal conditions, highlight potential constraints and fix required, and more importantly aggregating parameters for rating evaluation.

6.3 CONTRIBUTIONS

The main contributions of this research in the field of electrical distribution network optimisation are summarised as follows:

- **Deployment of rating aggregation model**: An elaborate step-by-step approach of the developed predictive asset rating model was presented in Section 3.5. The developed model is able to use a combination of the following parameters: type of electrical components, load profile, environmental and operating conditions. This approach allows the rating evaluation to be aggregated to consider the varying challenges faced by electrical distribution network. The evaluation process constitutes a step forward to the existing rating evaluation methods discussed in Section 2.5 as compared in Figure 6.1 with the developed model solving additional technical challenges faced by the industry.

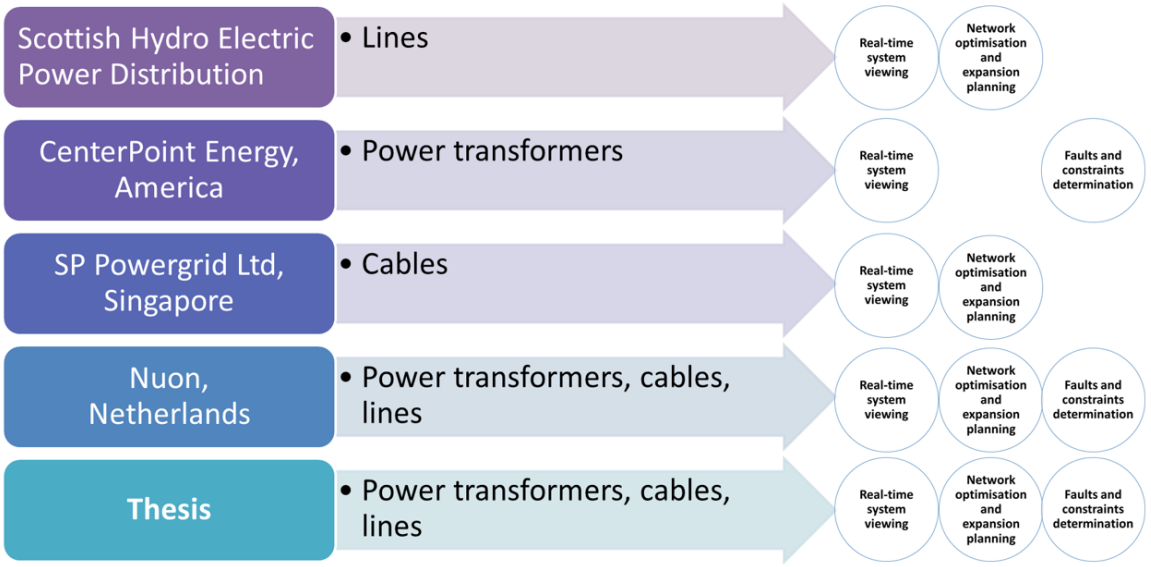

Figure 6.1 Comparison of technical challenges solved by model against existing methods

- **Analysis and evaluation of rating**: It has been shown in Section 5.3 that the developed model can be used to support decision making for electrical distribution network, catering for network control and operations, network planning, and asset management. The ability to sample the operating conditions at varying interval allows the asset performance to be evaluated in real-time, by day, month and year with possible criteria discussed in Section 4.4.2.2 and reprinted in Figure 6.2 for reference. The approach enables an improvement in performing targeted capacity utilisation studies.

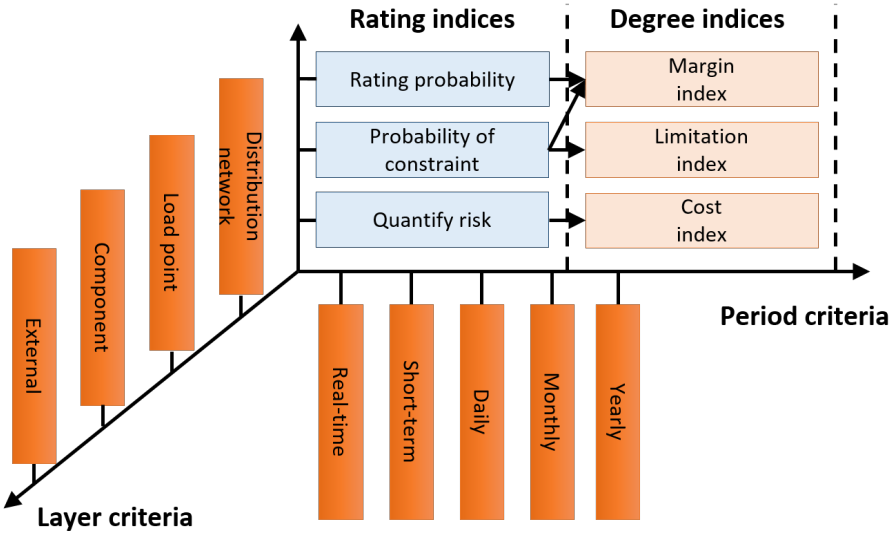

Figure 6.2 Simulation criteria and indices

- **In-depth analysis of line clearance evaluation**: As part of the work in constraint analysis for overhead lines, a feature rich LiDAR dataset were used where the LiDAR data point contains a label of the object it belongs to, along with the point height. This research provided findings of constraint consideration against multiple clearance limit to object and structures as discussed in Section 5.3.2. The approach to consider different types of non-electrical object is additional over current practices. The PAR model also consider clearance to underbuilt conductors with varying voltage level.

Contribution of the research work reported in this thesis have also been shared and reaffirmed by the industry as conference papers and awards received as listed in list of publications.

6.4 RECOMMENDATIONS FOR FUTURE WORK

The present iteration of the PAR model is seen as fit for purpose to solve the challenges faced in the electricity distribution network discussed in Chapter 2. There are some short-comings in the model which can be improved and will be discussed in the next sections, covering the following steps of the model:

(a) *processing raw data*,
(b) *asset rating computations and decision making process*,

6.4.1 Processing raw data

Data has been ingested, transformed and visualised throughout this study. Some data requires more processing whilst others are applied directly into the PAR model. Data that does not require further processing such as those categorised as static data in Chapter 4 does not require further changes. This section shall then focuses on the remaining data category:

(a) **Time-series data**
(b) **Financial data**

6.4.1.1 Time-series data

The data that falls under this category includes operational data such as circuit loading and environmental condition. The following section highlight some of the work that can be considered to further advance the model when considering time-series data.

(i) **Spatial interpolation**

The models ability to interpolate the raw data from field devices that's located further apart makes it easier for network operators to interpret and make use of the data. Despite not having raw data, pre-existing distribution has also been built into the model to cater for data that's not available. As highlighted in Chapter 4, the dataset were gathered from environmental stations located in the North Island of New Zealand. Due to this the datasets used for the spatial interpolation model are currently only applicable for network operators located in the North Island, covering Hawkes Bay and Rotorua region. The existing spatial interpolation grid covers an area approximately 91 km^2 for Hawkes Bay and 36 km^2 for Rotorua. The implemented inversed distance weighted (IDW) spatial interpolation model requires approximately 2 hours to map out the grid. This is a lot slower than propriety GIS software, ArcGis, which took less than 2 minutes to map out the same size grid. The implemented spatial interpolation model would work fine to interpolate a point at a time but was not efficient to interpolate larger sized grid. This part of the algorithm can be optimised further. A potential solution to speed up the IDW calculation as discussed by [ArcGIS 2007] is to limit the number of measured values used to predict the unknown points by only selecting nearby measured points. The distant measured points can be assumed zero with little influence to the final interpolation. The implemented IDW model assumes distant measured point to be equal to the static environmental value used by industrial standard such as 1.2 °C.m/W for soil thermal resistivity. Implementing this will greatly increase the speed of compute for larger size grid.

(ii) **Geographical considerations for soil data**

Data capture of soil thermal data that has direct impact to the rating of underground cable is difficult to achieve as the underground cables tend to be buried more than one meter below ground, below other buried services. Direct access to the soil conditions in close

proximity to the underground cables thus will require civil work which will be expensive to perform along the length of underground cables. Most publicly available soil data in New Zealand focuses more on top-soil conditions which were carried out for agriculture studies looking at soil properties up to 60 cm. Some of which were highlighted in Chapter 4. Propriety GIS software has the capabilities of including information from GIS layers such as the top-soil data layer which can be superimposed onto the IDW spatial interpolation to take additional geographical data into consideration when interpolating soil thermal data. As this method is done well by GIS softwares, the concept of superimposing the GIS layer wasn't investigated further. This step can help increase the accuracy of the soil thermal data which is used for cable rating calculations.

6.4.1.2 Financial data

The financial data looks at the capital expenditure (CAPEX) and operational expenditure (OPEX) on the network. This relates to item such as the cost of an equipment and network upgrade. A reference to financial data prepared by network operators in United Kingdom were discussed in Chapter 4. The financial data were not utilised in the end as the study would have divert away from the predictive asset rating model, as such the cost impact simulation were not simulated. As the developed model provides the ability to calculate the probability of rating and constraint on the network. The impact can be set quantitatively based on the financial data by assigning tiered range of financial impact to the business. Given that,

$$Risk = Probability\ (of\ a\ failure) * Impact\ (damage\ related\ to\ the\ failure) \tag{6.1}$$

the scenarios discussed in Chapter 5 can be paired to the financial data as shown in Table 6.1 to evaluate the risks. The risk index can then be calculated to provide additional matrix to network operators when making a business decision.

Table 6.1 Potential study for risk evaluation

Financial impact	Probabilistic studies to evaluate risks
Network performance	Load transfer scenario, network expansion scenario
Public safety	Constraint analysis scenario
Environmental impact	Constraint analysis scenario

6.5 DISCUSSION

The opportunities for improvement in the rating computations is highlighted in this section. As suggestion for improvement will also lead to better decision making process, the two will be discussed together. The asset rating computation revolves around the heat transfer equation to find the optimal operating temperature for varying network events. The next sections will look at how the rating computation can be improved to further optimise the capacity utilisation of the electrical components.

6.5.1 Distributed temperature sensing for rating studies

The validation of the cable rating model make use of the distributed temperature sensing (DTS) equipment available at Unison. Several comparison were made possible using the equipment and further studies were to be explored such as estimating the external soil thermal resistivity by looking at heating generated by the underground cables and measure the change of soil temperature over time. The plan was however short-lived due to damaged fibre which would require additional cost to access and repair it. The DTS would have provided better insight into the amount of heat dissipated to the external environment and provided the ability to measure the temperature in close proximity to the underground cables.

6.5.2 Loss of life considerations

The loss of life calculation for power transformer were discussed in Chapter 1 looking at the different calculation for the paper loss of life dependent on whether it is thermally-upgrade

paper or not based on the work done in AS/NZS 60076.7 [AS/NZS TC EL-008 2013b]. The calculation has been implemented in the model. The overhead and underground loss off life had also been considered. It was however not implemented in the final algorithm to focus on decision making based on rating and constraints computations. There has been substantive studies in ranking for replacement looking at the loss of life such as the work by by [Buhari *et al.* 2016] to estimate the replacement of cables based on Arrhenius and Weibull distribution through Monte Carlo simulation.

For power transformers, the latest research findings in its loss of life are presented in IEC 60076.7:2018 [IEC TC 14 2018]. The standard however hasn't been adapted by the AS/NZS. To maintain conformance with local standard, the highlighted changes in insulation life and temperature limits will be done as part of future work.

For overhead lines the model on the impact of annealing for varying operating temperature by [AS/NZS 7000 2016] is proposed. The model relates to the loss of tensile strength of the wires to the percentage reduction in cross-sectional area of the wire. The loss of tensile strength, W as a percentage, were given as,

$$W = W_a \left(1 - e^{-e^{\left(A' + \frac{B'}{T^*} \ln(t) + \frac{C'}{T^*} + D' \ln\left(\frac{R}{80}\right)\right)}} \right) \tag{6.2}$$

and the reduction in wire's cross-sectional area, R as a percentage, is given as,

$$R = 100 \left(1 - \left(\frac{D_w}{D_o} \right)^2 \right) \tag{6.3}$$

where, the constant of W_a, A', B', C', and D' is given in Table 6.2. T^* is the absolute wire temperature (K) and t the time duration (hours). D_o and D_w is the diameter (mm) of the wire before and after reduction. The value of R is to be substitute into (6.2) to calculate the final loss of tensile strength due to the elevated temperature operation.

Evaluating (6.2) at each time step shall then give the relative loss of life for overhead lines from

Table 6.2 Constants for annealing equation as given in [AS/NZS 7000 2016]

Alloy	W_a	A'	B'	C'	D'
1350-H19	56	7.8	150	-4700	7.5
6201A-T81	60	16.2	270	-9000	4
HDC (110A-H)	41	14	175	-6700	3

the original tensile strength. For 1350 alloy, the expected ageing after eight month of operation at the temperature 80°C, 100°C, 120°C, and 150°C is approximately 97%, 95%, 87%, and 70%.

For underground cables the majority of failures are due to natural ageing of insulation or water treeing. Partial discharge may be associated with cable failures but occurs mainly at joints or termination. Loss of life models for cables have looked at specific degradation mechanism such as the field emission and thermodynamic model that's seen as predominant to the ageing of the cable, also known as electrothermal stress. The three potential candidate for cable life model that looks at electrothermal stress are the Zhurkov [Zhurkov 1984, Aras *et al.* 2007], Crine [Crine *et al.* 1996] and Arrhenius [Buhari *et al.* 2016] model. The Zhurkov model looks at empirical relationship to characterise the thermal fluctuation of polymers under mechanical stress. Crine model suggested evaluating the electrothermal life of the insulation based on rate of Gibbs activation energy, relating to transition of state of electromagnetic energy. The Arrhenius model has been applied to estimate the replacement of cables. The work done by [Buhari *et al.* 2016] developed a reliability model and a prioritisation method for ageing underground cables. Two ranking method were given, one based on thermal loss-of-life, L_T,

$$L_T = \sum_{p=1}^{m} \frac{t_p}{L_p\left(\theta_{c,p}\right)} + \sum_{j=1}^{n} \frac{t_j}{L_p\left(\theta_{c,j}\right)} \tag{6.4}$$

Where, p and j denote historic and planning intervals, t_p and t_j is the duration and the remaining variables L_p L_j, $\theta_{c,p}$ and $\theta_{c,j}$ are temperature ($^{\circ}C$) . The second model is based on financial consequences, given as,

$$\begin{aligned} Cost = &\Delta SAIFI * SAIFI_{incentive} + \Delta SAIDI * SAIDI_{incentive} + \\ &Number\ of\ failures * Cost\ per\ failure \end{aligned} \tag{6.5}$$

Both methods can be used to compliment the developed model. The evaluation of (6.4) can be used to determine the probability constraint on the network and (6.5) can be used to quantify impact for risk evaluation. This will compliment the model to consider the cable's loss-of-life calculation and the financial evaluation. As the work was developed by a different research group based in India, this task is for future work should researchers wish to investigate further.

6.6 CONCLUSION

The uncertainties of future load demand due to technological shifts and consumer behaviour impose a challenge to network operators.The PAR model has been developed to present a quantitative analysis to support decision making and provide network operators access to new information, allowing them to optimise the capacity utilisation and achieve a reliable and safe power delivery. This study presented different ways data from the field such as environmental data, cooling operation data and geographical data can be used to understand the impact of external influences on the capacity utilisation of the electrical components. Additional consideration and improvements in the computation of rating for power transformers, overhead lines and underground cables were also presented. Some of the key findings includes the use of general beta distribution to enable multiple scenario studies; demonstrated the benefit of integrating constraint and rating calculation, improving the flexibility of the rating model. Lastly, the improved flexibility enables the Monte Carlo simulation to collectively consider different layers of the network, selective range of period and quantitative indices for decision making in an electrical distribution network. This study has looked at a broad range of scenarios experienced by network operators and presented measures to compare existing methodology with the developed model. This is in hope that the scenarios will prompt additional thinking and consideration of alternative solutions in the area of capacity planning, constraint analysis and network expansion planning. The use of the model to simulate potential outlook of the network is encouraged and should benefit current and future network operators where uncertainties exist.

REFERENCES

Adapa, R. and Douglass, D.A. (2005), 'Dynamic thermal ratings: monitors and calculation methods', In *Power Engineering Society Inaugural Conference and Exposition in Africa, 2005 IEEE*, pp. 163–167.

AIEE (1945), 'Guides for operation of transformers, regulators, and reactors', *American Institute of Electrical Engineers, Transactions of the*, Vol. 64, No. 11, pp. 797–805.

Anders, G.J. (1990), *Probability concepts in electric power systems*, John Wiley & Sons, Inc., Canada.

Aras, F., Alekperov, V., Can, N. and Kirkici, H. (2007), 'Aging of 154 kv underground power cable insulation under combined thermal and electrical stresses', *IEEE Electrical Insulation Magazine*, Vol. 23, No. 5, Sep., pp. 25–33.

ArcGIS (2007), 'Deterministic methods for spatial interpolation'.

AS TC EL-007 (2012), 'High-voltage switchgear and controlgear - common specifications'. AS Std. 62271.1.

AS/NZS 7000 (2016), 'Overhead line design-detailed procedures'.

AS/NZS TC EL-008 (2013a), 'Power transformers, part 2: Loading guide for oil-immersed power transformers'. AS/NZS 60076.7.

AS/NZS TC EL-008 (2013b), 'Power transformers, part 7: Loading guide for oil-immersed power transformers'. AS/NZS 60076.7.

ASTM D5334-14 (2014), 'Standard test method for determination of thermal conductivity of soil and soft rock by thermal needle probe procedure', www.astm.org.

ASTM E490 (2000), 'Standard solar constant and zero air mass solar spectral irradiance tables', www.astm.org.

Ausen, J., Fitzgerald, B.F., Gust, E.A., Lawry, D.C., Lazar, J.P. and Oye, R.L. (2006), 'Dynamic thermal rating system relieves transmission constraint', In *IEEE 11th International Conference on Transmission & Distribution Construction, Operation and Live-Line Maintenance, 2006. ESMO 2006.*

Baazzim, M.S., Al-Saud, M.S. and El-Kady, M.A. (2014), 'Comparison of finite-element and iec methods for cable thermal analysis under various operating environments', *International Journal of Electrical, Robotics, Electronics and Communication Engineering*, Vol. 8, No. 3, pp. 481–486.

Bauer, C.A. and Nease, R.J. (1957), 'A study of the superposition of heat fields and the kennelly formula as applied to underground cable systems', *Transactions of the American Institute of Electrical Engineers. Part III: Power Apparatus and Systems*, Vol. 76, No. 3, April, pp. 1330–1333.

Billinton, R. and Li, W. (1994), *Reliability assessment of electrical power systems using Monte Carlo methods*, Plenum Press, New York.

Brown, R.E. (2009), *Electric Power Distribution Reliability*, Power Engineering, CRC Press, Washington D.C., 2nd ed.

Buhari, M., Levi, V. and Awadallah, S.K.E. (2016), 'Modelling of ageing distribution cable for replacement planning', *IEEE Transactions on Power Systems*, Vol. 31, No. 5, Sep., pp. 3996–4004.

Castillo, W.A., Jagaduri, R.T. and Muralimanohar, P.K. (2012), 'Implementation of a transformer monitoring solution per ieee c57.91-1995 using an automation controller', In *Protective Relay Engineers, 2012 65th Annual Conference for*, pp. 442–448.

Chand, R. and Brown, C. (2017), 'Dynamic thermal monitoring and control of medium voltage cables', 21-23 June 2017.

CIGRE WG B2.12 (2002), 'Thermal behaviour of overhead conductors'.

Commerce Commission (2017), 'Electricity and the commerce comission's role', http://www.comcom.govt.nz/regulated-industries/electricity/. [Online] Accessed 06 July 2017.

Crine, J.., Dang, C. and Parpal, J.. (1996), 'Electrical aging of extruded dielectric cables: a physical model', In *Conference Record of the 1996 IEEE International Symposium on Electrical Insulation*, June, pp. 646–649 vol.2.

CYME (2012), 'Cymcap - power cable ampacity rating'.

Das, B., Phadnis, S., Janssens, S. and Raymond, S. (2015), 'Distribution transformer hot spot temperature monitoring based on fbg sensors', 24-26 June.

Degefa, M.Z., Humayun, M., Safdarian, A., Koivisto, M., Millar, R.J. and Lehtonen, M. (2014), 'Unlocking distribution network capacity through real-time thermal rating for high penetration of dgs', *Electric Power Systems Research*, Vol. 117, pp. 36–46.

Douglass, D.A. and Edris, A. (1999), 'Field studies of dynamic thermal rating methods for overhead lines', In *Transmission and Distribution Conference, 1999 IEEE*, pp. 842–851 vol.2.

Electricity Authority Commission (2017), '2010 statement of opportunities', https://www.ea.govt.nz/about-us/what-we-do/our-history/archive/operations-archive/statement-of-opportunities-soo/2010-soo/. [Online] Accessed 06 July 2017.

Electricity Authority of New Zealand (2018), 'Electricity in new zealand', https://www.ea.govt.nz/about-us/media-and-publications/electricity-nz/. [Online] Accessed 8 March 2019.

EPRI EL-2128 (1981), 'Soil thermal resistivity and thermal stability measuring equipment'.

European Commission JRC (2014), 'Smart grid projects outlook 2014'.

Halliburton (2011), 'Gemini hsi dts system'.

Hastings District Council (2015), 'Intramaps'.

IEC TC 14 (2005), 'Power transformers, part 7: Loading guide for oil-immersed power transformers'. IEC Std. 60076.7.

IEC TC 14 (2018), 'Power transformers, part 7: Loading guide for mineral-oil-immersed power transformers'. IEC Std. 60076.7.

IEC TC 20 (1985), 'Calculation of the cyclic and emergency current rating of cables'. IEC Std. 60853.

IEC TC 20 (2003), 'Electric cables - calculation of the current rating - finite element method'.

IEC TC 20 (2006), 'Electric cables - calculation of the current rating'. IEC Std. 60287.

IEC TC 65 (2008), 'Industrial platinum resistance thermometers and platinum temperature sensors'. IEC Std. 60751.

IEEE 442 (1996), 'Guide for soil thermal resistivity measurements'.

IEEE 738 (2013), 'Ieee standard for calculating the current-temperature relationship of bare overhead conductors'. IEC Std. 738-2012 (Revision of IEEE Std 738-2006 - Incorporates IEEE Std 738-2012 Cor 1-2013).

IEEE C57.91 (2012), 'IEEE guide for loading mineral-oil-immersed transformers and step-voltage regulators'. IEEE Std. C57.91.

Jalal, T.S., Vliet, B.v., Rashid, N. and Murrani, K.a. (2015), 'Challenges in implementing intelligent computational algorithms for smart distribution networks', 24-26 June 2015.

Johnson, N.L., Kotz, S. and Balakrishnan, N. (1995), *Chapter 12: Beta Distributions*, Vol. 1, Wiley, New York, 2nd ed., Chap. 12.

KEMA (2007), 'New zealand electric energy-efficiency potential study'.

Kulkarni, S.V. and A., K.S. (2004), *Transformer Engineering Design and Practice*, Marcel Dekker, New York, USA.

Landcare Research (2016), 'S-map online - the digital soil map for new zealand'.

Li, H.J. (2005), 'Estimation of soil thermal parameters from surface temperature of underground cables and prediction of cable rating', *Generation, Transmission and Distribution, IEE Proceedings-*, Vol. 152, No. 6, pp. 849–854.

Michiorri, A. (2010), *Power system real-time thermal rating estimation*, PhD thesis, Durham University.

Michiorri, A., Currie, R., Taylor, P., Watson, F. and Maclement, D. (2011), 'Dynamic line rating deployment on the orkney smart grid'.

Ministry of Business, Innovation & Employment (2018), 'Energy in new zealand 2018', https://www.mbie.govt.nz/building-and-energy/energy-and-natural-resources/energy-statistics-and-modelling/energy-statistics/electricity-statistics/. [Online] Accessed: 5 March 2019.

Mitas, L. and Mitasova, H. (2005), *Spatial interpolation*, Wiley, Chap. 34.

Mushamalirwa, D., Germay, N. and Steffens, J.C. (1988), 'A 2-d finite element mesh generator for thermal analysis of underground power cables', *Power Delivery, IEEE Transactions on*, Vol. 3, No. 1, pp. 62–68.

Neher, J.H. and McGrath, M.H. (1957), 'The calculation of the temperature rise and load capability of cable systems', *Power Apparatus and Systems, Part III. Transactions of the American Institute of Electrical Engineers*, Vol. 76, No. 3, pp. 752–764.

NIWA (2005), 'Solar energy'.

Nuijten, J.M.A., Geschiere, A., Smit, J.C. and Frijmersum, G.J. (2005), 'Future network planning and grid control', In *Future Power Systems, 2005 International Conference on*, pp. 7 pp.–7.

OSIsoft (2017), 'Pi system'. [Online] Accessed 16 July 2017.

Rahim, A.A., Abidin, I.Z., Tarlochan, F. and Hashim, M.F. (2010), 'Thermal rating monitoring of the tnb overhead transmission line using line ground clearance measurement and weather monitoring techniques', In *Power Engineering and Optimization Conference (PEOCO), 2010 4th International*, pp. 274–280.

Raniga, J.K. and Rayudu, R.K. (2000), 'Dynamic rating of transmission lines-a new zealand experience', In *Power Engineering Society Winter Meeting, 2000. IEEE*, pp. 2403–2409 vol.4.

Schell, P., Godard, B., De Wilde, V., Durieux, O., Lilien, J.L., Huu-Minh, N. and Lambin, J.J. (2012), 'Large penetration of distributed productions: Dynamic line rating and flexible generation, a must regarding investment strategy and network reliability', In *Integration of Renewables into the Distribution Grid, CIRED 2012 Workshop*, pp. 1–5.

Schneider Electric (2017), 'Scada system'. [Online] Accessed 16 July 2017.

Shepard, D. (1968), 'A two-dimensional interpolation function for irregularly-spaced data'.

Shun-Hsien, H., Wei-Jen, L. and Ming-Tse, K. (2006), 'On-line dynamic cable rating system for an industrial power plant in the restructured electric market', In *Industry Applications Conference, 2006. 41st IAS Annual Meeting. Conference Record of the 2006 IEEE*, pp. 1418–1424.

Simmons, D.M. (1932), 'Calculation of the electrical problems of underground cables', *The electric journal*.

Swift, G., Molinski, T.S. and Lehn, W. (2001), 'A fundamental approach to transformer thermal modeling', *IEEE Transactions on Power Delivery*, Vol. 16, No. 2, Apr, pp. 171–175.

Thas, O. (2010), *Comparing Distributions*, Vol. 1, Springer, New York, 1st ed., Chap. 3.

Transpower New Zealand (2017), 'Recent electricity demand', https://www.transpower.co.nz/system-operator/security-supply/electricity-demand. [Online] Accessed 04 July 2017.

Unison Networks Limited (2015), 'Asset management plan', http://www.unison.co.nz/tell-me-about/unison-group/publications-disclosures/asset-management-plan. [Online] Accessed: 7 August 2015.

Vector Limited (2015), 'Asset management plan', http://vector.co.nz/disclosures/electricity/amp. [Online] Accessed: 7 August 2015.

Wadhwa, C.L. (2012), *Electrical Power Systems*, New Academic Science, United Kingdom.

WG DNO UK (2017), 'Dno common network asset indices methodology'.

Willis, H.L. (2004), *Power Distribution Planning Reference Book, Second Edition*, Power Engineering, Marcel Dekker, Inc., New York.

Yang, J. and Strickland, D. (2014a), 'Thermal modelling for dynamic transformer rating in low carbon distribution network operation', In *Power Electronics, Machines and Drives (PEMD 2014), 7th IET International Conference on*, pp. 1–6.

Yang, J. and Strickland, D. (2014b), 'Thermal modelling for dynamic transformer rating in low carbon distribution network operation', In *Power Electronics, Machines and Drives (PEMD 2014), 7th IET International Conference on*, pp. 1–6.

Zhurkov, S. (1984), 'Kinetic concept of the strength of solids.', *International Journal of Fracture*, Vol. 26, No. 4, pp. 295 – 307.